Ferdowsi University of Mashhad

ISSN 2008-9147
Numbers: 20

JCMR

Journal of Cell and Molecular Research

Volume 10, Number 2, Winter 2019

بسم الله الرحمن الرحيم

Issuance License No. 124/902-27.05.2008 from Ministry of Culture and Islamic Guidance
Scientific Research Issuance License No. 161675 from the Ministry of Science, Research and Technology, Iran

Journal of Cell and Molecular Research (JCMR)

Volume 10, Number 2, Winter 2019

JCMR Office: Department of Biology, Faculty of Science, Ferdowsi University of Mashhad, Mashhad, Iran.
Postal Code: 9177948953
P.O. Box: 917751436
Tel: +98-513-8804063
Fax: +98-513-8795162
E-mail: jcmr@um.ac.ir
Online Submission: http://jcmr.um.ac

Table of Contents

Journal of Cell and Molecular Research (2019) 10 (2), 52-58 DOI: 10.22067/jcmr.v10i2.75890

Research Article

Investigating the Genotoxic Effect of Gamma Irradiation on L929 Cells after Vinblastine Treatment Using Micronucleus Assay on Cytokinesis-blocked Binucleated Cells

Zahra Jomehzadeh [1], Farhang Haddad[1]*, Maryam M. Matin[1,2], Shokouhozaman Soleymanifard [3]

[1] *Department of Biology, Faculty of Sciences, Ferdowsi University of Mashhad, Mashhad, Iran*
[2] *Novel Diagnostics and Therapeutics Research Group, Institute of Biotechnology, Ferdowsi University of Mashhad, Iran*
[3] *Department of Medical Physics, Mashhad University of Medical Sciences, Mashhad, Iran*

Received 10 October 2018 Accepted 20 January 2019

Abstract

There are several studies suggesting the role of aneuploidy in tumor formation. Aneuploid cells are different from normal ones in term of gene expression and proteome. Cells with different amount and kind of proteins might act differently to external stimuli, including ionizing irradiation. Currently, radiotherapy is one of the main methods in fight against cancer, therefore, it is important to understand the response of the aneuploidy-tumor cells to irradiation. To investigate the chromosomal effect of gamma irradiation on aneuploid cells, L929 cells were treated with 1.5 ng.ml^{-1} of vinblastine to induce aneuploidy. Vinblastine-treated cells were left to recover for 72 h and irradiated with 1 Gy of gamma radiation. Induced chromosomal damages were investigated using micronucleus (Mn) assay. Data showed that vinblastine and gamma irradiation both were able to significantly increase micronucleated-binucleated cells (MnBi) frequency. However, 1 Gy gamma irradiation of the cells after 72 h of vinblastine treatment led to the lower frequency of MnBi compared to irradiated cells. Results of this study suggest that vinblastine treatment of cells before irradiation not only did not sensitize the cells to radiation-induced chromosomal abnormalities, but also had radio-protective effect for these cells. This result could be useful in planning cancer therapy regimes.

***Keywords*:** Gamma, Vinblastine, L929 cells, Micronucleus assay, Binucleated cells

Introduction

Aneuploidy is an important incidence in cancer formation. Even low rates of chromosome mis-segregation lead to tumor formation (Silk et al., 2013). It has been reported in all solid tumors (Tanaka K, 2016). Aneuploidy by disturbing the genetic balance of the cell, affects several fetal cellular pathways involved in maintaining the integrity of genetic materials such as response of the cell to DNA damage and monitoring mechanisms of chromosome segregation during cell divisions (Nicholson and Duesberg, 2009). Carcinogens cause progressive anomalies in chromosomal integrity of the cells (Bloomfield et al., 2014). Therefore, aneuploid cells are more prone to genetic damages which may lead to transformation and cancer.

Agents capable of inducing chromosomal loss or non-disjunction do so by inducing anomalies in chromosome segregation during cell division. One of the strong aneugens is vinblastine, a Vinca alkaloid with strong aneugenic capability which has been suggested in several in vivo and in vitro studies (Cammerer et al., 2010; Leopardi et al., 2002; Zijno et al., 1996). It confers its effect by blocking tubulin dimers and preventing spindle fiber formation. It is able to induce aneuploidy even at very low doses (Cammerer et al., 2010).

Radiotherapy and chemotherapy are currently frequent approaches to cancer treatment (Blank et al., 2017; Franklin et al., 2017). Radiotherapy of cancer cells leads to harmful damages to the cells. Ionizing irradiation used in radiotherapy does so by inducing profound genetic damages to the cells. The harmful effect of ionizing radiation has been known for several years. It is able to induce damages and cuts to DNA which could end up as chromosomal breaks. It imposes damages to chromosomes by its direct effect on DNA or producing free radicals with high tendency to react with it (Ward, 1988).

Investigating the combined effects of radiation with other agents is advised by UNSCEAR (UNSCEAR, 2000). Chromosomal unbalanced cells may have different responses to other harmful agents compared to the normal ones. Because of the

*Corresponding author E-mail: haddad@um.ac.ir

important role of aneuploidy in cancer induction, it is important to know more about the reaction of aneuploid cells to other stimuli. A previous study showed that radiation-induced aneuploid cells showed higher sensitivity to radiation (Bakhoum et al., 2015). In this study we investigated the response of the vinblastine-induced aneuploid cells to ionizing radiation, which is a most common way of cancer treatment. It is for the first time that the co-treatment of two aneugen and clastogen agents is investigated on L929 cells.

Materials and Methods

Vinblastine treatment

L929 cell line was used in this experiment. Cells were cultured in DMEM LG (Gibco) supplemented with 10% FBS (Gibco) in 5% CO2 and 37ºC. Sub-culturing was taken place every 72 h in 1:5 ratios.
Vinblastine sulfate (GedeonIchter Ltd.) was dissolved in distilled water to the stock concentration of 1µg.ml^{-1}. L929 cells have been treated with three doses of 0.5 and 1.5 and 2 ng.ml-1 of vinblastine 24 h post culture initiation for next 24 h. For the second part of the experiment, cells have been treated with 1.5ng.ml^{-1} of vinblastine for 24 h. Culture medium was replaced with fresh vinblastine-free medium at the end of treatment. Cell harvest was performed at different time points of 24, 48 and 72 h post vinblastine removal. Cytochalasin-b (Cyto-b) was added to the cells at final concentration of 4ng.ml^{-1} 20 h before harvest for each time point.

Gamma irradiation

Gamma irradiation of the cells was performed with the rate of 0.99Gy/min at the final dose of 1Gy in T25 flask (60CO radiation therapy, Therateron, Canada). Cells which have been recovered at 72 h post vinblastine removal as well as non-treated cells were irradiated. Cyto-b was added to the cells at final concentration of 4ng.ml^{-1} 2 h after irradiation for 20 h.

Cell harvest and giemsa staining

Cell harvest was performed according to Fenech(Fenech, 2000) with some modifications. Briefly, 20 h post Cyto-b treatment, cells were detached from culture flasks by trypsin and centrifuged at 100g for 10 min. Cells were washed twice with 9:1 methanol: acetic acid fixator. Cell suspension was dropped on clean slides from height of 15-20 cm and left to air-dry.
Dried slides were placed in 10% giemsa solution for 20 min. They were washed with buffer phosphate and left to dry before scoring.

Scoring

Cell scoring took place at a 1000x magnification. In this study, cells with two detached nuclei with visible shared cytoplasm were scored as binucleated cell. From each culture flask at least three slides were coded, and on each slide at least 500 Bi as well as all mononucleated cells which were encountered were scored. In all Bi scored, cells harboring one or more small unattached nuclei considered as micronucleated-binucleated cell (MnBi). The frequency of MnBi was calculated as:

% MnBi= NO of MnBi/ All Bi scored x100

The Binucleated index (Bi index) was calculated as:

Bi index= NO of all Bi/ All Mono and Bi-nucleated cells scored x100

MTT test

Treated as well as untreated control cells were cultured in 96 wells culture plates. Cell viability test was performed for control and vinblastine treated cells harvested 24, 48 and 72 h post vinblastine removal. 100µg of tetrazolium salt (Sigma), dissolved in PBS, was added to 200 µl of cell culture medium and left for 6 h in 37◦C. Medium of each well was replaced with 150 µl of DMSO. Light absorbance of each well at 545 nm wavelength was recorded using ELISA reader (AWASENESS). Light absorbance value of each well was compared to control and its graph was prepared.

Statistical analysis

Statistical analysis was performed using MINITAB software version 14. The differences between control and treated cells as well as between treated groups were analyzed by one-way analysis of variance (ANOVA). For MTT analysis, the SD for all treatments was calculated using MINITAB software and the graphs were plotted using EXCEL software version 2013.

Results

Cyto-b blocked the cytokinesis of the cell division. Treatment of the cells with Cyto-b resulted in cells with two detached nuclei in one shared cytoplasm (Figure 1). Any break to chromosome structure which led to chromosome fragment or any chromosome loss resulted in binucleated cell harboring micronuclei (Mn) (Figure 2).

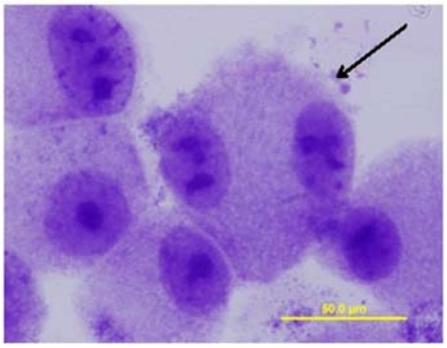

Figure 1. Binucleated cell

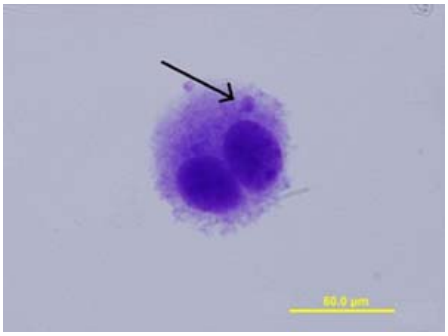

Figure 2. Binucleated cell harboring one micronucleus (MnBi)

Vinblastine treatment

Vinblastine treatment of the cells led to statistically significant increase in the frequency of MnBi (Table 1) compared to control at two highest doses used in this experiment (P<0.05). The highest increase was for 1.5 ng.ml^{-1} of vinblastine. The Bi index showed that vinblastine treatment significantly reduced the cell division activity at all doses used in this experiment (P<0.05) (Table 1).

Table 1. Vinblastine treatment of the L929 cells with different doses of 0.5, 1.5 and 2 ng.ml^{-1}

Doses of Vinblastine	Bi index ±SD	Frequency of MnBi±SD
0.0 ng.ml^{-1}	53.14 ± 3.62	1.89 ±1.64
0.5 ng.ml^{-1}	29.11 ± 2.46[a]	5.48 ±4.52
1.5 ng.ml^{-1}	27.90 ± 4.91[a]	15.26 ±7.58[a]
2 ng.ml^{-1}	26.82 ± 6.94[a]	10.63 ± 0.85[a]

[a]: Statistical difference with control (P<0.05)

The lowest dose that was able to induce the significant increase in MnBi frequency in this experiment was 1.5 ng.ml^{-1}. To minimize the probability of cell damage, we used this dose throughout the rest of the experiment.

Cell recovery after 1.5 ng.ml^{-1} vinblastine treatment

L929 cells were treated with 1.5 ng.ml^{-1} vinblastine for 24 h and cell harvest performed at different time intervals after cell culture replacement. The results of MnBi analysis are presented in Table 2. Vinblastine treatment of the cells led to statistically significant increase in the frequency of MnBi right after vinblastine removal compared to control (P<0.05). However, the frequency decreased in time dependent manner till reached to the control level at 72 h post culture replacement. Bi index although showed significant decrease compared to control right after vinblastine removal, but in all time points after vinblastine removal did not show any significant differences with control (Table 2).

Table 2. Effect of 24 h of vinblastine treatment at different time points after cell wash

		Binucleated index (Bi I)±SD	Frequency of MnBi±SD
control		44.89 ± 9.60	2.22 ± 1.06
Time points after vinblastine removal	0 h	27.90 ± 4.91[a]	15.26 ±7.58[a]
	24 h	39.56 ± 2.11	6.85 ± 0.39[a]
	48 h	44.04 ± 5.21	5.96 ± 2.92[a]
	72 h	35.78 ± 3.27	2.14 ± 0.51

[a]: Statistical difference with control (P<0.05)

Figure 3 represents the result of MTT assay after vinblastine treatment for 24 h at different time points post culture replacement. The results revealed that cells were able to gain their survival ability from harmful effect of vinblastine treatment 72 h post vinblastine removal. The cell viability reached to normal after 48 h.

Gamma irradiation of untreated and vinblastine treated cells

The results of gamma irradiation of L929 cells are represented in Table 3. Gamma irradiation of L929 cells caused significant increase in the frequency of MnBi compared to control (P<0.05). Recovered cells from 1.5 ng.ml^{-1} vinblastine treatment after 72 h of vinblastine removal did not show any significant difference in the frequency of MnBi compared to control. Irradiation of the

recovered cells 72 h after vinblastine treatment led to the significant increase in the frequency of MnBi in comparison to control (P<0.05), however, they also showed a significant decrease of MnBi frequency compared to non-vinblastine treated irradiated cells (P<0.05).

In all treatment regimes, Bi index did not show any significant difference in comparison to control (Table 3).

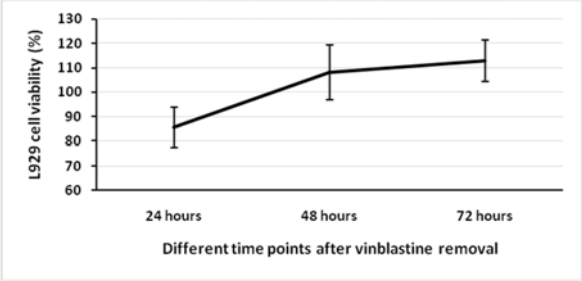

Figure 3. Cell viability after 24 h of 1.5ng.ml^{-1} vinblastine treatment at different time points post vinblastine removal

Table 3. Gamma irradiation of untreated and recovered cells 72 h after treatment with 1.5 ng.ml^{-1} vinblastine

	Binucleated index (Bi I)±SD	Frequency of MnBi±SD
Control	42.19 ± 12.06	2.45 ± 1.23
Cells recovered 72 h post vinblastine treatment	40.33 ± 6.30	2.63 ± 0.98
1 Gy gammairradiation of non-vinblastine treated cells	45.07 ± 5.96	10.40 ± 1.82[a,b]
1 Gy gamma irradiation of cells recovered 72 h post vinblastine treatment	48.83 ± 2.65	6.13 ± 1.01[a]

[a]: Statistically significant difference with control (P<0.05)

[b]: Statistically significant difference with vinblastine recovered cells after Irradiation (P<0.05)

Discussion

There are different conclusions about the role of aneuploidy and structural chromosomal aberrations in inducing cell transformation. Various kinds of numerical and structural chromosomal abnormalities have been reported in tumor cells. Although there is no doubt about the role of these two mechanisms in tumor formation, but the way these two react at the same time and how tumor cells which are involved in genetic instability react to therapy needs to be explained. Changes in the genetic composition of the cells leads to modification in time and quantity of gene expression and synthesis of proteins involve in cell division control and DNA repair, which would have profound consequences on the cell life(Nicholson and Duesberg, 2009). Ionizing irradiation of cancer cells is widely used in cancer therapy. It is suspected that cells with abnormal genetic equilibrium might act differently to the irradiation in comparison to normal cells. Aneuploid cells exhibit profound modifications in their gene expression profiles (Roschke et al., 2008) which may lead to different responses to other stimuli. In this study, we tried to investigate the effect of gamma irradiation in vinblastine-induced aneuploid cells.

Strong aneugenic capability of vinblastine has been investigated in several studies. It can induce chromosome loss or non-disjunction even at very low doses (Cammerer et al., 2010). Vinblastine is able to bind to DNA and in much higher affinity to tubulin (Pandya et al., 2014) and direct its effect through preventing tubulin polymerization during mitosis. Vinblastine treatment of the cells at the two highest doses used in this study were able to induce micronucleus formation. Judged by the nature of vinblastine action, it is possible to say that the increase in the frequency of micronucleus formation was because of high incidence of chromosome loss in treated cells. In other studies, also vinblastine treatment increased kinetochore positive micronuclei, which supports this argument (Marshall et al., 1996).

L929 cells are aneuploidy in nature. Chromosome analysis of this cell line has been revealed the chromosome number of 62-64 chromosomes (Sorokina et al., 1988). In current experiment, vinblastine treatment of these cells was performed to produced extra chromosomal instability in these cells.

Results of this experiment showed that treatment with vinblastine led to increase in the micronuclei frequency, although, it reached the base line frequency 48 h post treatment. The reduction in the frequency of induced micronuclei was started 24 h post vinblastine removal and reduced in a time dependent manner till reached the control level 72 h post vinblastine removal. Cell viability test also revealed that damaged cells were able to recover from vinblastine effect 48 h post vinblastine removal.

Reduction of the frequency of micronuclei after several cell divisions might be the result of

reintegration of micronuclei into main nuclei or simply by losing them during cytokinesis (Leach and Jackson-Cook, 2004). In both suggested reasons it is possible to expect that the result would be creation of aneuploid cells either by losing or gaining one or more chromosomes. Therefore, most of the recovered cells in this experiment could be considered as aneuploid cells.

Ionizing radiations are able to induce structural chromosomal damages in exposed cells (Shi et al., 2012). Cells which have been treated with doses of gamma irradiation showed a significant increase in the frequency of chromosomal damages which in micronucleus assay were represented as micronuclei (Hosseinimehr et al., 2009; Rao et al., 2011). Ionizing radiation imposes its harmful effects on chromosomes of the cells either through direct cuts of double or single strands of DNA or its indirect effect by increasing the free radicals capable of inducing breaks in DNA. Ionizing radiation by passing through water, produces highly active free radicals capable of attacking macromolecules of the cells including DNA. Induced one or double strand cuts in DNA molecule eventually lead to chromosomal structural aberrations including chromosome or chromatid breaks (Hall and Giaccia, 2012).

In several studies increase in the frequency of micronucleus in binucleated cells was proceeded the gamma irradiation of human peripheral lymphocytes (Hosseinimehr et al., 2009; Rao et al., 2011). In this study gamma irradiation of L929 cells also led to significant increase in the MnBi. The induced frequency of MnBi in our study was lower than the frequency of MnBi in human peripheral lymphocytes irradiated in vitro in both studies mentioned earlier (Hosseinimehr et al., 2009; Rao et al., 2011). This difference might be related to the higher dose of gamma-ray used in those studies.

On basis of the nature of damages imposed by ionizing radiation it is possible to expect that high frequency of micronuclei in exposed cells in the present study was mainly the result of chromosome or chromatid breaks. Those chromosomal parts were left behind in the cytoplasm during cell division and form micronuclei.

Cells already treated with vinblastine when exposed to 1 Gy gamma irradiation showed a lower frequency of MnBi compared to untreated cells. The vinblastine treated cells are expected to have unbalance composition of chromosomes and genetic materials. It is possible to consider the protective effect of aneuploidy against ionizing radiation through alteration in transcription and changing the amount of proteins and gene transcripts involved in radiation response of the cells. The gene expression modification in aneuploid cells could affect different aspects of cell response to external stimuli. The role of chromosomal instability in response to cancer therapy has been reviewed extensively (Rangel et al., 2017). Changes in the cell transcriptome by aneuploidy leads to increase in expression of a large group of genes appropriate for cancer formation (Gao et al., 2007). From these large group of genes some might be responsible for resistance to irradiation. These cells produce the higher amount of proteins with capability of radioprotection. Change in gene expression profile of the vinblastine-induced aneuploid cells results in producing higher amount of proteins involved in free radical scavenging and/or DNA repair mechanisms. The reduced frequency of MnBi in those aneuploid cells could be a result of alteration in quantity of gene products of those cells. The result of this study is in contrary with another study that suggests the higher sensitivity of aneuploid cells to ionizing radiation compared to normal cells (Bakhoum et al., 2015). The difference could be related to the way of inducing aneuploidy in those cells compared to ours. In that study aneuploidy was induced by irradiation whereas in ours it was induced by vinblastine treatment. Aneuploidy induction by irradiation would not be the only consequence of irradiation. Irradiation most definitely would be able to induce some forms of gene mutation which might reduce the resistance of the cells to subsequent irradiation. In our study aneuploidy was induced by vinblastine, which no evidences show its mutagenic capability. Therefore, it is possible to imagine that vinblastine induced aneuploid cells have no gene mutation which reduce their resistance to irradiation.

This lower frequency of chromosomal damages also could be the result of ability of vinblastine to reduce the harmful effect of ionizing radiation by its free radical scavenging capability. The radio-protective ability of vinblastine has been already suggested (Rajagopalan et al., 2003). Hence, despite vinblastine removal, the amount of vinblastine inside the cells could act as an antioxidant and protect the cells from clastogenic activity of gamma irradiation. To be able to understand this, the time interval between vinblastine removal and irradiation must be extended to several days.

Data of this study suggest that vinblastine treatment is able to protect the cells from ionizing radiation induced damages. The lower frequency of damages

induced by gamma irradiation in aneuploid cells reveals the need for more studies to create more effective cancer treatment protocols. The authors suggest longer interval time between vinblastine treatment and ionizing irradiation to reduce the probability of direct protection of vinblastine.

Acknowledgements

This work was supported financially by the Ferdowsi University of Mashhad under the grant No. 3/31476.

Conflict of Interest

The authors report no conflicts of interest.

References

1. Bakhoum S. F., Kabeche L., Wood M. D., Laucius C. D., Qu D., Laughney A. M., Reynolds G. E., Louie R. J., Phillips J., Chan D. A., Zaki B. I., Murnane J. P., Petritsch C. and Compton D. A. (2015) Numerical chromosomal instability mediates susceptibility to radiation treatment. Nat Commun 6:5990.
2. Blank O., von Tresckow B., Monsef I., Specht L., Engert A. and Skoetz N. (2017) Chemotherapy alone versus chemotherapy plus radiotherapy for adults with early stage Hodgkin lymphoma. Cochrane Database Syst Rev 4:CD007110.
3. Bloomfield M., McCormack A., Mandrioli D., Fiala C., Aldaz C. M. and Duesberg P. (2014) Karyotypic evolutions of cancer species in rats during the long latent periods after injection of nitrosourea. Mol Cytogenet 7:71.
4. Cammerer Z., Schumacher M. M., Kirsch-Volders M., Suter W. and Elhajouji A. (2010) Flow cytometry peripheral blood micronucleus test in vivo: determination of potential thresholds for aneuploidy induced by spindle poisons. Environ Mol Mutagen 51:278-284.
5. Fenech M. (2000) The in vitro micronucleus technique. Mutation Research/Fundamental and Molecular Mechanisms of Mutagenesis 455:81-95.
6. Franklin J., Eichenauer D. A., Becker I., Monsef I. and Engert A. (2017) Optimisation of chemotherapy and radiotherapy for untreated Hodgkin lymphoma patients with respect to second malignant neoplasms, overall and progression-free survival: individual participant data analysis. Cochrane Database Syst Rev 9:CD008814.
7. Gao C., Furge K., Koeman J., Dykema K., Su Y., Cutler M. L., Werts A., Haak P. and Vande Woude G. F. (2007) Chromosome instability, chromosome transcriptome, and clonal evolution of tumor cell populations. Proc Natl Acad Sci U S A 104:8995-9000.
8. Hall E. J. and Giaccia A. J. 2012. Radiobiology for the Radiologist. Lippincott Williams&Wilkins.
9. Hosseinimehr S. J., Mahmoudzadeh A., Ahmadi A., Mohamadifar S. and Akhlaghpoor S. (2009) Radioprotective effects of hesperidin against genotoxicity induced by gamma-irradiation in human lymphocytes. Mutagenesis 24:233-235.
10. Leach N. T. and Jackson-Cook C. (2004) Micronuclei with multiple copies of the X chromosome: do chromosomes replicate in micronuclei? Mutat Res 554:89-94.
11. Leopardi P., Marcon F., Dobrowolny G., Zijno A. and Crebelli R. (2002) Influence of donor age on vinblastine-induced chromosome malsegregation in cultured peripheral lymphocytes. Mutagenesis 17:83-88.
12. Marshall R. R., Murphy M., Kirkland D. J. and Bentley K. S. (1996) Fluorescence in situ hybridisation with chromosome-specific centromeric probes: a sensitive method to detect aneuploidy. Mutation Research/Fundamental and Molecular Mechanisms of Mutagenesis 372:233-245.
13. Nicholson J. M. and Duesberg P. (2009) On the karyotypic origin and evolution of cancer cells. Cancer Genet Cytogenet 194:96-110.
14. Pandya P., Agarwal L. K., Gupta N. and Pal S. (2014) Molecular recognition pattern of cytotoxic alkaloid vinblastine with multiple targets. J Mol Graph Model 54:1-9.
15. Rajagopalan R., Ranjan S. K. and Nair C. K. (2003) Effect of vinblastine sulfate on gamma-radiation-induced DNA single-strand breaks in murine tissues. Mutat Res 536:15-25.
16. Rajagopalan R R. S., Nair CK. (2003) Effect of vinblastine sulfate on gamma-radiation-induced DNA single-strand breaks in murine tissues. Mutat Res. 536:15-25.
17. Rangel N., Forero-Castro M. and Rondon-Lagos M. (2017) New Insights in the Cytogenetic Practice: Karyotypic Chaos, Non-Clonal Chromosomal Alterations and Chromosomal Instability in Human Cancer and Therapy Response. Genes (Basel) 8.
18. Rao B. N., Archana P. R., Aithal B. K. and Rao B. S. (2011) Protective effect of zingerone, a dietary compound against radiation induced genetic damage and apoptosis in human

lymphocytes. Eur J Pharmacol 657:59-66.
19. Roschke A. V., Glebov O. K., Lababidi S., Gehlhaus K. S., Weinstein J. N. and Kirsch I. R. (2008) Chromosomal instability is associated with higher expression of genes implicated in epithelial-mesenchymal transition, cancer invasiveness, and metastasis and with lower expression of genes involved in cell cycle checkpoints, DNA repair, and chromatin maintenance. Neoplasia 10:1222-1230.
20. Shi L., Fujioka K., Sun J., Kinomura A., Inaba T., Ikura T., Ohtaki M., Yoshida M., Kodama Y., Livingston G. K., Kamiya K. and Tashiro S. (2012) A modified system for analyzing ionizing radiation-induced chromosome abnormalities. Radiat Res 177:533-538.
21. Silk A. D., Zasadil L. M., Holland A. J., Vitre B., Cleveland D. W. and Weaver B. A. (2013) Chromosome missegregation rate predicts whether aneuploidy will promote or suppress tumors. Proc Natl Acad Sci U S A 110:E4134-4141.
22. Sorokina E. A., Novikova I., Grinchuk T. M. and Sal'nikov K. V. (1988) [Karyotype analysis of clone L929 murine fibroblasts by using differential chromosome staining]. Tsitologiia 30:197-204.
23. Tanaka K H. T. (2016) Chromosomal instability: A common feature and a therapeutic target of cancer. Biochim Biophys Acta. 1866:64-75.
24. UNSCEAR. (2000) The United Nations Scientific Committee on the Effects of Atomic Radiation Report Vol. II: Sources and effects of ionizing radiation. Annex H: Combined effects of radiation and other agents, UNSCEAR, Vienna.
25. Ward J. F. (1988) DNA damage produced by ionizing radiation in mammalian cells: identities, mechanisms of formation, and reparability. Prog Nucleic Acid Res Mol Biol 35:95-125.
26. Zijno A., Marcon F., Leopardi P. and Crebelli R. (1996) Analysis of chromosome segregation in cytokinesis-blocked human lymphocytes: non-disjunction is the prevalent damage resulting from low dose exposure to spindle poisons. Mutagenesis 11:335-340.

Journal of Cell and Molecular Research (2019) 10 (2), 59-66 DOI: 10.22067/jcmr.v10i2.76835

Research Article

Cell type-specific Effect of miRZip-21 to Suppress miR-21 in Human Glioma Cell Lines

Hamideh Monfared[1], Yavar Jahangard[1], Maryam Nikkhah[2], Seyed Javad Mirnajafi-Zade[3], Seyed Javad Mowla[1*]

[1] *Department of Molecular Genetics, Faculty of Biological Science, Tarbiat Modares University, Tehran, Iran*
[2]*Department of Nanobiotechnology, Faculty of Biological Science, Tarbiat Modares University, Tehran, Iran*
[3]*Department of Physiology, Faculty of Medical Science, Tarbiat Modares University, Tehran, Iran*

Received 27 November 2018 Accepted 12 January 2019

Abstract

There are different subtypes of brain tumors, classified according to the origin of the abnormally proliferated glial cells. Glioblastoma multiforma (GBM) is the grade 4 of brain tumors, gliomas, with the least life expectancy. microRNAs (miRNAs) are small, single stranded, non-coding RNAs with 20-25 nt length with post-transcriptional gene regulatory activities. An altered expression of miRNAs is linked to developmental disorders and some diseases, most importantly cancers. miR-21 is a well-known microRNA, overexpressed in almost all cancer types, including brain tumors. It targets several genes with vital roles in cellular pathways involve in proliferation, invasion and metastatic behaviors. Exosomes are 30-100 nm extracellular vesicles which are packed with various molecules, including miRNAs. Here, we suppressed miR-21 expression level in HEK-293T cells by transfecting them with the miRZip-21 vector. However, when U87-MG cells were cultured in the presence of exosomes isolated from conditioned medium of engineered HEK-293T cells derived exosomes, we did not observe any suppressing effect on host cells' miR-21 expression level. Moreover, by analyzing the effects of miRZip-21-enriched cell's conditioned media on three other brain cell lines including 1321N1, A-172 and DAOY, cell type-specific effects of exocrine miRZip-21 were revealed. These data suggested that cell lines from different brain tumor subtypes could exert different responses to microRNA-based therapies, based on their cellular origin and clinical behaviors.

***Keywords*:** miR-21, Brain tumors, Glioblastoma multiforma, Exosomes

Introduction

Brain tumor is a neoplasm that occurs by an abnormal and uncontrolled cell division of glial cells within the central nervous system (CNS). Tumors of the CNS have a wide spectrum of subtypes according to the WHO classification, their cellular origin and histological characteristics of each particular tumor. The most frequent brain cancers in children are pilocytic astrocytomas, ependymomas and medulloblastomas, while, in adults diffuse astrocytic tumors (including astrocytoma, anaplastic astrocytomas, and glioblastomas), oligodendrogliomas, and meningiomas (Collins and Psychiatry, 2004; Louis et al., 2007; Louis et al., 2016) are most frequent brain cancer subtypes. Glioblastoma multiforma (GBM) is the grade 4 of brain tumors, which it's life expectancy about 18 months after diagnosis (Paolillo et al., 2018).

microRNAs (miRNAs) are small, single stranded, non-coding RNAs with 20-25 nt length that have post-transcriptional gene regulatory activities. miRNAs play crucial roles in variable biological events such as development, differentiation and apoptosis. Misregulations in expression level of miRNAs can lead to some diseases including cancers. Therefore, investigating the expression profile of various miRNAs can provide useful diagnostic, prognostic and therapeutic information for the future therapeutic challenges (Gulyaeva and Kushlinskiy, 2016; Hayes et al., 2014; Paul et al., 2018). miR-21 is a well-known miRNA that is overexpressed in almost all cancer types, including brain tumors. It targets several important genes in cellular processes, with regulatory effects on proliferation, invasion and metastatic behaviors. PDCD4 (Programmed cell death protein 4) and RECK (Reversion-inducing-cysteine-rich protein with kazal motifs) are two important miR-21 target genes, with some key regulatory roles in apoptotic and metastatic pathways (Corsten et al., 2007; Gabriely et al., 2008; Gao et al., 2007; Gaur et al., 2011; Malhotra et al., 2018; Papagiannakopoulos et al., 2008; Sekar et al., 2015). Inhibition of miR-21 expression or activity via different techniques promoted apoptotic cell death, sensitivity to chemotherapy/radiotherapy and cancer suppression (Belter et al., 2016;

*Corresponding author E-mail: sjmowla@modares.ac.ir

Devulapally et al., 2015; Lu et al., 2008; Sicard et al., 2013; Yang et al., 2014).

Extracellular vesicles (EVs) are membrane fragments budding from cells' surfaces to transfer cytoplasmic or membrane cargoes to target cells (Ratajczak et al., 2006; Tkach and Théry, 2016; Yuana et al., 2013). Exosomes are 30-100 nm extracellular vesicles with important roles in signaling pathways (Arscott et al., 2013; Kucharzewska et al., 2013; Mittelbrunn et al., 2011). They contain a variety of cellular components, including proteins and genetic materials such as miRNAs (Nouraee et al., 2015; Yu et al., 2016; Zhang et al., 2015).

Here, we tried to downregulate miR-21 expression in HEK293T cells by transfecting them with an anti-miR-21 (miRZip-21) construct. Then, engineered exosomes enriched from HEK293T cells' conditioned media were transferred into glioblastoma cells to explore their suppressing effects on host cells' miR-21 expression level. Our data revealed that exosome enriched with miRZip-21 have differential effects on different glioma cell lines.

Materials and Methods

Cell culture and transfection

HEK-293T cells were obtained from Iranian biological resource center and cultured in DMEM-F12 (Gibco, USA), supplemented with 10% fetal bovine serum (Gibco, USA) and 1% penicillin-streptomycin (Bio Basic, Canada) and were seeded in a 12-well plate (SPL Life Science, South Korea). To suppress miR-21 expression level, miRZip-21 purchased from System Bioscience (SBI, USA). Stable cell line colonies expressing miRZip-21 were generated by transfecting cells at %70 confluencies with lipofectamin 3000 (Invitrogen, USA). Successfully transfected cells were selected by using 4 µg/ml Puromycin (Sigma, Germany). Then, cells were expanded while antibiotic concentration reduced gradually.

RNA extraction and RT-PCR

RNA extraction performed by Trizol (for cells) and Trizol LS (for cell's conditioned media and exosomes) reagents (Invitrogen, USA). After cDNA synthesis with TAKARA cDNA synthesis kit (Japan), Real-time PCR was performed for detecting miR-21 expression level using SYBR Green (Bio Fact, Korea) and Stem-loop method (Kramer, 2011). Then, the expression levels of PDCD4 and RECK, as miR-21 target genes, were analyzed (Supplementary table 1).

Co-culture experiments

In order to analyze miRZip-21 effects on target cells, stable transfected HEK-293T cells were seeded in 6-well plates (2×104 cells per well, SPL Life Science, South Korea). 24 hours later, target cells (U87-MG cells, obtained from Iranian biological resource center) were seeded on inserts with 0.4 µm pore sizes (SPL Life Science, South Korea), within the same plates of transfected HEK-293T cells (23×103 cells/insert). RNA extraction was performed for both HEK-293T and U87-MG cells after 24 and 48 hours of co-culture experiments.

Exosome purification and characterization

miRZip-21-expressing stable cell lines were cultured in T75 cell culture flasks in the presence of exosome-depleted FBS (Huan et al., 2013). Cell's conditioned media were collected every 2-3 days, and total exosomes were extracted by several steps of centrifugation (300 g for10 min, 2000 g for 10 min, 10000 g for 30 min, 20000 g for 60 min, 100000 g for 70 min) (Théry et al., 2006). DLS analysis (with 10 minutes sonication), and Bradford assay were respectively used to determine size and concentration of isolated exosomes. 20 µl of our exosome preparations were applied for scanning electron microscopy (SEM). To visualize size and shapes of extracted exosomes, SEM images were achieved by using gold coating with physical vapour deposition (PVD) method, done with Sputter coater instrument (SBC 12 model) and KYKY-EM3200 instruments (26 KV).

Investigating effects of exosomes on U87-MG cells: U87-MG cells were seeded in a 24-well plate in RPMI media (Gibco, USA) (supplemented with 10% FBS and 1% Penicillin/streptomycin). Then, they exposed to 50 µg/ml of miRZip-21 enriched exosomes for 24 to 48 hours. Following cell lysis, total RNA extraction performed for all samples to investigate the expression levels of miR-21 and miR target genes.

Analyzing effects of conditioned media from miRZip-21 producing HEK-293T cells on other brain related cell lines: 1321N1, A172 and DAOY cell lines were obtained from Iranian biological resource center, cultured in RPMI media (Gibco, USA) containing 10% fetal bovine serum (Gibco, USA) and 1% penicillin-streptomycin (Bio Basic, Canada), in 24-well plate (SPL Life Science, South Korea). Upon reaching 70% confluencies, their medium exchanged with an equal mixture of RPMI and conditioned media of miRZip-21 producing HEK-293T cells (1:1).

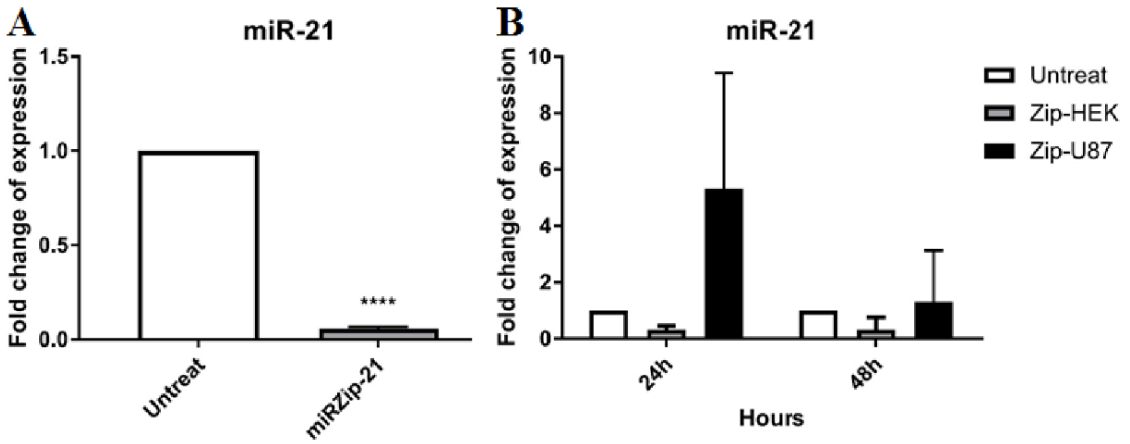

Figure 1. A) Down-regulation of miR-21 expression in HEK-293T stable cell lines exogenously expressing miRZip-21, in comparison to untransfected cells ($p < 0.0001$). B) miR-21 expression level in U87-MG cells, 24 and 48 hours following co-culturing with HEK-293T cells stably expressing miRZip-21. As demonstrated no significant downregulation observed for treated cells.

Statistical analysis

All experiments were repeated at least 2-3 times. Statistical analysis performed using GraphPad Prism 6 software and ordinary ANOVA test. Data were presented as Mean +/- SD, and differences were considered significant, when p value were less than 0.05.

Results

miRZip-21 decreases miR-21 expression level in HEK-293T cells: We employed miRZip-21 to downregulate miR-21 expression level. Following transfecting HEK-293T cells with miRZip-21 vector and producing stable cell lines, the expression levels of miRZip-21 and miR-21 were determined by a real-time PCR approach. In miRZip-21 expressing stable cell line, miR-21 expression level significantly decreased in comparison to untransfected cells ($p < 0.0001$; Figure 1A). Gene expression levels were normalized to the expression of GAPDH (Glyceraldehyde 3-phosphate dehydrogenase) as our house keeping gene.

miR-21 expression level of U87-MG cells exert modifications upon co-culturing with HEK-293T cells expressing miRZip-21: Primary glioblastoma cell line U87-MG was employed to analyze the effects of secreted miRZip-21 in a co-culture system, in which the cells were physically separated from each other. After 24 and 48 hours of conditioned media contact between U87 and miRZip-21 expressing HEK-293T cells, miR-21 expression measured quantitatively. Our experiments revealed that although, miRZip-21 decreases miR-21 expression level in HEK-293T, but it fails to decrease miR-21 level in U87-MG target cells (Figure 1B). As it is evident in Figure 1, we even observed an unexpected elevation of miR-21 levels in U87-MG target cells following 24 h and 48 h of co-culture experiments.

miRZip-21 successfully packaged into the exosomes of transfected cells: To examine the possibility of miRZip-21 packaging in the exosomes of transfected cells, we purified exosomes by means of ultracentrifugation. General characteristics of isolated exosomes including their size and shape evaluated and confirmed by performing DLS analysis and electron microscopy. Particle size analysis revealed a sharp and single peak on 83.46 nm point for purified vesicles (Figure 2A). Uniform shape and proper size of isolated exosomes (mostly under 100 nm) were also confirmed following scanning electron microscopy experiments (Figure 2B).

We then analyzed the level of miR-21 expression in exosomes isolated from conditioned media of HEK-293T miRZip-21 expressing stable cell line, in comparison to untransfected cells. Our data revealed a diminished level of miR-21 in the miRZip-21 expressing cells; however, it was not statistically significant (Figure 3).

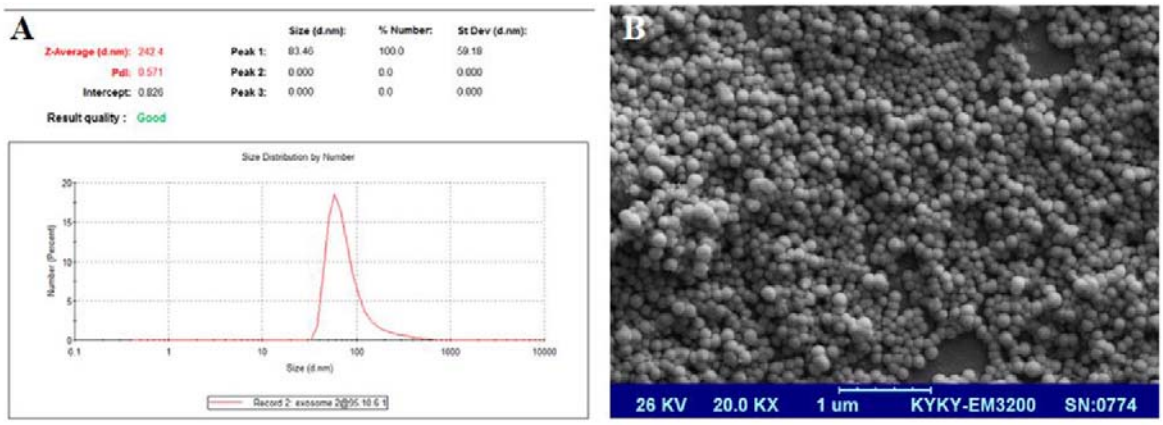

Figure 2. Characterizing the purity and identity of extracted exosomes. A) DLS experiments demonstrated a good quality and normal size distribution (with a unique peak under 100 nm; average 83.46 nm) for purified exosomes. B) SEM micrograph obtained from our exosome preparation, indicated proper concentration of exosomes in our investigated sample with ideal size distribution between 30-170 nm (mostly under 100nm).

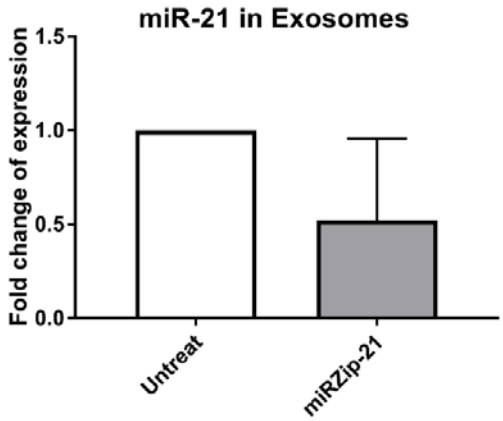

Figure 3. miR-21 expression levels in exosomes isolated from miRZip-21 expressing HEK-293T cells, in comparison to the exosomes extracted from untransfected cells.

Engineered exosomes had no miR-21 suppression effect on U87-MG cells: Despite our expectations, miRZip-21 containing exosomes failed to exert any suppression effects on miR-21 expression levels of U87-MG cells as our target cell (Figure 4A). Interestingly, a noticeable, but not statistically significant, increase in the level of miR-21 was observed in the cells, 24h after co-culture experiments. To explore the possibility of a similar effect of miRZip-21 containing exosomes on miR-21 target genes, we quantified the expression levels of PDCD4 and RECK genes, two important target genes of miR-21, in treated cells. As was expected, miRZip-21 containing exosomal treatments caused a reverse effect on the expression of PDCD4 and RECK genes in treated cells, although, these changes were also not statistically significant (Figure 4B, C).

Investigating miRZip-21 effects on other brain cancer cell lines: To further examine the effects of miRZip-21 on other cell lines, we performed similar experiments on some other glioma cell lines (table 1). Our data revealed a differential effect on the above mentioned cell lines exposed to the miRZip-21-enriched conditioned media of HEK-293T stable cells (Fig 5). In 1321N1 astrocytoma cell line, miR-21 level elevated in 24 hours, but dramatically dropped down after 48 hours of treatment. In case of A172 cells, which are classified as non-tumorgenic glioblastoma cell line, a significant downregulation of miR-21 observed in all investigated time points. Finally, DAOY cells showed an upregulation of miR-21 expression at both 24 and 48 hours. However, differences were not statistically significant.

Discussion

Glioblastoma multiforma is the most malignant form of brain tumors (Collins and Psychiatry, 2004; Louis et al., 2007; Louis et al., 2016). Finding a new therapeutic approach for treating brain tumors is of great importance. Despite new molecular and surgical approaches (Gilbert, 2011; Van Meir et al., 2010), finding an effective cure is still remained to be introduced.

microRNAs are demonstrated to have important roles in cancer initiation and progression (Gulyaeva and Kushlinskiy, 2016; Hayes et al., 2014; Paul et al., 2018). We have already reported that miR-21 is upregulated in esophageal tumors and that the upregulation was mainly confined to the fibroblast-like stromal cells adjacent to cancer cells, rather than tumor cells (Nouraee et al., 2013). The latter finding suggests a role for secreted miR-21 as a microenvironmental communication signal between

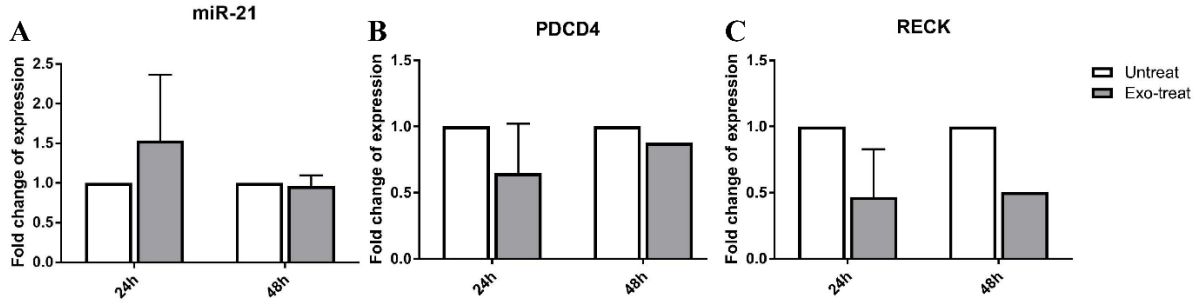

Figure 4: A) Expression of miR-21 in U87-MG cells exposed to the engineered exosomes isolated from conditioned media of miRZip-21 expressing HEK-293T cells by ultracentrifugation. **B, C)** Expression of PDCD4 and RECK in U87-MG cells following treatment with exosomes obtained from conditioned media of genetically modified HEK293T cells. As demonstrated similar expression pattern observed for miR-21 target genes, PDCD4 and RECK, 24 and 48 hours post-treatments. It should be notified that these modifications were not statistically significant.

Table 1: Characteristics of brain tumor cell lines applied in the present study.

Investigated Cell lines	Properties	Tumorgenic?
U87-MG	Human primary glioblastoma	Yes
1321N1	astrocytoma	?
A172	glioblastoma	No
DAOY	Desmoplastic cerebellar medulloblastoma	Yes

**Data submitted from ATCC site*

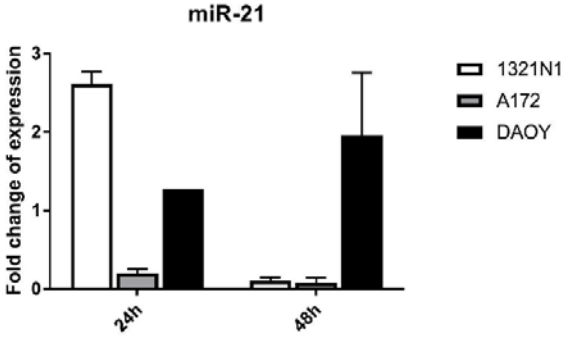

Figure 5: miR-21 expression levels in 1321N1, A172 and DAOY cell lines after treatment with conditioned media obtained from miRZip-21 stably expressing HEK-293T cells. Note that different cell lines responded differentially to the treatment with miRZip-21-containing conditioned media.

cancer cells and their adjacent non-tumor cells. Cancer cell communications is an important target point to be considered for inhibition of cancer development. Most of these secretory signaling molecules are released in the form of exosomes. GBM cells apply these microvesicles to increase tumor cell communication for proliferation, invasion and even metastatic behaviors (Arscott et al., 2013; Kucharzewska et al., 2013; Mittelbrunn et al., 2011). The presence of microRNAs within exosomes have been already reported (Collino et al., 2010; Ogata-Kawata et al., 2014; Yuana et al., 2013), including the packaging and release of miR-21 within exosomes of different cancer cell types (Tanaka et al., 2013; Tian et al., 2014; Tsukamoto et al., 2017; Wang et al., 2015). miR-21 silencing was also carried out with effective results in both *in vitro* and *in vivo* trials (Belter et al., 2016; Devulapally et al., 2015; Lu et al., 2008; Sicard et al., 2013; Yang et al., 2014).

Here, we tried to supress miR-21 expression in glioblastoma cell line U87-MG, employing engineered exosomes carrying the miRZip-21 construct. While miRZip-21 downregulated miR-21 expression level in transfected HEK-293T stable cell line, its effect on target cells treated with miRZip-21 containing exosomes was unexpected. There is no rational explanation for elevated expression of miR-21 in U87-MG cells. To find out if the aforementioned effect is caused by a general mechanism, we examined the effect of miRZip-21 producing stable HEK-293T conditioned media on three other brain cancer cell lines. The cerebellar medulloblatoma cell line, DAOY, showed almost similar results as U87-MG, with an upregulation of miR-21 after 24h and 48h of treatment. The effect of miRZip-21 on A172 cells was in contrast with what observed on U87-MG, with a downregulation of miR-21 expression level at both 24 and 48h of treatment. The astrocytoma cell line 1321N1 (Gundemir et al., 2017; Toll et al., 2011) showed a surprising response after treatment with miRZip-21 containing conditioned media, with an upregulation of miR-21 at 24h and a dramatic downregulation 48

hours following treatment.
Altogether, our data revealed different response of various brain cell lines to a single treatment. This is in agreement with previous findings that brain tumor subtypes response differently to different treatment approaches (Gundemir et al., 2017; Toll et al., 2011; Verhaak et al., 2010). Therefore, the therapeutic application of miR-21 suppression requires to determine the subclass of tumors, as the current proposed therapy is cell-line dependent.

Acknowledgements

This study was supported by a research grant from the Iranian Council of Cognitive Sciences and Technologies.

Conflict of Interest
No competing financial interests exist.

References

1. Arscott W. T., Tandle A. T., Zhao S., Shabason J. E., Gordon I. K., Schlaff C. D., Zhang G., Tofilon P. J. and Camphausen K. A. J. T. o. (2013) Ionizing radiation and glioblastoma exosomes: implications in tumor biology and cell migration. 6:638-IN636.
2. Belter A., Rolle K., Piwecka M., Fedoruk-Wyszomirska A., Naskręt-Barciszewska M. Z. and Barciszewski J. J. S. R. (2016) Inhibition of miR-21 in glioma cells using catalytic nucleic acids. 6:24516.
3. Collino F., Deregibus M. C., Bruno S., Sterpone L., Aghemo G., Viltono L., Tetta C. and Camussi G. J. P. o. (2010) Microvesicles derived from adult human bone marrow and tissue specific mesenchymal stem cells shuttle selected pattern of miRNAs. 5:e11803.
4. Collins V. J. J. o. N., Neurosurgery and Psychiatry. (2004) Brain tumours: classification and genes. 75:ii2-ii11.
5. Corsten M. F., Miranda R., Kasmieh R., Krichevsky A. M., Weissleder R. and Shah K. J. C. r. (2007) MicroRNA-21 knockdown disrupts glioma growth in vivo and displays synergistic cytotoxicity with neural precursor cell–delivered S-TRAIL in human gliomas. 67:8994-9000.
6. Devulapally R., Sekar N. M., Sekar T. V., Foygel K., Massoud T. F., Willmann J. r. K. and Paulmurugan R. J. A. n. (2015) Polymer nanoparticles mediated codelivery of antimiR-10b and antimiR-21 for achieving triple negative breast cancer therapy. 9:2290-2302.
7. Gabriely G., Wurdinger T., Kesari S., Esau C. C., Burchard J., Linsley P. S., Krichevsky A. M. J. M. and biology c. (2008) MicroRNA 21 promotes glioma invasion by targeting matrix metalloproteinase regulators. 28:5369-5380.
8. Gao F., Zhang P., Zhou C., Li J., Wang Q., Zhu F., Ma C., Sun W. and Zhang L. J. O. r. (2007) Frequent loss of PDCD4 expression in human glioma: possible role in the tumorigenesis of glioma. 17:123-128.
9. Gaur A. B., Holbeck S. L., Colburn N. H. and Israel M. A. J. N.-o. (2011) Downregulation of Pdcd4 by mir-21 facilitates glioblastoma proliferation in vivo. 13:580-590.
10. Gilbert M. R. 2011. Recurrent glioblastoma: a fresh look at current therapies and emerging novel approaches. In Seminars in oncology. Vol. 38. Elsevier. S21-S33.
11. Gulyaeva L. F. and Kushlinskiy N. E. J. J. o. t. m. (2016) Regulatory mechanisms of microRNA expression. 14:143.
12. Gundemir S., Monteagudo A., Akbar A., Keillor J. W. and Johnson G. V. J. N.-o. (2017) The complex role of transglutaminase 2 in glioblastoma proliferation. 19:208-218.
13. Hayes J., Peruzzi P. P. and Lawler S. J. T. i. m. m. (2014) MicroRNAs in cancer: biomarkers, functions and therapy. 20:460-469.
14. Huan J., Hornick N. I., Shurtleff M. J., Skinner A. M., Goloviznina N. A., Roberts C. T. and Kurre P. J. C. r. (2013) RNA trafficking by acute myelogenous leukemia exosomes. 73:918-929.
15. Kramer M. F. J. C. p. i. m. b. (2011) Stem-loop RT-qPCR for miRNAs. 95:15.10. 11-15.10. 15.
16. Kucharzewska P., Christianson H. C., Welch J. E., Svensson K. J., Fredlund E., Ringnér M., Mörgelin M., Bourseau-Guilmain E., Bengzon J. and Belting M. J. P. o. t. N. A. o. S. (2013) Exosomes reflect the hypoxic status of glioma cells

and mediate hypoxia-dependent activation of vascular cells during tumor development.201220998.
17. Louis D. N., Ohgaki H., Wiestler O. D., Cavenee W. K., Burger P. C., Jouvet A., Scheithauer B. W. and Kleihues P. J. A. n. (2007) The 2007 WHO classification of tumours of the central nervous system. 114:97-109.
18. Louis D. N., Perry A., Reifenberger G., Von Deimling A., Figarella-Branger D., Cavenee W. K., Ohgaki H., Wiestler O. D., Kleihues P. and Ellison D. W. J. A. n. (2016) The 2016 World Health Organization classification of tumors of the central nervous system: a summary. 131:803-820.
19. Lu Z., Liu M., Stribinskis V., Klinge C., Ramos K., Colburn N. and Li Y. J. O. (2008) MicroRNA-21 promotes cell transformation by targeting the programmed cell death 4 gene. 27:4373.
20. Malhotra M., Sekar T. V., Ananta J. S., Devulapally R., Afjei R., Babikir H. A., Paulmurugan R. and Massoud T. F. J. O. (2018) Targeted nanoparticle delivery of therapeutic antisense microRNAs presensitizes glioblastoma cells to lower effective doses of temozolomide in vitro and in a mouse model. 9:21478.
21. Mittelbrunn M., Gutiérrez-Vázquez C., Villarroya-Beltri C., González S., Sánchez-Cabo F., González M. Á., Bernad A. and Sánchez-Madrid F. J. N. c. (2011) Unidirectional transfer of microRNA-loaded exosomes from T cells to antigen-presenting cells. 2:282.
22. Nouraee N., Mowla S. J., Calin G. A. J. G., Chromosomes and Cancer. (2015) Tracking miRNAs' footprints in tumor–microenvironment interactions: insights and implications for targeted cancer therapy. 54:335-352.
23. Nouraee N., Van Roosbroeck K., Vasei M., Semnani S., Samaei N. M., Naghshvar F., Omidi A. A., Calin G. A. and Mowla S. J. J. P. O. (2013) Expression, tissue distribution and function of miR-21 in esophageal squamous cell carcinoma. 8:e73009.
24. Ogata-Kawata H., Izumiya M., Kurioka D., Honma Y., Yamada Y., Furuta K., Gunji T., Ohta H., Okamoto H. and Sonoda H. J. P. o. (2014) Circulating exosomal microRNAs as biomarkers of colon cancer. 9:e92921.
25. Paolillo M., Boselli C. and Schinelli S. J. B. s. (2018) Glioblastoma under siege: an overview of current therapeutic strategies. 8:15.
26. Papagiannakopoulos T., Shapiro A. and Kosik K. S. J. C. r. (2008) MicroRNA-21 targets a network of key tumor-suppressive pathways in glioblastoma cells. 68:8164-8172.
27. Paul P., Chakraborty A., Sarkar D., Langthasa M., Rahman M., Bari M., Singha R. S., Malakar A. K. and Chakraborty S. J. J. o. c. p. (2018) Interplay between miRNAs and human diseases. 233:2007-2018.
28. Ratajczak J., Wysoczynski M., Hayek F., Janowska-Wieczorek A. and Ratajczak M. J. L. (2006) Membrane-derived microvesicles: important and underappreciated mediators of cell-to-cell communication. 20:1487.
29. Sekar D., Saravanan S., Karikalan K., Thirugnanasambantham K., Lalitha P. and IH Islam V. J. C. p. b. (2015) Role of microRNA 21 in mesenchymal stem cell (MSC) differentiation: a powerful biomarker in MSCs derived cells. 16:43-48.
30. Sicard F., Gayral M., Lulka H., Buscail L. and Cordelier P. J. M. T. (2013) Targeting miR-21 for the therapy of pancreatic cancer. 21:986-994.
31. Tanaka Y., Kamohara H., Kinoshita K., Kurashige J., Ishimoto T., Iwatsuki M., Watanabe M. and Baba H. J. C. (2013) Clinical impact of serum exosomal microRNA-21 as a clinical biomarker in human esophageal squamous cell carcinoma. 119:1159-1167.
32. Théry C., Amigorena S., Raposo G. and Clayton A. J. C. p. i. c. b. (2006) Isolation and characterization of exosomes from cell culture supernatants and biological fluids. 30:3.22. 21-23.22. 29.
33. Tian T., Zhu Y.-L., Zhou Y.-Y., Liang G.-F., Wang Y.-Y., Hu F.-H. and Xiao Z.-D. J. J. o. B. C. (2014) Exosome uptake through clathrin-mediated endocytosis and macropinocytosis and mediating miR-21 delivery.jbc. M114. 588046.
34. Tkach M. and Théry C. J. C. (2016) Communication by extracellular

vesicles: where we are and where we need to go. 164:1226-1232.
35. Toll L., Jimenez L., Waleh N., Jozwiak K., Woo A.-H., Xiao R.-P., Bernier M., Wainer I. J. J. o. P. and Therapeutics E. (2011) β2-adrenergic receptor agonists inhibit the proliferation of 1321N1 astrocytoma cells. 336:524-532.
36. Tsukamoto M., Iinuma H., Yagi T., Matsuda K. and Hashiguchi Y. J. O. (2017) Circulating exosomal microRNA-21 as a biomarker in each tumor stage of colorectal cancer. 92:360-370.
37. Van Meir E. G., Hadjipanayis C. G., Norden A. D., Shu H. K., Wen P. Y. and Olson J. J. J. C. a. c. j. f. c. (2010) Exciting new advances in neuro-oncology: the avenue to a cure for malignant glioma. 60:166-193.
38. Verhaak R. G., Hoadley K. A., Purdom E., Wang V., Qi Y., Wilkerson M. D., Miller C. R., Ding L., Golub T. and Mesirov J. P. J. C. c. (2010) Integrated genomic analysis identifies clinically relevant subtypes of glioblastoma characterized by abnormalities in PDGFRA, IDH1, EGFR, and NF1. 17:98-110.
39. Wang J.-J., Wang Z.-Y., Chen R., Xiong J., Yao Y.-L., Wu J.-H. and Li G.-X. J. A. P. J. C. P. (2015) Macrophage-secreted exosomes delivering miRNA-21 inhibitor can regulate BGC-823 cell proliferation. 16:4203-4209.
40. Yang C. H., Yue J., Pfeffer S. R., Fan M., Paulus E., Hosni-Ahmed A., Sims M., Qayyum S., Davidoff A. M. and Handorf C. R. J. J. o. B. C. (2014) MicroRNA-21 promotes glioblastoma tumorigenesis by down-regulating insulin-like growth factor-binding protein-3 (IGFBP3). 289:25079-25087.
41. Yu X., Odenthal M. and Fries J. W. J. I. j. o. m. s. (2016) Exosomes as miRNA carriers: formation–function–future. 17:2028.
42. Yuana Y., Sturk A. and Nieuwland R. J. B. r. (2013) Extracellular vesicles in physiological and pathological conditions. 27:31-39.
43. Zhang J., Li S., Li L., Li M., Guo C., Yao J., Mi S. J. G., proteomics and bioinformatics. (2015) Exosome and exosomal microRNA: trafficking, sorting, and function. 13:17-24.

Table S1. Primers sequence

Name	Forward / Reverse	Sequence
miR-21 cDNA Synthesis	–	5'- GTC GTA TCC AGT GCA GGG TCC GAG GTA TTC GCA CTG GAT ACG ACT CAA CA -3'
miR-21 PCR	Forward	5'- CCG GCC TAG CTT ATC AGA CTG -3'
	Reverse	5'- AGTG CAG GGT CCG AGG TA -3'
5S rRNA	Forward	5'- GTCTACGGCCATACCACCCTG -3'
	Reverse	5'- AAAGCCTACAGCACCCGGTAT -3'
PDCD4	Forward	5'- CAGTTGGTGGGCCAGTTTATTG -3'
	Reverse	5'- AGAAGCACGGTAGCCTTATCCA -3'
RECK	Forward	5'- GACTCTTCTCCTGGTCCATCTC -3'
	Reverse	5'- CTATCCGTTGGGTTCCTCAT -3'
GAPDH	Forward	5'- ATGGGGAAGGTGAAGGTCG -3'
	Reverse	5'- GGGGTCATTGATGGCAACAATA -3'

Journal of Cell and Molecular Research (2019) 10 (2), 67-75 DOI: 10.22067/jcmr.v10i2.74806

Research Article

Induction of AHR Gene Expression in Colorectal Cancer Cell Lines by Cucurbitacin D, E, and I

Younes Aftabi[1,3], Habib Zarredar[1], Mohammadreza Sheikhi[2], Zahra Khoshkam[2], Abasalt Hosseinzadeh Colagar[3*]

[1] Tuberculosis and Lung Disease Research Center, Tabriz University of Medical Sciences, Tabriz, Iran
[2] Department of Molecular and Cell Biology, Faculty of Basic Sciences, University of Tehran, Tehran, Iran
[3] Department of Molecular and Cell Biology, Faculty of Basic Sciences, University of Mazandaran, Babolsar, Mazandaran, Iran

Received 15 August 2018 Accepted 8 March 2019

Abstract

Aryl hydrocarbon receptor (AHR) is a ligand-activated transcription factor and its induction may result in suppressing of cell proliferation in colorectal cancer (CRC). Cucurbitacin D (CucD), E (CucE) and I (CucI) are plant derived metabolites that inhibit cancer cells. This study aimed to evaluate the possible potency of the cucurbitacins for activation of AHR expression in CRC cell lines SW-480 and HT-29. The MTT assay was used to find the IC50 value of the metabolites in the cell lines. Afterwards, the cells were incubated with the IC50 concentrations of the cucurbitacins and AHR-mRNA expression assessed using RT-PCR. The IC50 values of CucD, CucE, and CucI were 4.5, 6.8, and 3.8 µM in HT-29 cell line and 35, 19, 17.5 µM in SW-480 cells, respectively. The SW-480 cells were more resistant against cucurbitacins in comparison with HT-29 cells and all three cucurbitacins led to more AHR-mRNA expression in HT-29 cells. CucE had the lowest effect on AHR-mRNA expression in the cell lines and CucI was a common metabolite for both HT-29 and SW-480 cells, which showed the lowest IC50 value (the highest toxicity) and the highest effect on AHR-mRNA expression. CucI may have a potential AHR-induction role and it could be applicable as an AHR-expression inducer in CRC studies.

Keywords: Aryl hydrocarbon receptor, Colon cancer, Cucurbitacin, HT-29, SW-480

Introduction

It is predicted that the global burden of colorectal cancer (CRC) will increase by 60% to more than 2.2 million new cases and 1.1 million deaths by 2030 (Arnold et al., 2017). The Aryl-hydrocarbon receptor (AHR) is a ligand-activated transcription factor that upon activation, translocates to the nucleus and associates with ARNT, binds to the cognate dioxin responsive elements (DRE) and transactivates target genes, particularly the phase I and II drug-metabolizing enzymes (Nebert et al., 2004; Kawajiri and Fujii-Kuriyama, 2007). It controls a wide range of developmental and toxicological processes (Stockinger et al., 2014; Liu et al., 2014; Esser and Rannug, 2015). Moreover, AHR gene communicates with several cellular signal transduction cascades to lead cell proliferation, cell cycle arrest, and apoptosis (Marlowe and Puga A, 2005).

Some studies suggest that AHR may act as a tumor suppressor and its induction has been proposed as a potential target for cancer treatment (Fan et al., 2010; Wang et al., 2017; Kolluri et al., 2017). It is reported that lung cancer cell migration is inhibited by AHR overexpression (Tsai et al., 2017) and ligand-activation of the AHR exhibits enhanced antitumor effects in colon cell lines (Megna et al., 2017). The AHR-mRNA expression level is reported to be moderate in normal colon tissue and it has been shown that AHR pathway is active in CRC cell lines (Li et al., 1998; Koliopanos et al., 2002). Although, AHR has a critical role in suppression of intestinal carcinogenesis (Kawajiri et al., 2009), the molecular features of this event is not clarified convincingly. However, it was revealed already that the sustained AHR activation results in G1 phase cell cycle arrest (Levine-Fridman et al., 2014).

AHR activation could be reached through several ways: 1- Toxic ligands (Morrow et al., 2014), 2- Rapidly metabolized or relatively non-toxic ligands (Koliopanos et al., 2002; Ehrlich and Kerkvliet, 2017), 3- Nontoxic ligands (Goettel et al., 2016) and 4- An indirect ligand-independent event (Maayah et al., 2013). However, most ligands of this protein have been disqualified for pharmaceutical development regarding their toxicity potentials (Ehrlich and Kerkvliet, 2017). But, ligand-independent induction of AHR has been reported as

*Corresponding author E-mail: ahcolagar@umz.ac.ir

a useful strategy in cancer cell suppressing (Gluschnaider et al., 2010). Therefore, identifying appropriate molecules, which perform such function, could help in developing more successful cancer suppressing drugs.

Cucurbitacins (Cucs) are diverse plant derived metabolites that have been introduced as candidates for cancer cell inhibition (Lee et al., 2010). Structurally, they are a multiplex category of triterpenes such as cucurbitacin D (CucD), E (CucE) and I (CucI) found in the members of Cucurbitaceae plants and several other families and possess immense pharmacological potential (Kaushik et al., 2015). The STAT3 and F-actin are the two main identified molecular targets of Cucs. They induce G2/M (CucD and CucI) and/or S-phase (CucD) cell cycle arrest and exhibit an effective inhibitory action on many cells, including CRC cell lines (Chen et al., 2012). Cucs are not ligands of AHR and therefore, if they could induce AHR activity indirectly, they would be useful chemicals in the study of cancer cell inhibition via AHR-ligand independent activation. This study aimed to evaluate the effects of CucD, CucE, and CucI on AHR-mRNA expression in human primary colorectal adenocarcinoma cell lines SW-480 and HT-29.

Materials and Methods

Chemicals and cell culture

All solvents and reagents used were purchased from Sigma (USA). The human cancer cell lines HT-29 and SW-480 were provided from Iranian Biological Resources Center's Cell Bank (Tehran, Iran). CucD, CucE, and CucI were obtained from Extrasynthese, Genay, France. HT-29 and SW-480 cells were cultured in the RPMI-1640 mix with sodium bicarbonate, streptomycin/penicillin, l-glutamine and 10% FBS. The cells were incubated at 37 °C in a water-saturated atmosphere of 5% CO_2 and 95% air until confluence. All reagents and medium were prepared just before use.

Cell viability assay and IC50 determining

Mortality of CRC cell lines SW-480 and HT-29 under CucD, CucE and CucI treatment was investigated by the colorimetric MTT assay (Edmondson et al., 1998). Cells were divided into a 96-well plate (15×10^3 cells/well for both cell lines) in the culture medium for 24 h. Next, they were treated with different concentrations of CucD, CucE and CucI (0.25, 1, 3, 5, 8, 12, 16, 30 and 50 µM for HT-29; 3, 7, 12, 18, 24, 28, 36, 40 and 50 µM for SW-480 cell line) in 0.1% (v/v) dimethyl sulfoxide with at least 3 repeats for 24 h. Blank was also measured in the absence of cells. Cells in culture medium and DMSO (0.1%, v/v) in the absence of drugs were considered as controls. Every assay was repeated three times. For the colorimetric MTT assay, 20 µl MTT, a soluble tetrazolium salt solution, (5 mg/ml in PBS), was added to the wells containing 80 µl medium in the absence of drugs. Plates were incubated for 3 h at 37◦C in the dark. Cells were then solubilized by adding 100 µl of 0.04 N DMSO and formazan absorbance was recorded at 550 nm using a Microplate Reader RT2100C spectrophotometer (Rato Life and Analytical Sciences Co., China). Cell growth percentage was calculated as [mean of the test well (3 repeats) − mean of the blank wells] × 100/ [mean of control wells − mean of blank wells]. Plots of viable cells percentage against Cucs concentration series were drawn. The IC50 values (concentration of Cucs that decreases cell viability by 50%) were derived from the data plots using corresponding horizontal and vertical lines.

Assessing of the AHR-mRNA expression

SW-480 and HT-29 cells (5×10^5 cells per well) were seeded into 6-well plates and were grown to 80% confluency. 24 h after treatment with cucurbitacins D, E, and I at IC50 concentrations, cells were harvested and total RNA was extracted from the cells by RNX-Plus solution (Sinaclon Labware & Container, Iran) according to the manufacturer's instructions. The cDNA was synthesized using Easy cDNA Synthesis Kit (Cat. No. A101161, Parstous Biotechnology, Iran) according to the manufacturer's instructions. The real-time PCR experiments were performed at least in duplicate using a 48 well Step One Real-Time PCR System and Real Q Plus Master Mix Green kit (Ampliqon A/S, Denmark) with the following conditions: 95 °C for 15 min, 40 amplification cycles consisting of 95 °C for 15 sec, 60 °C for 30 sec, and 72 °C for 60 sec. Melting curves were then determined with temperature ranging from 60 to 95 °C. GAPDH was chosen as an internal control. SYBR Green reagents were used for all real time PCR reactions. The expression of the genes was analyzed based on the cycle threshold (Ct) and relative expression levels were determined as $2^{-[\Delta\Delta C(t)]}$. The specific primers were used for AHR (F: CCATCCCCATACCCCACTAC, R: TTCTGGCTGGCACTGATACA) and GAPDH (F: GACCCCTTCATTGACCTCAACTAC; R: TCGCTCCTGGAAGATGGTGATGG).

Statistical analysis

In order to make it possible to compare Cucs effect on AHR-mRNA expression, the quantity of

mRNA upregulation under a specific Cuc (folds of expression increasing) divided into the IC50 value of corresponding cucurbitacin and named Index A. Therefore, the index A implies the upregulation amount of AHR-mRNA per each concentration unit of a particular Cuc. Indeed, characteristic drug features are reflected in the gene expression profile (Iskar et al., 2010). One-way ANOVA test and LSD post hoc analysis was used to evaluate IC50 and AHR-mRNA expression data. The statistical significance level was set at $P<0.05$. SPSS version 20.0 was employed for the data analyzing.

Results

Cell viability and IC50

Figure 1A and Figure 2A depict the cell viability vs. gradually increasing concentration of the Cucs in HT-29 and SW-480 cell lines, respectively. The behavior of CucD, CucE, and CucI in two cell lines was different, but in the final stage, CucI showed more toxicity in both of them. The IC50 values of CucD, CucE, and CucI were 4.5, 6.8, and 3.8 µM in HT-29 cells (Figure 1B) and 35, 19, 17.5 µM in SW-480 cell line, respectively (Figure 2B). Comparison of IC50 values of CucE and CucI in SW-480 cells showed no significant difference but other comparisons result in significant differences (Table 1). However, in HT-29 cells the IC50 values of all Cucs were significantly different with each other (Table 1). In controls, which were treated with DMSO (0.1%, v/v) and medium, no significant change in cell viability was detected.

Table 1. Comparison of IC50s and AHR-mRNA expression in the cell lines after treating with Cucs

Cell line	Compared Cucs	P-value of IC50s comparison	P-value of index A* comparison
HT-29	D, E	0.000	0.000
	D, I	0.007	0.226
	E, I	0.000	0.000
SW-480	D, E	0.000	0.085
	D, I	0.000	0.000
	E, I	0.347	0.000

*Index A: Folds of AHR-mRNA expression increasing/IC50 concentration of Cucs.

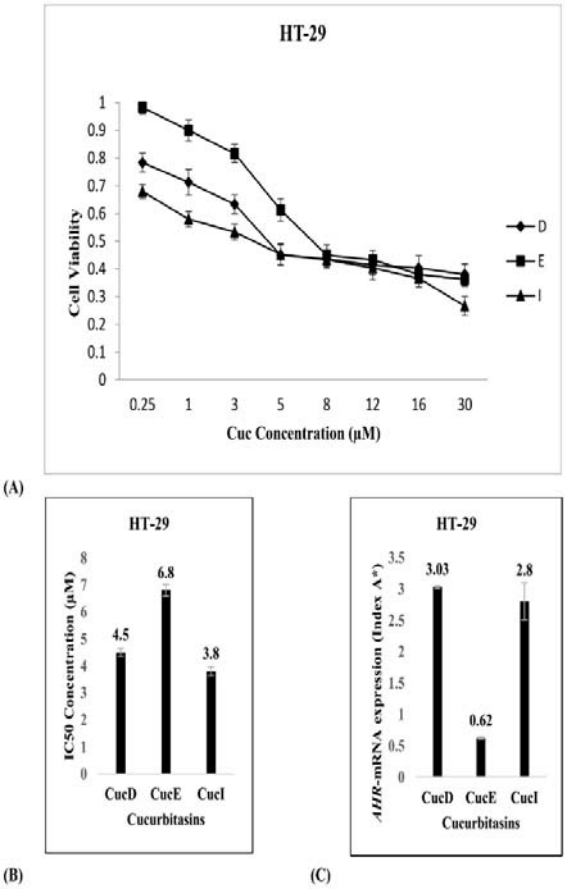

Figure 1. Cell viability, IC50 value and AHR-mRNA expression under CucD, CucE and CucI treatment in HT-29 cells. (A) The lethality of the gradually increasing concentration of CucD, CucE and CucI in HT-29 cell line. Results represented as a percentage of control recovery, which was considered to be 100%. All data were reported as the mean (±S.E.M.) of at least three separate experiments. (B) IC50 concentrations of cucurbitacins in HT-29 cell line. (C) AHR-mRNA expression after treatment with the cucurbitacins in HT-29 cells. *Index A: Folds of AHR-mRNA expression increasing/IC50 concentration of Cucs.

AHR-mRNA expression

Melting curves showed that the primers are efficient for gene expression analysis (Figure 3). AHR-mRNA expression upregulated in HT-29 cells after treatment with CucD, CucE, and CucI 13.63, 4.21 and 10.64 folds, respectively. Moreover, in SW-480 cells AHR-mRNA increased 3.5, 1.14 and 8.05 folds under CucD, CucE and CucI treatments, respectively. In HT-29 cells, index A was not significantly different for CucD, CucI comparison (Table 1). Also, in the SW-480 cell line difference between the index A of CucD and CucE was not statistically significant. All other comparisons of the

index A for Cucs showed a significant difference (Table 1).

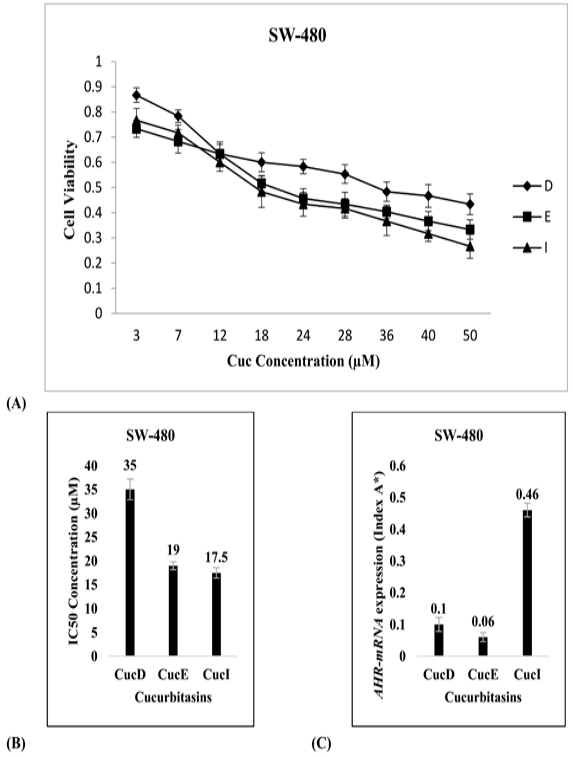

Figure 2. IC50 value and AHR-mRNA expression under CucD, CucE and CucI treatment in SW-480 cell lines. (A) The lethality of the gradually increasing concentration of CucD, CucE, and CucI in SW-480 cell line. Results represented as a percentage of control recovery, which was considered to be 100%. All data were reported as the mean (±S.E.M.) of at least three separate experiments. IC50 concentrations of cucurbitacins in SW-480 cell line. (B) IC50 concentrations of cucurbitacins in SW-480 cells. (C) AHR-mRNA expression after treatment with the cucurbitacins in SW-480 cell line. *Index A: Folds of AHR-mRNA expression increasing/IC50 concentration of Cucs.

Discussion

Colorectal cancer is the third most commonly diagnosed malignancy and the fourth leading cause of cancer-related deaths in the world. Its incidence and mortality rates are rising rapidly in many countries and the number of patients with CRC will continue to increase in future decades. Therefore, improvement of treatment options of CRC is a vital issue (Arnold et al., 2017).

The AHR gene contributes to cell proliferation, cell cycle arrest and apoptosis and therefore has a crucial role in cancer-related molecular pathways (Marlowe and Puga A, 2005; Fan et al., 2010). However, the role of AHR gene in cancer has remained controversial and recent evidence supports both pro- and anti-carcinogenic properties of AHR signaling (Xie and Raufman, 2015). Besides, the induction of tumor suppressor and anti-metastatic function of AHR has been proposed as a potential target for cancer treatment (Kolluri et al., 2017; Tsai et al., 2017; Denison and van den Berg, 2017). Recently, it is reported that AHR activation may induce p21cip1/waf1 and lead to anti-proliferative effects (O'Donnell et al., 2017). Especially, it is also shown recently that AHR may represent a potential putative target for novel anticancer agents for CRC (Megna et al., 2017). AHR pathway role in intestinal cancers has been subject of many molecular studies and its protective role in tumorigenesis has been emphasized (Kawajiri et al., 2009; Díaz-Díaz et al., 2014; Ikuta et al., 2016; Ikuta et al., 2013; Ronnekleiv-Kelly et al., 20126; Oh-oka et al., 2017). Altogether, Ikuta et al. concluded that in normal intestine tissue, AHR is associated with tumor prevention by regulating gut immunity, whereas in tumor cells, it is involved in growth suppression (Hall et al., 2010).

AHR could be activated by toxic ligands, rapidly metabolized or relatively non-toxic ligands, non-toxic ligands, and even ligand independently and then prevent cancer cell growth and migration (Koliopanos et al., 2002; Morrow et al., 2014; Ehrlich and Kerkvliet, 2017; Hall et al., 2010; Safe et al., 2010; Chen et al., 2001). However, given that many AHR agonists are potential oxidative stress inducers (Qiang et al., 2004; Abdelrahim et al., 2006), ligand-independent or nontoxic metabolites-dependent induction of AHR may have a priority for using as AHR inducers (Ehrlich and Kerkvliet, 2017). For instance, Megna et al. (2017) showed that piperidone analogues of curcumin, an AHR ligand, exhibit enhanced antitumor effects in colon cell lines due to the ability of these compounds in AHR activation. In the same way, Gluschnaider et al. indicated a ligand-independent strategy of boosting AHR expression as a means of suppressing prostate cancer (Gluschnaider et al., 2010). Indeed, there are compounds such as Sunitinib (Maayah et al., 2013) Omeprazole and Ketoconazole (Novotna et al., 2014; Jin et al., 2014), which facilitate AHR activity and induce AHR-dependent pathways, but they are not AHR ligands or represent a weak affinity (Platten et al., 2015).

Cucurbitacins are plant-derived highly oxygenated triterpenes that exhibit anti-cancer activity. Indeed, many plants, which have been used in folk medicine to treat cancer, contain these

metabolites (Lee et al., 2010; Alghasham, 2013; Platten et al., 2015; Jafargholizadeh et al., 2018). Among different Cucs, it is shown previously that CucD, CucE and CucI exhibit a potent inhibitory

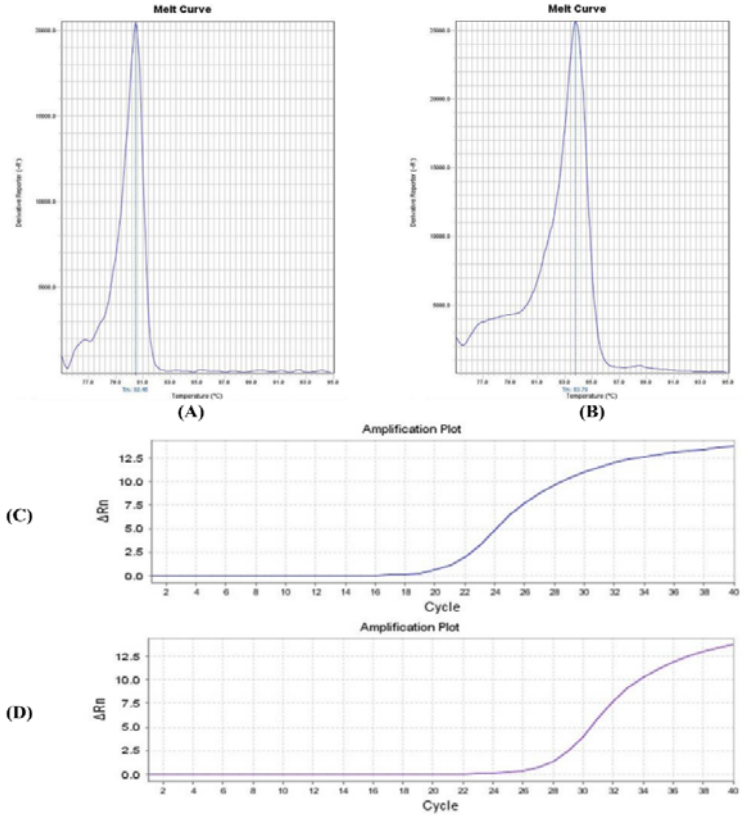

Figure 3. Melting Curves of GAPDH (A) and AHR (B). Amplication plots of GAPDH (C) and AHR (D).

effect on the CRC cells (Jayaprakasam et al., 2003). For instance, Hsu et al. (2014) showed that CRC primary cells accumulated in metaphase due to G2/M arrest after treating with 2.5-7.5 µM of CucE. Feng et al (2014) found that it inhibits SW-480 cells proliferation and modulates the expression of cell cycle regulators through Wnt/β-catenin signaling activation and upregulation of a tumor suppressor. Further, Kim et al. (2014) reported that up to 500 nM CucI reduces SW-480 cells proliferation by enhancing apoptosis and cell cycle arrest at the G2/M phase with a decreased expression of cell cycle proteins and increased caspases activities. Also, Song et al. (2015) demonstrated that CucI decreases the viability of COLO205 cell line significantly (IC50=200 nM/24h) and suppresses cell migration and invasion and decreases expression of p-STAT3 and MMP-9.

In the current study, the comparison of IC50 value between CucD and CucE; CucD and CucI; and CucE and CucI in HT-29 cells showed that there are significant differences between them (Table1). However, AHR-mRNA expression per concentration unit (Index A) of CucD in comparison with CucE showed no significant difference in HT-29 cells (Table1). Also, in SW-480 cell line CucE and CucI showed no significant difference in IC50 value, however, the AHR expression per concentration unit of CucE and CucI in this cell line was significantly different (Table1). Indeed, in SW-480 cells CucI causes to 7.67 folds more AHR-mRNA expression in comparison with CucE (Figure 2C). Regarding that alongside common effects, there are some different induced pathways by these two cucurbitacins (Chen et al., 2012), the difference of AHR-mRNA induction sounds reasonable.

The SW-480 cells were more resistant against Cucs in comparison with HT-29 cells. Indeed, in comparison with HT-29 cells, respectively 7.78, 2.8 and 4.6 folds more of CucD, CucE and CucI were needed to kill 50 percent of SW-480 cells. Also, all three Cucs lead to more AHR-mRNA expression in HT-29 cells. In other words, each concentration unit of CucD, CucE and CucI results in 33, 10.3 and 6.09 folds more AHR-mRNA expression in HT-29 cells in comparison with SW-480 cells.

In the HT-29 cells, the order of Cucs from the highest cytotoxicity to the lowest was: CucI>CucD>CucE (Figure 1B). However, the

cytotoxicity order of metabolites in SW-480 cell line was CucI>CucE>CucD without significant difference between CucI and CucE (Figure 2B, Table 1). In a similar manner, it is previously reported that compared to CucD, CucI and CucE represent a higher toxicity in SW-1353 cell line (Abbas et al., 2013). Index A comparison revealed that in HT-29 cells the order of metabolites in affecting AHR-mRNA expression from the highest to the lowest could be shown as CucD>CucI>CucE (Figure 1C) and there was no significant difference between CucD and CucI (Table 1). In SW-480 cells the order of metabolites regarding their effect on AHR-mRNA expression was: CucI>CucD>CucE, without significant difference between CucD and CucE (Figure 2C).

The CucE in HT-29 cells had the lowest cytotoxicity and lowest effect on AHR-mRNA expression (Figures 1B and C). CucI showed higher cytotoxicity and higher effect on AHR-mRNA expression in SW-480 cell line (Figures 2B and C). However, regarding that there is no significant difference between CucD and CucI in AHR-mRNA expression in HT-29 cells, it could be inferred that among studied three cucurbitacins the CucI is a common metabolite for both HT-29 and SW-480 cell lines that has the lowest IC50 value (the highest toxicity) and the highest effect on AHR-mRNA expression.

According to recent reports, it seems that Cucs effect and AHR pathway have overlapping features in cancerous cells. The IDO-AHR-IL6-STAT3 signaling loop maintains indoleamine-2,3-dioxygenase (IDO) expression in human cancers (Litzenburger et al., 2014). Induction of IDO and IDO-mediated tryptophan catabolism has been introduced as an important immunoregulatory mechanism, which depends on AHR expression (Nguyen et al., 2014). Initial studies showed that the CucI is a selective inhibitor of JAK/STAT3 activation and reduces the levels of activated STAT3 in human cancer cell lines (Blaskovich et al., 2003). Then, it could be hypothesized that after incubating cells with CucI and disruption of IDO-AHR-IL6-STAT3 signaling loop via STAT3 inhibiting, AHR expression may upregulate to compensate the reduction of the loop outcome, however, excessive amounts of AHR protein results in increased expression of DRE-containing genes and lead to growth inhibition and apoptosis (Nebert et al., 2000). Also, a recent study revealed that CucE modulates AHR signaling in $CD4^+$ T cells and stimulates Cyp1A expression, which is hallmark of AHR activation (Jevtić et al., 2016). Furthermore, the activation of AHR results in cyclin D inhibiting and promotes S-phase arrest (Marlowe and Puga A, 2005) in a same way as CucD performs (Chan et al., 2010).

In conclusion, our findings revealed that the cucurbitacin D, E and I show different lethal concentrations in colorectal cancer cell lines HT-29 and SW-480. Also, there was a different level of AHR-mRNA expression under treatment with these metabolites. In comparison with SW-480 cells, the HT-29 cells were more vulnerable against the cucurbitacins and this cell line represented more AHR-mRNA expression too. Cucurbitacin I was common metabolite that resulted in the highest toxicity and the highest AHR-mRNA expression in HT-29 and SW-480 cells. Therefore, it may potentially be useful as an indirect activator of AHR pathway in colorectal cancer cells.

Acknowledgements

This study was supported by a grant from the University of Mazandaran, dedicated to the PhD thesis of Younes Aftabi.

Conflict of Interest

The author(s) declared no potential conflicts of interest with respect to the research, authorship, and/or publication of this article.

References

1. Abbas S., Vincourt J. B., Habib L., Netter P., Greige-Gerges H. and Magdalou J. (2013) The cucurbitacins E, D and I: investigation of their cytotoxicity toward human chondrosarcoma SW 1353 cell line and their biotransformation in man liver. Toxicology letters 216:189-199.
2. Abdelrahim M., Ariazi E., Kim K., Khan S., Barhoumi R., Burghardt R., Liu S., Hill D., Finnell R., Wlodarczyk B. and Jordan, V. C. (2006) 3-Methylcholanthrene and other aryl hydrocarbon receptor agonists directly activate estrogen receptor α. Cancer research 66:2459-2467.
3. Alghasham A. A. (2013) Cucurbitacins–a promising target for cancer therapy. International journal of health sciences 7:77.
4. Arnold M., Sierra M. S., Laversanne M., Soerjomataram I., Jemal A. and Bray F. (2017) Global patterns and trends in colorectal cancer incidence and mortality. Gut 66:683-691.
5. Blaskovich M. A., Sun J., Cantor A., Turkson J., Jove R. and Sebti S. M. (2003) Discovery of JSI-124 (cucurbitacin I), a selective Janus kinase/signal transducer and activator of

transcription 3 signaling pathway inhibitor with potent antitumor activity against human and murine cancer cells in mice. Cancer research 63:1270-1279.
6. Chan K. T., Meng F. Y., Li Q., Ho C. Y., Lam T. S., To Y., Lee W. H., Li M., Chu K. H. and Toh M. (2010) Cucurbitacin B induces apoptosis and S phase cell cycle arrest in BEL-7402 human hepatocellular carcinoma cells and is effective via oral administration. Cancer letters 294:118-124.
7. Chen I., Hsieh T., Thomas T. and Safe, S. (2001) Identification of estrogen-induced genes downregulated by AhR agonists in MCF-7 breast cancer cells using suppression subtractive hybridization. Gene 262:207-214.
8. Chen X., Bao J., Guo J., Ding Q., Lu J., Huang M. and Wang Y. (2012) Biological activities and potential molecular targets of cucurbitacins: a focus on cancer. Anti-cancer drugs 23:777-787.
9. Denison M. S. and van den Berg M. (2017) Editorial overview: The aryl hydrocarbon (Ah) receptor: From toxicology to human health. Current opinion in toxicology 2:i-iv.
10. Díaz-Díaz C. J., Ronnekleiv-Kelly S. M., Nukaya M., Geiger P. G., Balbo S., Dator R., Megna B. W., Carney P. R., Bradfield C. A. and Kennedy G.D. (2016) The Aryl Hydrocarbon Receptor is a Repressor of Inflammation-associated Colorectal Tumorigenesis in Mouse. Annals of surgery 264:429-436.
11. Edmondson J. M., Armstrong L. S. and Martinez A. O. (1988) A rapid and simple MTT-based spectrophotometric assay for determining drug sensitivity in monolayer cultures. Journal of tissue culture methods 11:15-17.
12. Ehrlich A. K. and Kerkvliet N. I. (2017) Is chronic AhR activation by rapidly metabolized ligands safe for the treatment of immune-mediated diseases?. Current opinion in toxicology 2:72-78.
13. Esser C. and Rannug A. (2015) The aryl hydrocarbon receptor in barrier organ physiology, immunology, and toxicology. Pharmacological reviews 67:259-279.
14. Fan Y., Boivin G. P., Knudsen E. S., Nebert D. W., Xia Y. and Puga A. (2010) The aryl hydrocarbon receptor functions as a tumor suppressor of liver carcinogenesis. Cancer research 70:212-220.
15. Feng H., Zang L., Zhao Z. X. and Kan Q. C. (2014) Cucurbitacin-E inhibits multiple cancer cells proliferation through attenuation of Wnt/β-catenin signaling. Cancer biotherapy and radiopharmaceuticals 29:210-214.
16. Gluschnaider U., Hidas G., Cojocaru G., Yutkin V., Ben-Neriah Y. and Pikarsky E. (2010) β-TrCP inhibition reduces prostate cancer cell growth via upregulation of the aryl hydrocarbon receptor. PloS one 5:e9060.
17. Goettel J. A., Gandhi R., Kenison J. E., Yeste A., Murugaiyan G., Sambanthamoorthy S., Griffith A. E., Patel B., Shouval D. S., Weiner H. L. and Snapper S.B. (2016) AHR activation is protective against colitis driven by T cells in humanized mice. Cell reports 17:1318-1329.
18. Hall J. M., Barhoover M. A., Kazmin D., McDonnell D. P., Greenlee W. F. and Thomas, R. S. (2010) Activation of the aryl-hydrocarbon receptor inhibits invasive and metastatic features of human breast cancer cells and promotes breast cancer cell differentiation. Molecular endocrinology 24:359-369.
19. Hsu Y. C., Huang T. Y. and Chen M. J. (2014) Therapeutic ROS targeting of GADD45γ in the induction of G2/M arrest in primary human colorectal cancer cell lines by cucurbitacin E. Cell death & disease 5:e1198.
20. Ikuta T., Kobayashi Y., Kitazawa M., Shiizaki K., Itano N., Noda T., Pettersson S., Poellinger L., Fujii-Kuriyama Y., Taniguchi S.I. and Kawajiri K. (2013) ASC-associated inflammation promotes cecal tumorigenesis in aryl hydrocarbon receptor-deficient mice. Carcinogenesis 34:1620-1627.
21. Ikuta T., Kurosumi M., Yatsuoka T. and Nishimura Y. (2016) Tissue distribution of aryl hydrocarbon receptor in the intestine: Implication of putative roles in tumor suppression. Experimental cell research 343:126-134.
22. Iskar M., Campillos M., Kuhn M., Jensen L. J., Van Noort V. and Bork, P. (2010) Drug-induced regulation of target expression. PLoS computational biology 6:e1000925.
23. Jafargholizadeh N., Zargar S. J. and Aftabi Y. (2018) The cucurbitacins D, E, and I from Ecballium elaterium (L.) upregulate the LC3 gene and induce cell-cycle arrest in human gastric cancer cell line AGS. Iranian journal of basic medical sciences 21:253.
24. Jayaprakasam B., Seeram N. P. and Nair M. G. (2003) Anticancer and antiinflammatory activities of cucurbitacins from Cucurbitaandreana. Cancer letters 189:11-16.
25. Jevtić B., Djedović N., Stanisavljević S., Despotović J., Miljković D. and Timotijević G. (2016) Cucurbitacin E potently modulates the activity of encephalitogenic cells. Journal of agricultural and food chemistry 64:4900-4907.
26. Jin U. H., Lee S. O., Pfent C. and Safe S. (2014) The aryl hydrocarbon receptor ligand omeprazole inhibits breast cancer cell invasion and metastasis. BMC cancer 14:498.
27. Kaushik U., Aeri V. and Mir S. R. (2015) Cucurbitacins–an insight into medicinal leads from nature. Pharmacognosy reviews 9:12.
28. Kawajiri K. and Fujii-Kuriyama Y. (2007) Cytochrome P450 gene regulation and physiological functions mediated by the aryl

hydrocarbon receptor. Archives of biochemistry and biophysics 464:207-212.
29. Kawajiri K., Kobayashi Y., Ohtake F., Ikuta T., Matsushima Y., Mimura J., Pettersson S., Pollenz R. S., Sakaki T., Hirokawa T. and Akiyama T. (2009) Aryl hydrocarbon receptor suppresses intestinal carcinogenesis in ApcMin/+ mice with natural ligands. Proceedings of the national academy of sciences 106:13481-13486.
30. Kim H. J., Park J. H. Y. and Kim J. K. (2014) Cucurbitacin-I, a natural cell-permeable triterpenoid isolated from Cucurbitaceae, exerts potent anticancer effect in colon cancer. Chemico-biological interactions 219:1-8.
31. Koliopanos A., Kleeff J., Xiao Y., Safe S., Zimmermann A., Büchler M. W. and Friess H. (2002) Increased arylhydrocarbon receptor expression offers a potential therapeutic target for pancreatic cancer. Oncogene 21:6059.
32. Kolluri S. K., Jin U. H. and Safe S. (2017) Role of the aryl hydrocarbon receptor in carcinogenesis and potential as an anti-cancer drug target. Archives of toxicology 91:2497-2513.
33. Lee D. H., Iwanski G. B. and Thoennissen N. H. (2010) Cucurbitacin: ancient compound shedding new light on cancer treatment. The scientific world journal 10:413-418.
34. Levine-Fridman A., Chen L. and Elferink C. J. (2004) Cytochrome P4501A1 promotes G1 phase cell cycle progression by controlling aryl hydrocarbon receptor activity. Molecular pharmacology 65:461-469.
35. Li W., Harper P. A., Tang B. K. and Okey A. B. (1998) Regulation of cytochrome P450 enzymes by aryl hydrocarbon receptor in human cells: CYP1A2 expression in the LS180 colon carcinoma cell line after treatment with 2, 3, 7, 8-tetrachlorodibenzo-p-dioxin or 3-methylcholanthrene. Biochemical pharmacology 56:599-612.
36. Litzenburger U. M., Opitz C. A., Sahm F., Rauschenbach K. J., Trump S., Winter M., Ott M., Ochs K., Lutz C., Liu X. and Anastasov N. (2014) Constitutive IDO expression in human cancer is sustained by an autocrine signaling loop involving IL-6, STAT3 and the AHR. Oncotarget 5:1038.
37. Liu H., Ramachandran I. and Gabrilovich D. I. (2014) Regulation of plasmacytoid dendritic cell development in mice by aryl hydrocarbon receptor. Immunology and cell biology 92:200-203.
38. Maayah Z. H., El-Gendy M. A., El-Kadi A. O. and Korashy H. M. (2013) Sunitinib, a tyrosine kinase inhibitor, induces cytochrome P450 1A1 gene in human breast cancer MCF7 cells through ligand-independent aryl hydrocarbon receptor activation. Archives of toxicology 87:847-856.
39. Marlowe J. L. and Puga A. (2005) Aryl hydrocarbon receptor, cell cycle regulation, toxicity, and tumorigenesis. Journal of cellular biochemistry 96:1174-1184.
40. Megna B. W., Carney P. R., Depke M. G., Nukaya M., McNally J., Larsen L., Rosengren R. J. and Kennedy G.D. (2017) The aryl hydrocarbon receptor as an antitumor target of synthetic curcuminoids in colorectal cancer. Journal of surgical research 213:16-24.
41. Morrow D., Qin C., Smith III, R. and Safe, S. (2004) Aryl hydrocarbon receptor-mediated inhibition of LNCaP prostate cancer cell growth and hormone-induced transactivation. The Journal of steroid biochemistry and molecular biology 88:27-36.
42. Nebert D. W., Dalton T. P., Okey A. B. and Gonzalez F. J. (2004) Role of aryl hydrocarbon receptor-mediated induction of the CYP1 enzymes in environmental toxicity and cancer. Journal of biological chemistry 279:23847-23850.
43. Nebert D. W., Roe A. L., Dieter M. Z., Solis W. A., Yang Y. I. and Dalton T. P. (2000) Role of the aromatic hydrocarbon receptor and [Ah] gene battery in the oxidative stress response, cell cycle control, and apoptosis. Biochemical pharmacology 59:65-85.
44. Nguyen N. T., Nakahama T., Le D. H., Van Son L., Chu H. H. and Kishimoto T. (2014) Aryl hydrocarbon receptor and kynurenine: recent advances in autoimmune disease research. Frontiers in immunology 5:551.
45. Novotna A., Korhonova M., Bartonkova I., Soshilov A. A., Denison M. S., Bogdanova K., Kolar M., Bednar P. and Dvorak Z. (2014) Enantiospecific effects of ketoconazole on aryl hydrocarbon receptor. Plos one 9: e101832.
46. O'Donnell E. F., Jang H. S., Pearce M., Kerkvliet N. I. and Kolluri S. K. (2017) The aryl hydrocarbon receptor is required for induction of p21cip1/waf1 expression and growth inhibition by SU5416 in hepatoma cells. Oncotarget 8:25211.
47. Oh-oka K., Kojima Y., Uchida K., Yoda K., Ishimaru K., Nakajima S., Hemmi J., Kano H., Fujii-Kuriyama Y., Katoh R. and Ito, H. (2017) Induction of colonic regulatory T cells by mesalamine by activating the aryl hydrocarbon receptor. Cellular and molecular gastroenterology and hepatology 4:135-151.
48. Platten M., von Knebel Doeberitz N., Oezen I., Wick W. and Ochs, K. (2015) Cancer immunotherapy by targeting IDO1/TDO and their downstream effectors. Frontiers in immunology 5:673.
49. Qiang M. A., Kinneer K., Yongyi B. I. and KAN, Y. W. (2004) Induction of murine NAD (P) H: quinone oxidoreductase by 2, 3, 7, 8-tetrachlorodibenzo-p-dioxin requires the CNC (cap n collar) basic leucine zipper transcription

factor Nrf2 (nuclear factor erythroid 2-related factor 2): cross-interaction between AhR (aryl hydrocarbon receptor) and Nrf2 signal transduction. Biochemical journal 377:205-213.
50. Ronnekleiv-Kelly S. M., Nukaya M., Díaz-Díaz C. J., Megna B. W., Carney P. R., Geiger P. G. and Kennedy G. D. (2016) Aryl hydrocarbon receptor-dependent apoptotic cell death induced by the flavonoid chrysin in human colorectal cancer cells. Cancer letters 370:91-99.
51. Safe S., Wormke M. and Samudio, I. (2000) Mechanisms of inhibitory aryl hydrocarbon receptor-estrogen receptor crosstalk in human breast cancer cells. Journal of mammary gland biology and neoplasia 5:295-306.
52. Song J., Liu H., Li Z., Yang C. and Wang C. (2015) Cucurbitacin I inhibits cell migration and invasion and enhances chemosensitivity in colon cancer. Oncology reports 33:1867-1871.
53. Stockinger B., Meglio P. D., Gialitakis M. and Duarte J. H. (2014) The aryl hydrocarbon receptor: multitasking in the immune system. Annual review of immunology 32:403-432.
54. Tsai C. H., Li C. H., Cheng Y. W., Lee C. C., Liao P. L., Lin C. H., Huang S. H. and Kang J.J. (2017) The inhibition of lung cancer cell migration by AhR-regulated autophagy. Scientific reports 7:41927.
55. Wang Z., Monti S. and Sherr D. H. (2017) The diverse and important contributions of the AHR to cancer and cancer immunity. Current opinion in toxicology 2:93-102.
56. Xie G. and Raufman J. P. (2015) Role of the aryl hydrocarbon receptor in colon neoplasia. Cancers 7:1436-1446.

Journal of Cell and Molecular Research (2019) 10 (2), 76-89 DOI: 10.22067/jcmr.v10i2.76133

Research Article

Population Genetic Analysis of *Zucchini yellow mosaic virus* based on the CI Gene Sequence

Zohreh Moradi[1], Mohsen Mehrvar[1], Ehsan Nazifi[2*]

[1] *Department of Plant Pathology, Faculty of Agriculture, Ferdowsi University of Mashhad, Mashhad, Iran*
[2] *Department of Biology, Faculty of Basic Sciences, University of Mazandaran, Babolsar, Iran*

Received 22 October 2018 Accepted 27 January 2019

Abstract

Zucchini yellow mosaic virus (ZYMV) is one of the most economically important viruses infecting cucurbits worldwide. Population genetic analysis of ZYMV was conducted based on the virus cylindrical inclusion (CI) gene sequences of 10 isolates identified in this study and 94 other isolates from different countries in six continents: Asia, Europe, Oceania, Africa, North and South America. The overall mean value of nucleotide sequence diversity among all isolates was 0.074±0.006. Phylogenetic analysis showed that ZYMV isolates fell into three main phylogroups with significant F_{ST} values (>0.55) and almost tended to cluster according to their geographical position. Group I was predominant and contained isolates originated from different parts of the world. Iranian isolates clustered into group I, sharing 87.7-99.7% and 92.5–100% nucleotide and amino acid identity, with other isolates of this group. Group II was a new group that included only Singapore isolates. Group III including East Timor, Reunion Island and Australia-Kununurra isolates which were genetically differentiated from other populations. ZYMV populations from different geographic origins were composed of multiple lineages. With exception of the Oceanian population which was strongly differentiated from the American population, most other geographical populations showed low to moderate genetic differentiation. There was moderate to high level of gene flow despite large separating geographic distances. Analysis of the synonymous-to-nonsynonymous ratio showed strong purifying selection in the CI gene. The analyses indicated that in addition to selection, random processes such as genetic drift and founder effects are important determinants for the genetic structure of populations of ZYMV.

***Keywords*:** Cylindrical inclusion, Evolutionary forces, Genetic variability, *Zucchini yellow mosaic virus*

Introduction

Zucchini yellow mosaic virus (ZYMV; genus *Potyvirus,* family *Potyviridae*) is a damaging plant pathogen that infects a wide range of cucurbit crops worldwide (Desbiez and Lecoq, 1997; Lisa and Lecoq, 1984), with major economic impact and significant yield losses. The virus was first isolated in Italy in 1973, described in 1981 by Lisa et al. (1981), subsequently in France by Lecoq et al. (1981). As other potyviruses, ZYMV has flexuous filamentous particles of 680–730 nm long, which encapsidate a single-stranded, positive-sense RNA of approximately 10 kb. The viral genome, which has a poly (A) tail at its 3′end and a VPg structure at its 5′ end, consists of a unique large open reading frame (ORF) which encodes a single large polyprotein that is self-hydrolyzed after translation into 10 putative functional proteins (from N- to C-termini): P1 protein, helper component proteinase (HC-Pro), P3 protein, 6K1, cylindrical inclusion protein (CI), 6K2, nuclear inclusion protein a (NIa) (VPg+Pro), nuclear inclusion protein b (NIb) and coat protein (CP) (Adams et al., 2005a; Urcuqui-Inchima et al., 2001; Riechmann et al., 1992; Adams et al., 2012). In addition, a pretty interesting *Potyviridae* ORF, which is embedded in the P3-coding region, encodes a small putative protein PIPO (Chung et al., 2008). ZYMV, which is aphid-transmitted in a non-persistent manner (Lecoq et al., 1991; Desbiez et al., 1996; Gal-On, 2007), can infect wild and agronomically important cucurbit plants, some non-cucurbitaceous weeds, and some ornamental plants (Al-Musa, 1989; Desbiez and Lecoq, 1997; Coutts and Jones, 2005; Chen and Hong, 2008; Choi et al., 2002). Seed transmission, although at very low rates, has been reported in some cases (Desbiez and Lecoq, 1997; Tobias and Palkovics, 2003; Schrijnwerkers et al., 1991; Coutts et al., 2011; Simmons et al., 2011, 2013), which could explain ZYMV worldwide distribution (Desbiez et al., 2002). Several studies have been published in recent years on ZYMV biological and molecular variability in the world (Coutts et al., 2011; Desbiez et al., 1996, 2002; Glasa et al., 2007;

*Corresponding author E-mail: E.Nazifi@umz.ac.ir

Maina et al., 2017; Novakova et al., 2014; Yakoubi et al., 2008) as well as in Iran (Bananej et al., 2008; Masumi et al., 2011). Most of the molecular studies were based on analysis of CP and or partial NIb-CP sequences. Based on these phylogenetic analyses, ZYMV isolates have been classified into two or three major phylogroups (Desbiez et al., 2002; Zhao et al., 2003; Simmons et al., 2008; Ha et al., 2008a; Bananej et al., 2008; Yakoubi et al., 2008; Masumi et al., 2011; Coutts et al., 2011; Maina et al., 2017). On the other hand, in the absence of complete genomic sequence, cylindrical inclusion (CI)-coding region is the most suitable part for diagnostic and taxonomy purposes, rather than the CP (Ha et al., 2008b; Adams et al., 2005b, Lee et al., 1997). Molecular evolutionary studies of viruses focused on understanding effects of variation caused by mutation, recombination, selection pressure, and host or geography driven adaptation in viral populations (Moury et al., 2002; Gibbs and Ohshima, 2010). So, studying the molecular evolutionary history of plant viruses and understanding their genetic variation and the causative factors producing variation in viral populations is important for developing sustainable management strategies. Despite worldwide distribution of this virus, molecular evolution and population genetic structure are poorly understood and further investigation is required. This study was aimed to investigate population genetic structure and genetic diversity of ZYMV to identify the sources of genetic variation operating in the ZYMV population. It is based on analysis of the CI genomic region, which is a region that, to date, has not been analyzed in other studies. According to the Adams et al. (2005b) comparisons of the CI gene most accurately reflected those for the complete ORF, and this region would be the best for diagnostic and taxonomic studies if only a sub-portion of the genome were sequenced and was therefore selected for this study. Here, the CI nucleotide sequences of ten ZYMV isolates were obtained and analyzed together with those retrieved from the GenBank.

Materials and Methods

Virus sources, RT-PCR, cloning and sequencing

During the growing season of 2013, cucurbit and tomato plants with symptoms of ZYMV infection (including systemic mosaic, yellowing, vein clearing and banding, stunting, blistering, shoestring and leaf and fruit deformations) were collected from northern (Mazandaran, Golestan) and eastern (Razavi Khorasan) areas of Iran (Table 1). Total RNA was isolated and used as a template for reverse transcription (RT). One pair of degenerate primer including CI For/CI Rev corresponding to CI coding region in the potyvirus genome (Ha et al., 2008b) was used in the RT-PCR reactions. The first strand cDNA was synthesized using antisense primer and the Moloney murine leukemia virus (MMuLV) reverse transcriptase (Thermo Scientific, USA) according to the manufacturer's instructions. PCR was carried out using Taq PCR Master Mix (Ampliqon, Denmark) according to the manufacturer's instructions. PCR was performed under the following conditions: 94 °C for 3 min; followed by 35 cycles of 94°C for 30 s, 52°C for 30 s, and 72 °C for 90 s and ended with a final extension at 72 °C for 10 min. The expected PCR products (of ~700 base pairs) were purified and ligated into pTZ57R/T vector (Thermo Scientific, USA), according to the manufacturer's instructions. The ligation mix was transformed into *Escherichia coli* strain *DH5α*. Plasmid DNA from recombinant clones was purified using a Plasmid Miniprep Kit (Qiagen, Germany), and a purified clone from each isolate was subjected to sequencing in both directions (Macrogen Inc., South Korea). Sequence data were assembled using the Contig Express program in the Vector NTI 11 software (Invitrogen, USA).

Sequences, phylogenetic and recombination analysis

High nucleotide sequence similarity to ZYMV was indicated using BLAST N analysis. Analyses were conducted using 104 CI nucleotide sequences, including 10 nucleotide sequences obtained in this work and 94 retrieved from GenBank (Table 2). Out of ZYMV CI sequences retrieved from GenBank, three were from Iran and the others were from other countries in the world. The CI nucleotide sequences were translated to amino acids using ExPASy translate tool (http://web.expasy.org/translate/). Alignments were performed with Clustal W implemented in BioEdit v.7.2.5 (Hall, 1999). The pairwise nucleotide (nt) and amino acid (aa) sequence identity scores were displayed as color-coded cells using SDT v.1.2 software (Muhire et al., 2014). Phylogenetic trees were generated by the maximum-likelihood (ML) and neighbor-joining (NJ) methods implemented in MEGA7 (Kumar et al., 2016), with 1000 bootstrap replicates. Genetic distance between and within phylogenetic groups of ZYMV CI gene was calculated using MEGA7 with 1000 bootstrap replicates. Recombination analysis was performed on the aligned nucleotide sequences using RDP4 package (Martin et al., 2015). The occurrence of

Table 1. Characteristics of samples which identified as ZYMV after analyzing with BLAST and their origin, host, symptom and accession numbers

Isolates	Province (region)	Host plant	Symptom	Accession number
Gj1	Razavi Khorasan (Jovein)	*Solanum lycopersicum*	YM/MO	KJ135782
Kj	Mazandaran (Juybar)	*Cucurbita moschata*	M/B/Y	KJ135786
KHB2	Mazandaran (Babolsar)	*Cucurbita moschata*	M/MO/VB	KJ135785
KB	Mazandaran (Babolsar)	*Cucurbita moschata*	VC/M	KJ135784
KB2	Mazandaran (Babolsar)	*Cucurbita pepo*	VC/YSP	MF766014
Gj2	Razavi Khorasan (Jovein)	*Solanum lycopersicum*	MO/B/YM	MF766013
KS1	Mazandaran (Sari)	*Cucurbita pepo*	GB/D/M	MF766018
KF1	Mazandaran (Nowshahr)	*Cucurbita pepo*	M/B/D	MF766015
KG1	Golestan (Gorgan)	*Cucurbita pepo*	M/GB/D	MF766016
KG2	Golestan (Gorgan)	*Cucurbita pepo*	GB/D/S	MF766017

Abbreviations: VC; Vein clearing, VB; Vein banding, M; Mosaic, B; Blistering, GB; Green blistering, MO; Mottling; YSP; Yellow spots, YM; Yellow mosaic, Y; Yellowing, D; Deformation, S; Shoestring.

recombination events was assessed by at least four programs using default parameters, and a *P* value threshold of 0.05.

Population genetic analysis

Population genetic parameters of CI gene sequences obtained in this study and those from GenBank were estimated using DnaSP v. 6.10.04 software (Rozas et al., 2017) based on phylogenetic groups and geographic origins. Nucleotide sequences alignment of the CI gene were assessed to estimate number of haplotypes (H), haplotype diversity (Hd), number of polymorphic sites (S), total number of mutations (η), average pairwise nucleotide diversity (π) using the Jukes and Cantor correction (Jukes and Cantor, 1969), average number of nucleotide differences between sequences from the same population (K), and the ratio of non-synonymous to synonymous nucleotide diversity (dN/dS), also known as ω. In general, ω = 1, < 1 and > 1 indicates neutral evolution, negative (purifying) selection and positive (diversifying) selection, respectively. The nucleotide diversity measures the average pairwise variation among sequences with values ranging from 0 (no variation) to 0.1 (extreme variation). The haplotype diversity indicates the frequency of haplotypes in a sample with values ranging from 0 to 1.000 (Tsompana et al., 2005).

Population genetic differentiation

Genetic differentiation between populations was examined using several statistics: *Ks**, *Z*, *Z**, *Kst** and *Snn* based on permutation statistical tests with 1000 replicates. *Ks** and *Z* are the sequence-based statistics considered by Hudson (2000). Under the null hypothesis (no genetic differentiation), *Kst** is expected to be near zero, but if *Ks**, *Kst** test statistics is supported by small *P* value (<0.05), the null hypothesis is rejected (Hudson et al., 1992a). The *Z* statistic is calculated from ranking distances between all pairs of sequences. *Z** statistic is a logarithmic variant of *Z* statistic and if it is too small and supported by significant *P* value (<0.05) the null hypothesis of no genetic differentiation is rejected (Hudson et al., 1992b). The frequency of the nearest neighbor sequences in the same locality is measured by the *Snn* test statistic, whose values may range from 1 (when populations from different localities are genetically distinct) to 1/2 in the case of panmixia (Hudson, 2000). The degree of genetic differentiation or the level of gene flow between ZYMV populations was calculated by estimating the absolute value of the standardized variance in allele frequencies across populations (*Fst*) (Wright, 1951). The *Fst* values ranges from 0 (indicating no differentiation between the populations) to 1 (when the populations are clearly differentiated) (Rozas et al., 2003). These analyses were performed using DnaSP6 (Rozas et al., 2017).

Results

CI nucleotide sequences

PCR amplification of partial CI region yielded fragments of about 700 bp. Sequences of the CI gene from ten Iranian ZYMV isolates were successfully generated, submitted to the GenBank,

Table 2. GenBank accession number and origin of some of the previously reported ZYMV used for phylogenetic comparison of the nucleotides sequence of the CI coding region

Populations	Geography		Country	Number	Isolates/strains (host of origin)	Accession numbers
I	Asia		Iran	13	Fars (Cpe), IKA/strain A (Sq), SANRU (Cpe)	JN183062, KU528623, KU198853
			India	1	AP Gherkin (Can)	KT778297
			Turkey	35	YUN8-4 (Cpe), Y4 (Cpe), Y23 (Cpe), S3 (Cme), KZ1 (Cpe), KAR15-1 (Cmo), KAR12-4 (Cpe), K3 (Cpe), K17 (Cpe), H1M (Cs), G3 (Cpe), G2 (Cpe), G1 (Cpe), ER6-8 (Cpe), E-7 (Cme), AYS7 (Cpe), D14 (Cs), C5 (Cmo), C17 (Cme), C13 (Cmo), C11(Cmo), BRD4 (Cmo), BRD2 (Cmo), BE7 (Cmo), BE6 (Cpe), BE26 (Cpe), BE15 (Cpe), BE10 (Cpe), AS5 (Cpe), AS1 (Cpe), AS11 (Cpe), AKS6-2 (Cpe), AKS5-7 (Cpe), AKS2-5 (Cmo), KZN1 (Cpe)	KP828427, KP828426, KP828425, KP828424, KP828423, KP828422, KP828421, KP828420, KP828419, KP828418, KP828417, KP828416, KP828415, KP828414, KP828413, KP828412, KP828411, KP828410, KP828409, KP828408, KP828407, KP828406, KP828405, KP828403, KP828402, KP828400, KP828397, KP828395, KP828394, KP828393, KP828392, KP828391, KP828390, KP828389, KP828388
			Israel	3	AG (-), NAT (-), B* (France-Israel) (-)	EF062583, EF062582, AY188994
			South Korea	5	RDA (Cpe), KR-PS (Cmo),KR-PE (Cmo), KR-PA (Cmo), A (Ar)	AB369279, AY279000, AY278999, AY278998, AJ429071
			Japan	4	2002 (Cs), Z5-1 (Cs), 169 (Cme), M (-)	AB188116, AB188115, AB020477, AB020478
			China	9	WS (Cpe), zz (Sin), SXSG (La), CJLX30535 (Crayfish), spider131932 (Spiders), WG (Bh), SG (Lc), CU (Cs), WM (Cl)	KX664482, KX421104, KX249747, KX884565, KX884570, AJ316229, AJ316228, AJ307036, AJ515911
			Taiwan	3	TW-TN3 (Lc), Begonia (Begonia), TW-TN3 (Lc)	NC_003224, AM422386, AF127929
	Africa		Egypt	1	EG (Sq)	LC153708
	Europe		Slovakia	2	Kuchyna (Cpe), SE04T (Cpe),	DQ124239, KF976713
			Czech Republic	1	H (Cpe)	KF976712
			Spain	1	Vera (Cpe)	KX499498
	Americas	N. America	USA	11	leaf23 (Cpe), leaf17 (Cpe), leaf1 (Cpe), SG5 (Cpe), SG4 (Cpe), SG1 (Cpe), FG2 (Cpe), PA_2006 (Cpe), California (Cmo), - (Cpe), - (Cpe)	KJ923769, KJ923768, KJ923767, KC665635, KC665634, KC665631, KC665630, JQ716413, L31350, KJ875864, KJ875865

		S. America	Argentina	1	10itSDE (Cma)	KT598222
	Oceania		Australia: Broome, WA	3	13Br (Cpe), 20Br (Cpe), 56Br (Cpe)	KY225555, KY225550, KY225549
			Australia: Darwin, NT	2	38NT (Cme, honeydew), 75NT (Cme, rockmelon)	KY225548, KY225547
II	Asia		Singapore	2	Singapore (-), Singapore (Cs)	U60962, AF014811
	Africa		Reunion Island	1	Reunion Island (Mch)	L29569
	Oceania		East Timor	3	TM40 (Cs), TM16 (Pu), TM39 (Pu)	KY225556, KY225545, KY225544
III			Australia: Kununurra, WA	3	694K (Pu), 695K (P), 697K (Cme, honeydew)	KY225543, KY225542, KY225546

Cpe: *Cucurbita pepo*, Cme: *Cucumis melo*, Cma: *Cucurbita maxima*, Cmo: *Cucurbita moschata*, Cs: *Cucumis sativus*, Can: *Cucumis anguria*, Mch: *Momordica charantia,* Cl: *Citrullus lanatus*, Sin: *Sesamum indicum,* La: *Luffa aegyptiaca*, Lc: *Luffa cylindrica, Bh: Benincasa hispida,* Ar*: Althaea rosea,* Pu: Pumpkin, Sq: Squash, -: unknown isolate or host

and assigned the accession numbers KJ135782, KJ135784, and MF766013-MF766018 (Table 1). Names and accession numbers of the previously reported ZYMV isolates have been also presented in Table 2.

Sequence comparisons

The pairwise sequence identity of partial CI gene of all 104 ZYMV isolates ranged from 79.0 to 100.0% at the nt sequence level (Figure 1) and from 91.2 to 100% at the aa sequence level (Figure S1). All 13 Iranian isolates (ten from this study and three retrieved from GenBank) revealed 93.5–99.1% and 94.3–100% identity at the nt and aa levels, respectively. The lowest nt identity (79.0%) was observed between Gj1 and TM40 (KY225556) and TM39 (KY225544) isolates from East Timor. In addition, the highest nt identity (99.7%) was identified between KG1 and AG, NAT and B isolates from Israel. Amino acid sequence identity in the CI gene of all ZYMV isolates was over 91%. The minimum aa sequence identity of the CI gene between the Iranian isolates and those deposited in GenBank was between isolates Gj1, Gj2 and KB and isolate TM39 (KY225544, East Timor) (91.2%), respectively. Some Iranian isolates (Fars, SANRU, KS1, KG1, KG2, KF1) showed 100% aa identity with isolates from Slovakia (SE04T, Kuchyna), Czech Republic (H), Israel (NAT, B, AG), Japan (169) and Turkey (KZN1, AKS2-5, AKS5-7, AKS6-2, AS11, AS5, BE10, BE15, BE26, BE6, BE7, BRD4, C11, C13, C17, C5, D14, E-7, ER6-8, G1, G2, G3, H1M, K3, KZ1, KAR12-4, KAR15-1, S3).

Phylogenetic analysis

The ZYMV CI coding region sequences were subjected to phylogenetic analyses, with that of *Watermelon mosaic virus* (WMV) isolate (IR02-54, EU660584) as outgroup. Both the ML and NJ trees showed a similar topology. As shown in Figure 1, all the 104 ZYMV isolates were divided into three distinct phylogroups: I, II and III. Group I is a large and geographically widespread group which was further clustered into several subgroups (IA, IB, IC and ID). Group I included a range of isolates (n=95) from different parts of the world including all 13 Iranian isolates plus isolates from Egypt (n=1), Turkey (n=35), Australia (n=5), Argentina (n=1), USA (n=11), Spain (n=1), India (n=1), Slovakia (n=2), Czech Republic (n=1), Israel (n=3), Taiwan (n=3), Japan (n=4), South Korea (n=5), and China (n=9). The between-subgroup genetic distance of the four subgroups in group I was significantly higher than the within-subgroup ones (Table S1) which providing evidence for a phylogenetic grouping. The overall mean value of nucleotide sequence diversity between Iranian and other isolates in subgroup IA was 0.031±0.003. Group II included two isolates from Singapore. Group III contained three isolates from East Timor, one from Reunion Island and three from Australia. The overall mean distance among all ZYMV isolates was 0.077±0.006. Based on pairwise comparisons, genetic distance within groups was 0.052±0.004, 0.000±0.000 and 0.130±0.010 for

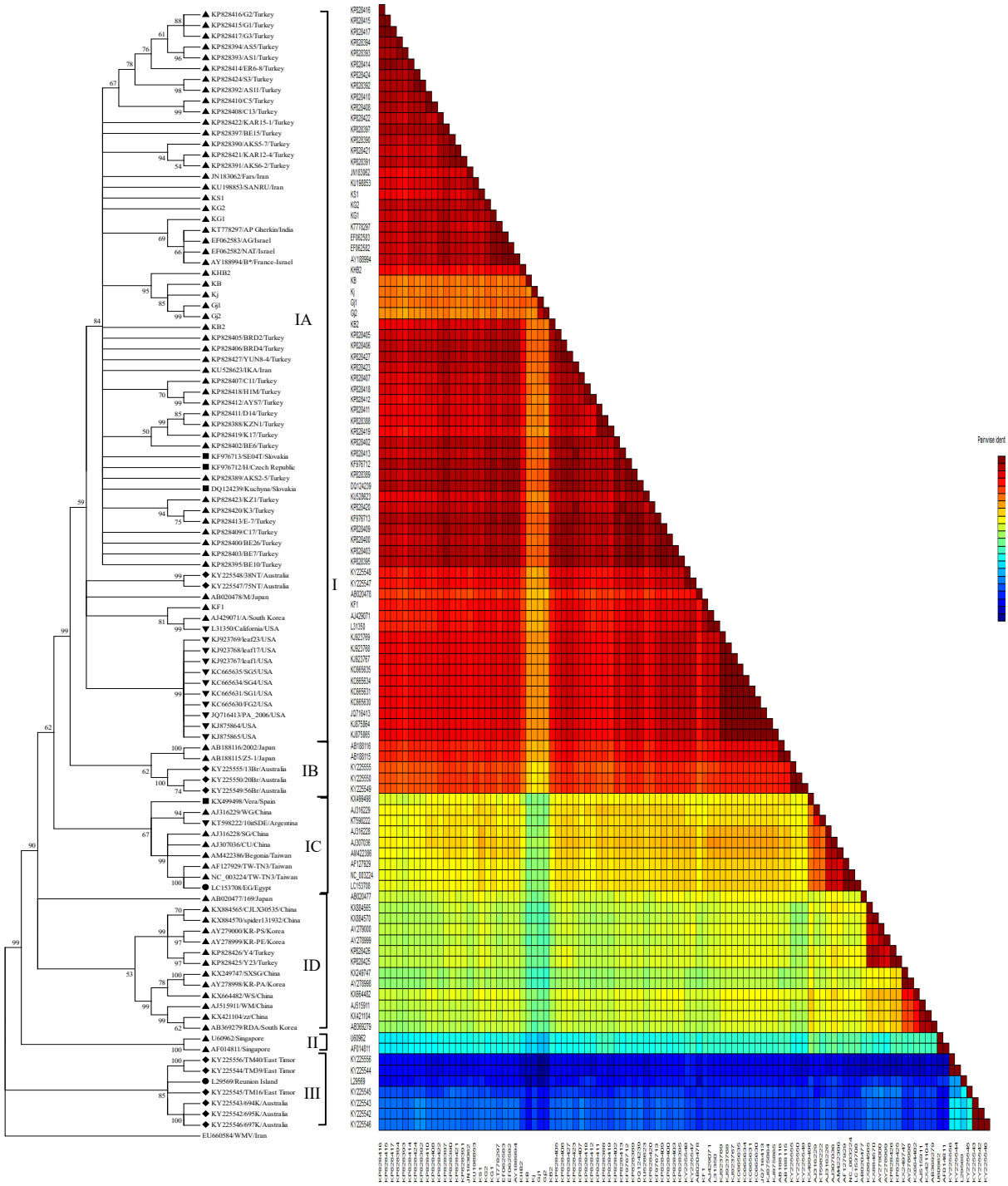

Figure 1. Maximum-likelihood phylogenetic tree constructed from the partial cylindrical inclusion (CI) gene nucleotide sequences of 104 ZYMV isolates, and graphical representation of pairwise nucleotide identity. The phylogenetic tree was generated in MEGA7 and bootstrapped with 1000 replicates. Bootstrap values ≥ 50% are shown at the branch internodes. Two dimensional nucleotide diversity plot constructed based on SDT MUSCLE alignment. The Asian isolates are indicated by "▲", European isolates by "■", American isolates by "▼", Oceanian isolates by "♦" and African isolates by "●".

group I, II and III, respectively. In addition, the genetic diversity between groups was 0.144±0.015, 0.220±0.018 and 0.231±0.019 for group I versus II, I versus III and II versus III, respectively. As expected, the genetic distances between the three groups were significantly greater than the within-group ones, supporting the results of phylogenetic grouping.

Table 3. Population genetic parameters calculated for the CI genes of *Zucchini yellow mosaic virus* on the basis of phylogroups identified in Figure 1 and geographical origin

Phylogroup	H	Hd	S	η	K	π	SS	NS	dN	dS	ω
All	72	0.986	280	373	46.46	0.074	154.67	526.33	0.00784	0.27345	0.0286
Group I (n=95)	67	0.985	**234**	**278**	33.026	0.050	154.64	526.36	0.00549	0.2496	**0.0219**
Group II (n=2)	1	0.000	0	0	0	0.000	153.67	527.33	0.0000	0.0000	0.0000
Group III (n=7)	4	0.810	172	179	**77.619**	**0.126**	155.38	525.62	0.01117	0.87953	0.0127
Geographic origins											
Asia (n=75)	60	0.994	**236**	**288**	37.767	0.058	154.68	526.32	0.00648	0.30088	**0.02153**
Europe (n=4)	2	0.500	53	53	26.500	0.041	154.50	526.50	0.00382	0.20613	0.01853
America (n=12)	3	0.318	55	56	10.000	0.015	154.47	526.53	0.00063	0.07950	0.0079
Oceania (n=11)	7	0.909	194	211	89.127	0.148	154.67	526.33	0.01605	1.70054	0.00943
Africa (n=2)	2	1.000	126	126	**126.000**	**0.212**	156.17	524.83	0.01930	3.48410	0.005539

H, number of haplotypes, Hd, haplotype diversity; S: number of polymorphic sites; η (eta): total number of mutations; k: average number of nucleotide differences between sequences; π: nucleotide diversity, with Jukes & Cantor correction; SS: total number of synonymous sites analyzed; NS: total number of non-synonymous sites analyzed; dN, average number of nonsynonymous substitutions per nonsynonymous site; dS, average number of synonymous substitutions per synonymous site, with the Jukes and Cantor correction; dN/dS, average ratio between nonsynonymous and synonymous substitutions in sequence pairs. Maximum respective values between groups are in bold.

It is worth noting that no recombination event was found between ZYMV isolates in CI gene. Also, no signatures of recombination were detected between ZYMV group I, II and III subpopulations, indicating significant genetic differentiation and limited gene flow between isolates in these phylogenetic groups, probably due to the presence of quarantine and physical barriers between them or existence of other host plants.

Genetic diversity of ZYMV

Pairwise comparisons showed that members of group I shared 87.7-100% nt sequence identity, with an average nt identity value of 97.05%, members of group II were 100% identical, and members of group III shared 84.6-100% nt sequence identities, with an average nt identity value of 92.68% (Figure 1). This suggested that group III ZYMVs had a higher level of genetic variation than those belonging to group I and II. Group I did not show a clear division in terms of geographical distribution. However, groups II and III were more phylogenetically clustered by geographical origin. Haplotype diversity and nucleotide diversity for all ZYMV isolates were 0.986 and 0.074, respectively, indicating a relatively high genetic diversity in ZYMV populations and among lineage subpopulations (Table 3). The haplotype diversity for group I and group III was 0.985 and 0.810, whereas nucleotide diversity for these two groups was 0.050 and 0.126, respectively. Notably, it was impossible to perform these statistical tests for ZYMV group II isolates, due to limited data. The highest nucleotide diversity (π=0.126) between the isolates and the greatest overall average number of differences, k (78 nucleotides), were calculated for the phylogroup III. However, the largest number of segregation sites, (S=234), and mutations within the segregating sites, (η=278), were found in the phylogroup I (Table 3). In the geographical populations, the highest values of π (=0.212) and k (126 nucleotides), were calculated for the Africa population. However, the highest values of S (236), and η (288), were found in Asia population (Table 3). The lowest π (0.015) and k (10 nucleotides) were estimated for the America population. The global selection pressure (dN/dS) for all ZYMV isolates was 0.0286. Furthermore, the dN to dS ratio (ω) for each population was <1. The highest

and lowest pressure was calculated for Asian (ω=0.021) and African (ω=0.005) populations. These results indicated that all ZYMV populations are under negative selection but subjected to distinct constraints. To determine the gene- and site-specific selection pressures acting on the ZYMV CI cistron, different codon-based maximum-likelihood algorithms within the HYPHY software package as implemented in Datamonkey server (www.datamonkey.org) were used to estimate the value of ω at each codon site. All of the codons were under negative selection or neutral evolution, which revealed that strong purifying evolutionary constraint is driving CI gene evolution in ZYMV.

Differentiation of phylogroups and geographical populations

As mentioned, genetic distinction of ZYMV populations was defined in two categories: phylogenetic populations and geographical populations. With exception of insignificant *Snn* value for group II vs. III, the independent statistical tests of population differentiation (*Ks**, *Kst**, *Z** and *Snn*) were significant (Table 4), supporting the genetic differentiation between lineage groups of ZYMV isolates. Strong genetic differentiation confirmed by high F_{ST} (>0.549). Additionally, gene flow and genetic differentiation between the Asian, American, European, Oceanian and African populations of the ZYMV isolates were determined using the *Ks**, *Kst**, *Z**, *Snn* and F_{ST} statistical tests. Among the ZYMV geographical populations, American and Oceanian populations with significant *Kst**, high Snn (mostly near 1.000) and F_{ST} (0.352) values are statistically distinct. However, nonsignificant *Ks**, *Kst**, *Z** and *Snn* values were indicated no significant differentiation between European population with the Asian and the African populations. Such a nonsignificant differentiation was also associated with low F_{ST} value (<0.104). Genetic differentiation between Asia vs. America, Asia vs. Oceania, and Europe vs. America confirmed by *Kst**, *Z**, *Snn*, and relatively high F_{ST} value (0.223-0.232), suggesting significant genetic differentiation. Also, no genetic differentiation was observed between Asia vs. Europe and Oceania vs. Africa, due to negative F_{ST} values or nonsignificant *Ks**, *Kst**, *Z** and *Snn* values (Table 4). Genetic isolation was less pronounced between the African population with the Asian and the European populations, indicating frequent gene flow. There was frequent gene flow between the European ZYMV with Oceanian and American with African populations, because the related F_{ST} values were <0.33. In addition, nonsignificant *Z*, *Z** or *Snn* values indicated these population pairs were not well differentiated (Table 4). Taken together, there is some significant correlation between geographical position and genetic distances among the geographical populations, showing that observed genetic differentiation could be explained by distance isolation.

Discussion

Analysis of genetic variation in ZYMV populations from different geographical locations can provide relevant information for understanding its emergence, epidemiology, and gene flow. Phylogenetic analysis and genetic differentiation of 104 ZYMV isolates, revealed that the population structure of the three ZYMV phylogroups somewhat correlated with their geographical locations; which was supported by the subsequent genetic distance analyses. Previous ZYMV studies used complete or partial CP sequences to distinguish phylogenetic groups. Desbiez et al. (2002) classified ZYMV isolates into two main groups based on the analyses of 47 partial nt sequences of CP gene. After analyzing the complete CP nt sequences of 39 ZYMV isolates, Zhao et al. (2003) designated three groups (I-III): I, worldwide; II, containing isolates only from Asia; and III, containing isolates only from China. Subsequently, Ha et al. (2008a) analyzed the complete CP nt sequences of 61 ZYMV isolates into three main clusters: I, distributed worldwide; II, comprising Reunion Island, Singapore and Vietnam isolates; and III, consisting of Vietnam and China isolates. By comparison of 208 partial CP sequences (231 nt), Bananej et al. (2008) suggested two main groups. Group A was a worldwide group that included three subgroups, and B comprised isolates from China, Reunion Island, Singapore and Vietnam. By analyzing the 143 complete CP sequences, Coutts et al. (2011) classified ZYMV isolates into three main groups as proposed by Ha et al. (2008a). Similarly, Massumi et al. (2011) got the same results in analyses based on the nucleotide sequences of the whole CP gene and the NIb-CP gene fragment. Finally, Maina et al. (2017) analyzed ZYMV populations from East Timorese and northern Australia and found connectivity

Table 4. Results of genetic differentiation analysis between subpopulations from pairwise comparison of *Zucchini yellow mosaic virus* sequences based on phylogroups identified in Figure 1 and geographical populations

Comparisons	*Ks** (*P*-value)	*Kst** (*P*-value)	*Z* (*P*-value)	*Z** (*P*-value)	*Snn* (*P*-value)	F_{ST}
Phylogroup						
Group I vs. II	3.217 (0.000)	0.015 (0.000)	2233.150 (0.000)	7.411 (0.000)	1.000 (0.003)	0.809
Group I vs. III	3.242 (0.000)	0.054 (0.000)	2307.149 (0.000)	7.418 (0.000)	1.000 (0.000)	0.549
Group II vs. III	3.700 (0.0450)	0.087 (0.045)	10.904 (0.033)	2.293 (0.026)	1.000 (0.056 ns)	0.700
Geography						
Asia vs. Europe	3.295 (0.559 ns)	-0.001 (0.559 ns)	1559.699 (1.000 ns)	7.041 (0.525 ns)	0.875 (0.875 ns)	-0.041
Asia vs. America	3.054 (0.000)	0.067 (0.000)	1765.184 (0.001)	6.938 (0.000)	0.942 (0.000)	0.223
Asia vs. Oceania	3.398 (0.000)	0.039 (0.000)	1698.290 (0.000)	7.061 (0.000)	0.994 (0.000)	0.232
Asia vs. Africa	3.331 (0.015)	0.016 (0.015)	1414.834 (0.020)	6.949 (0.017)	0.961 (0.253 ns)	0.085
Europe vs. America	1.192 (0.000)	0.355 (0.000)	47.472 (0.002)	3.656 (0.00)	0.875 (0.002)	0.226
Europe vs. Oceania	3.582 (0.035)	0.078 (0.035)	50.564 (0.292 ns)	3.567 (0.066 ns)	1.000 (0.001)	0.263
Europe vs. Africa	1.994 (0.138 ns)	0.419 (0.138 ns)	4.500 (0.138 ns)	1.445 (0.138 ns)	0.500 (0.584 ns)	0.104
America vs. Oceania	2.407 (0.000)	0.246 (0.000)	102.046 (0.000)	4.275 (0.000)	0.956 (0.000)	0.352
America vs. Africa	1.032 (0.025)	0.470 (0.014)	34.500 (0.025)	3.447 (0.019)	0.786 (0.138 ns)	0.208
Oceania vs. Africa	3.935 (0.019)	0.047 (0.019)	36.809 (0.093 ns)	3.308 (0.061ns)	0.846 (0.097 ns)	-0.058

Note: Probability (*P*-value) obtained by the permutation test (PM test) with 1000 replicates. ns, not significant. The analysis was done using DnaSP v. 6.10.04.

between them either in the genome-based tree or the CP-based tree. In this study, pairwise comparisons and phylogenetic analysis based on partial CI gene nt sequences clearly showed the existence of three groups, in which phylogroups I (worldwide) and III (East Timor, Reunion Island and Australia-Kununurra) were consistent with the genomic nt sequence phylogroup classification of Maina et al. (2017) but phylogroup II (containing only two Singapore isolates) was an additional one. Group I was the largest and widespread group including most of the ZYMV isolates from Asia, Europe, North and South America, Africa and Australia, in accordance with previous reports by Desbiez et al. (2002), Bananej et al. (2008), Coutts et al. (2011) (they denoted group I as group A), Ha et al. (2008a), Massumi et al. (2011) and Maina et al. (2017). This study also suggested four minor groups within group I, in which subgroups A, B, C, and D corresponded to the reported subgroups II, I, IV+V, and III, respectively (Maina et al., 2017). However, subgroup IV along with the previously reported WG and 10itSDE isolates in subgroup V were integrated into subgroup IC. As mentioned above, the geographical origins of the isolates in group I were the most diverse and the overall nt and aa identity within CI sequences in this group was >87.0% and >92.0%, respectively, which suggest the common origin of distantly distributed isolates. International trading of infected seeds, plants or fruits can be a possible explanation for such sequence similarities observed between the intercontinental isolates of ZYMV (Desbiez et al., 2002; Lecoq et al., 2003; Simmons et al., 2008; Simmons et al., 2011, 2013). In some cases, the CI gene data was more phylogenetically classified by geographical situation than anticipated by chance alone, as depicted in subgroups IC (expect Argentinian isolate) and ID. Analysis of ZYMV population differentiation indicated that three phylogroups were completely distinct with significant *Ks**, *Kst**, *Z*, Snn* and very high F_{ST} values (>0.500). The ω estimates for group I and group III were respectively 0.022 and 0.013 (Figure 1, Table 3), and in concordance with the result of genetic differentiation analysis (Table 4). The result showed that group I was subjected to more intense purifying selection than group III. Recombination is one of the principal forces driving plant virus evolution (Garcia-Arenal et al., 2003), however no recombination event was detected in CI gene of studied isolates, suggesting that this potent evolutionary force has not shaped the emergence of ZYMV CI gene variants. Meanwhile, the partial genome fragment could not provide accurate results. A previous study provided evidence for the presence of recombination cold spots within the full-length polyprotein of 14 ZYMV isolates from northern Australia (n=10, Broome, Kununurra), East Asia (n=2, Japan, China) and Southeast Asia (n=2, Singapore, East Timor) (Maina et al., 2017). Among them, Z5-1 from Japan was lone isolate identified as a recombinant in the CI coding region plus 6k2, NIa-Vpg and NIa-Pro coding regions and the lower frequency of recombination occurred in these regions than elsewhere in genomic RNA. Overall, there were a low frequency of recombination in most of ZYMV isolates (Maina et al., 2017); one possible explanation is strong selective pressure against survival of new ZYMV recombinants. In genetic diversity analyses (Table 3), the African population showed the most nucleotide diversity (π), followed by the Oceanian population. However, American and European populations exhibited low haplotype diversity (0.318, 0.500) and nucleotide diversity (0.015, 0.041). Low level of genetic diversity among American isolates as well as European ZYMV isolates was in contrast to the diversity reported from other parts of the world. Geographical population cluster levels of genetic differentiation ranged from -0.041–0.352 in the F_{ST} values. The highest and lowest F_{ST} values were found for Oceania versus America and Africa populations, respectively (Table 4). Except African population, all the populations were differentiated from the American and Oceanian ZYMV populations because the *Kst** values were well above zero and supported by high significant *P*-value (0.000). The extent of genetic differentiation between most of the geographical population pairs was moderate ($0.085<F_{ST}<0.104$) to great ($0.223<F_{ST}<0.263$), indicating moderate to high gene flow between these geographical

ZYMV populations. The exception was Oceanian and American ZYMV populations, which had complete genetic difference (infrequent gene flow) (F_{ST} =0.352). Genetic differentiation between American and Oceanian ZYMV populations also confirmed by all statistical tests. This could be due to long distances between these geographic regions, indicative of a correlation between genetic and geographical distances. Based on these test statistics, geographical isolation may have played a role in ZYMV population structure especially in Oceanian and American isolates. The dN/dS ratio for Asian isolates was the highest, indicating that CI is under tighter functional constraints for these isolates. There were no codons identified as being under positive selection for all lineages. Strong negative selection on the CI of the ZYMV suggests the crucial role of this protein in helicase activities, RNA replication, cell-to-cell and systemic movement or other vital yet unknown functions (Carrington et al., 1998; Klein et al., 1994). In the phylogenetic analysis all ZYMV populations were polyphyletic and distributed in more than one phylogenetic groups (Figure 1). This indicates that ZYMV isolates were dispersed to other geographical areas with unknowingly infected seed (despite low levels of seed transmission) (Tobias and Palkovics, 2003; Desbiez and Lecoq, 1997; Schrijnwerkers et al., 1991; Simmons et al., 2011) or vegetative propagules and evolved via genetic drift (founder effect). As mentioned, the sequence variation along the CI gene of ZYMV isolates is controlled by purifying selection pressure (<1). Alternatively, in situ evolution within several countries, with human activity in widespread seed transmission playing a main role in ZYMV dispersal, as suggested by Simmons et al. (2008) in analysis of ZYMV CP gene. Therefore, when an isolate becomes settled down in a place, without positive selection within the population, little change could occur unless a new variant is introduced, as the case for Australian isolates (Kununurra in northern Australia which are highly different from other Australian isolates) (Coutts et al., 2011). Moreover, the Kununurra sequences grouped together with the three East Timorese sequences within major phylogroup III (previously called the Southeast Asian/Reunion Island phylogroup), which seems adapted to tropical conditions (Maina et al., 2017). The close relationship between the CI sequences (as well as complete genomic sequences) from Kununurra and East Timor suggest recent ZYMV introduction across the sea from Southeast Asia to Kununurra. Such grouping could be attributed to monsoonal winds (from East Timor toward northern Australia) which could bring viruliferous insect vectors or migrating birds with infected seed in their guts, thus introducing viruses (Eagles et al., 2013). The Iranian ZYMV isolates in the subgroup IA shared 93.5–99.1% CI nucleotide sequence identity with each other and 87.7-99.7% with other isolates of this subgroup. Iranian isolates were more resembling to isolates from Middle East (Israel, Turkey and India,), Far East (China, Japan and South Korea), Europe (Spain, Czech Republic, and Slovakia), Australia and USA in partial CI nucleotide sequence. So, how ZYMV first entered Iran is difficult to determine, but there are several possible pathways. During commercial exchanges, infected cucurbit material such as plants, fruits or seeds may have entered from elsewhere, providing the initial virus source. In the present study, tomato was found to be a new natural host of ZYMV, broadening the understanding of the genetic diversity of the pathogen in pathogenicity to plants. The analyses done in this study provide evidence for important evolutionary forces driving ZYMV evolution such as selection, genetic drift and founder effects by exchange infected plant products between different geographical regions. These findings provide an insight into the ZYMV population structure and are helpful for designing proper strategies to the management of this virus.

References

1. Adams M.J., Antoniw J.F. and Beaudoin F. (2005a) Overview and analysis of the polyprotein cleavage sites in the family *Potyviridae*. Molecular Plant Pathology 6:471–487.
2. Adams M.J., Antoniw J.F. and Fauquet C.M. (2005b) Molecular criteria for genus

and species discrimination within the family *Potyviridae*. Archives of Virology 150:459–479.
3. Adams M.J., Zerbini F.M., French R., Rabenstein F., Stenger D.C. and Valkonen J.P.T. (2012) Family *Potyviridae*. In: King AMQ, Adams MJ, Carstens EB, Lefkowitz EJ, eds. Virus taxonomy: Classification and nomenclature of viruses. Ninth report of the ICTV. London, UK: Academic Press, 1069–1089.
4. Al-Musa A.M. (1989) Over summering hosts for some cucurbit viruses in the Jordan Valley. Journal of Phytopathology 127:49–54.
5. Bananej K.A., Keshavarz T., Vahdat A., Hosseini Salekdeh G. and Glasa M.J. (2008) Biological and molecular variability of *Zucchini yellow mosaic virus* in Iran. Journal of Phytopathology 156:654-659.
6. Chen Y.K. and Hong Y.H. 2008. First report of Begonia chlorotic ringspot caused by *Zucchini yellow mosaic virus* in Taiwan. Plant Disease 92:1247.
7. Choi S.K., Yoon J.Y., Ryu K.H., Choi J.K. and Park W.M. (2002) First report of *Zucchini yellow mosaic virus* on hollyhock (*Althaea rosea*). Plant Pathology Journal 18:121–125.
8. Coutts B.A. and Jones R.A.C. (2005) Incidence and distribution of viruses infecting cucurbit crops in the Northern Territory and Western Australia. Australian Journal of Agricultural Research 56:847–858.
9. Coutts B.A., Kehoe M.A., Webster C.G., Wylie S.J. and Jones R.A. (2011) *Zucchini yellow mosaic virus*: biological properties, detection procedures and comparison of coat protein gene sequences. Archives of Virology 156:2119-31.
10. Chung BY-W., Miller W.A., Atkins J.F. and Firth A.E. (2008) An overlapping essential gene in the *Potyviridae*. Proceedings of the National Academy of Sciences of the USA 105:5897–5902.
11. Desbiez C., Wipf-Scheibel C., Granier F., Robaglia C., Delaunay T. and Lecoq H. (1996) Biological and molecular variability of *Zucchini yellow mosaic virus* in the island of Martinique. Plant Disease 80:203–207.
12. Desbiez C. and Lecoq H. (1997) *Zucchini yellow mosaic virus*. Plant Pathology 46: 809-829.
13. Desbiez C., Wipf-Scheibel C. and Lecoq H. (2002) Biological and serological variability, evolution and molecular epidemiology of *Zucchini yellow mosaic virus* (ZYMV, *Potyvirus*) with special reference to Caribbean islands. Virus Research 85:5–16.
14. Eagles D., Walker P.J., Zalucki M.P. and Durr P.A. (2013) Modelling spatio-temporal patterns of long-distance Culicoides dispersal into northern Australia. Preventive Veterinary Medicine 110: 312-322.
15. Gal-On A. (2007) *Zucchini yellow mosaic virus*: insect transmission and pathogenicity-the tails of two proteins. Molecular Plant Pathology 8:139–150.
16. Garcı´a-Arenal F., Fraile A. and Malpica J.M. (2003) Variation and evolution of plant virus populations. International Microbiology 6:225–232.
17. Gibbs A. and Ohshima K. (2010) Potyviruses and the digital revolution. Annual Review of Phytopathology 48: 205–223.
18. Glasa M., Svoboda J. and Novakova S. (2007) Analysis of the molecular and biological variability of *Zucchini yellow mosaic virus* isolates from Slovakia and Czech Republic. Virus Genes 35:415–421.
19. Ha C., Revill P., Harding R.M., Vu M. and Dale J.L. (2008a) Identification and sequence analysis of potyviruses infecting crops in Vietnam. Archives of Virology 153:45–60.
20. Ha C., Coombs S., Revill P.A., Harding R.M., Vu M. and Dale J.L. (2008b) Design and application of two novel degenerate primer pairs for the detection and complete genomic characterization of potyviruses. Archives of Virology 153:25-36.
21. Hall T.A. (1999) BioEdit: a user-friendly biological sequence alignment editor and analysis program for Windows 95/98/NT. Nucleic Acids Symposium Series 41:95–98.
22. Hudson R.R., Boos D.D. and Kaplan N.L. (1992a) A statistical test for detecting geographic subdivision. Molecular Biology and Evolution 9:138–151.
23. Hudson R.R., Slatkin M. and Maddison W.P. (1992b) Estimation of levels of gene flow from DNA sequence data. Genetics 132:583–589.
24. Hudson R.R. (2000) A new statistic for detecting genetic differentiation. Genetics 155: 2011–2014.

25. Carrington J.C., Jensen P.E. and Schaad M.C. (1998) Genetic evidence for an essential role for potyvirus CI protein in cell-to-cell movement. Plant Journal 14: 393–400.
26. Jukes T.H. and Cantor C.R. (1969) Evolution of protein molecules. In: Munro HN (ed) Mammalian protein metabolism. Academic Press, NewYork, pp 21–132.
27. Klein P.G., Klein R.R., Rodriguez-Cerezo E., Hunt A.G. and Shaw J.G. (1994) Mutational analysis of the *Tobacco vein mottling virus* genome. Virology 204:759-769.
28. Kumar S., Stecher G., and Tamura K. (2016) MEGA7: Molecular Evolutionary Genetics Analysis version 7.0 for bigger datasets. Molecular Biology and Evolution 33:1870-1874.
29. Lecoq H., Pitrat M. and Clément M. (1981) Identification et caractérisation d'un potyvirus provoquant la maladie du rabougrissement jaune du melon. Agronomie 1:827–834.
30. Lecoq H., Bourdin D., Raccah B., Hiebert E. and Purcifull D.E. (1991) Characterization of a *Zucchini yellow mosaic virus* isolates with a deficient helper component. Phytopathology 81: 1087-1091.
31. Lecoq H., Desbiez C., Wipf-Scheibel C. and Girard M. (2003) Potential involvement of melon fruit in the long-distance dissemination of cucurbit potyviruses. Plant Disease 87:955–959.
32. Lee K.C., Mahtani P.H., Chng C.G. and Wong S.M. (1997) Sequence and phylogenetic analysis of the cytoplasmic inclusion protein gene of *Zucchini yellow mosaic potyvirus*: its role in classification of the *Potyviridae*. Virus Genes 14: 41–53.
33. Lisa V., Boccardo G., D'Agostino G., Dellavalle G. and d'Aquilio M. (1981) Characterization of a potyvirus that causes *Zucchini yellow mosaic virus*. Phytopathology 71: 667-672.
34. Lisa V. and Lecoq H. (1984) *Zucchini yellow mosaic virus*. CMI/AAB Description of Plant Viruses, No. 282.
35. Martin D.P., Murrell B., Golden M., Khoosal A. and Muhire B. (2015) RDP4: detection and analysis of recombination patterns in virus genomes. Viral evolution 1:vev003.
36. Massumi H., Shaabanian M., Heydarnejad J., Hosseini Pour A. and Rahimian H. (2011) Host range and phylogenetic analysis of Iranian isolates of *Zucchini yellow mosaic virus*. Journal of Plant Pathology 93:187-193.
37. Maina S., Coutts B.A., Edwards O.R., Almeida L., Kehoe M.A., Ximenes A., and Jones R.A.C. (2017) *Zucchini yellow mosaic virus* populations from East Timorese and Northern Australian Cucurbit Crops: Molecular Properties, Genetic Connectivity, and Biosecurity Implications. Plant Disease 101:1236-1245.
38. Moury B., Morel C., Johansen E. and Jacquemond M. (2002) Evidence for diversifying selection in *Potato virus Y* and in the coat protein of other potyviruses. Journal of General Virology 83:2563-2573.
39. Muhire B.M., Varsani A. and Martin D.P. (2014) SDT: A Virus Classification Tool Based on Pairwise Sequence Alignment and Identity Calculation. PLoS ONE 9: e108277.
40. Novakova S., Svoboda J. and Glasa M. (2014) Analysis of the complete sequences of two biologically distinct *Zucchini yellow mosaic virus* isolates further evidences the involvement of a single amino acid in the virus pathogenicity. Acta Virologica 58:364 – 367.
41. Riechmann J.L., Lain S. and Garcia J.A. (1992) Highlights and prospects of *Potyvirus* molecular biology. Journal of General Virology 73:1–16.
42. Rozas J., Sanchez-DeI Barrio J.C., Messeguer X. and Rozas R. (2003) DnaSP, DNA polymorphism analyses by the coalescent and other methods. Bioinformatics 19:2496–2497.
43. Rozas J., Ferrer-Mata A., S anchez-DelBarrio J.C., Guirao-Rico S., Librado P., Ramos-Onsins S.E. and Sanchez-Gracia A. (2017) DnaSP 6: DNA sequence polymorphism analysis of large datasets. Molecular Biology and Evolution 34:3299-3302.
44. Schrijnwerkers C.C.F.M., Huijberts N. and Bos L. (1991) *Zucchini yellow mosaic virus*; two outbreaks in the Netherlands and seed transmissibility. Netherlands Journal of Plant Pathology 97:187–191.
45. Simmons H.E., Holmes E.C. and Stephenson A.G. (2008) Rapid evolutionary dynamics of *Zucchini yellow mosaic virus*. Journal of General Virology 89:1081–1085.

46. Simmons H.E., Holmes E.C., Gildow F.E., Bothe-Goralczyk M.A. and Stephenson A.G. (2011) Experimental Verification of Seed Transmission of *Zucchini yellow mosaic virus*. Plant Disease 95:751–754.
47. Simmons H.E., Dunham J.P., Zinn K.E., Munkvold G.P., Holmes E.C. and Stephenson A.G. (2013) *Zucchini yellow mosaic virus* (ZYMV, *Potyvirus*): Vertical transmission, seed infection and cryptic infections. Virus Research 176:259–264.
48. Tobias I. and Palkovics L. (2003) Characterization of Hungarian isolates of *Zucchini yellow mosaic virus* (ZYMV, *Potyvirus*) transmitted by seeds of *Cucurbita pepo* var. Styriaca. Pest Management Science 59:493–497.
49. Tsompana M., Abad J., Purugganan M. and Moyer J.W. (2005) The molecular population genetics of the *Tomato spotted wilt virus* (TSWV) genome. Molecular Ecology 14:53–66.
50. Urcuqui-Inchima S., Haenni A. and Bernardi F. (2001) *Potyvirus* proteins: a wealth of functions. Virus Research 74:157-175.
51. Wright S. (1951) The genetical structure of populations. Annals of eugenics 15:323–354.
52. Yakoubi S., Desbiez C., Fakhfakh H., Wipf-Scheibel C., Fabre F., Pitrat M., Marrakchi M. and Lecoq H. (2008) Molecular, biological and serological variability of *Zucchini yellow mosaic virus* in Tunisia. Plant Pathology 57:1146–1154.
53. Zhao M.F., Chen J., Zheng H.Y., Adams M.J. and Chen J.P. (2003) Molecular analysis of *Zucchini yellow mosaic virus* isolates from Hangzhou, China. Journal of Phytopathology 151:307-311.

Table S1. Genetic distances within and between subgroups in group I

	Subgroups			
	IA	**IB**	**IC**	**ID**
Subgroup IA	0.022 ± 0.002			
Subgroup IB	0.038 ± 0.005	0.019 ± 0.004		
Subgroup IC	0.079 ± 0.009	0.080 ± 0.010	0.034 ± 0.004	
Subgroup ID	0.099 ± 0.011	0.102 ± 0.011	0.090 ± 0.009	0.057 ± 0.006

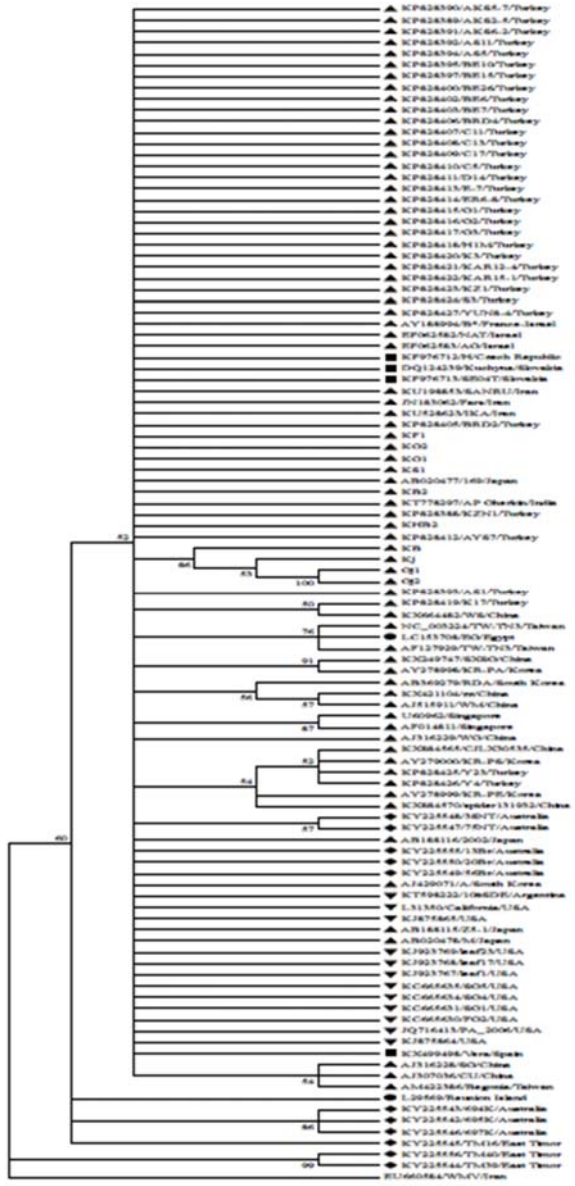

Figure S1. Maximum likelihood phylogenetic tree illustrating the phylogenetic relationships between Iranian and other ZYMV isolates. Tree was drawn by MEGA7 using the CI amino acid sequence. WMV (*Watermelon mosaic virus*) included as out-group. The GenBank accession number, the name of each isolate and its country of origin are listed. Numbers at each node indicate bootstrap percentages based on 1000 replications. Values are shown only when the values are equal or greater than 50%.

Journal of Cell and Molecular Research (2019) 10 (2), 90-96 DOI: 10.22067/jcmr.v10i2.73401

Research Article

Prefractionation in Proteome Profile Analysis of ANXC4 Gene Mutant in *Aspergillus Fumigatus*

Elham Erami[1*], Fereydoun Sadeq-zadeh[2]

[1]*Department of Quality Control, Research and Production Complex, Pasteur Institute of Iran, Tehran, Iran*
[2] *Green Environment and Sustainable Chemistry, Tehran, Iran*

Received 9 June 2018 Accepted 8 March 2019

Abstract

Aspergillus fumigatus is one of the pathogenic filamentous fungi that could cause opportunistic infection, allergy and poisoning. Since, genetic sequencing of some of these fungi has been completed, identifying the protein profile of these fungus cells is necessary. One of these genes is the Annexin family. Annexin C4 is a new member of fungal annexins. This study investigates the effect of ANXC4 mutant gene in proteome profile of *Aspergillus Fumigatus*. Moreover, in order to enhance the power of protein complex separation, we used an optimized prefractionation method. Using reverse phase-high performance liquid chromatography eight fractions were separated. Then to confirm the protein concentration, each fraction was tested by SDS-PAGE. Protein profile of these fractions was analyzed using 2-DE, and Image Master software. Among the proteins identified statistically, two emerging proteins were observed. The results show that the expression of ANXC4 could affect the expression of some proteins in *A.Fumigatus*. To accurately identify these proteins, further experiments are needed including Mass spectrometry analysis.

***Keywords*:** *Aspergillus Fumigatus*, RP-HPLC, 2-DE, Prefractionation, Proteome profile

Introduction

The genus *Aspergillus* contains nearly 200 species, only approximately 2 dozen of which are known to cause human disease; primarily *A. fumigatus, A. flavus, A. niger, A. terreus,* and *A. nidulans,* with each species at times causing unique clinical infections (W.J. Steinbach 2018). *A. Fumigatus*is an opportunistic filamentous fungus that causes prevalent infections in diseases such as tuberculosis, asthma and cystic fibrosis colonization of this fungus leads to respiratory tract destruction (Dagenais and Keller, 2009). Immunosuppression is the primary factor for the opportunistic infections that are generally called aspergillosis (Debeaupuis *et al.*, 1997)(Latgé, 2001). Secretion of extracellular proteins such as toxins and enzyme play a significant role in pathogenesis of this fungus. The need to study *A. fumigatus'* pathogenesis side mechanisms and its similar strains, and the necessity to develop disease prevention and treatment methods, have been the causes of getting more attention to genetic studies of these strains (Ronning *et al.*, 2005). Given the fact that, genetic sequencing of some fungi has been completed, identifying the protein profile of these fungus cells is necessary. One in particular that is at the center of our study is the Annexin family that is made up of more than a thousand members (KamandKhalaj et al. 2015).

Annexins are multifunctional proteins that bind to phospholipid membranes in a calcium-dependent manner (Maria Maryam 2019). They are expressed in most strains and branches of eukaryotes. These proteins have different functions in the cell, for example, participation in organization of exocytosis and endocytosis performance of the cell membrane, membrane integration and regulation of calcium channels. Annexins have been divided into five major families (A, B, C, D and E). Fungal annexins belong to group C. This gene is structurally different from other annexins (Gerke and Moss, 2002)(Moss and Morgan, 2004). In the past, *ANXC3.1* and *ANXC3.2* have been surveyed. Khalaj*et al.* (2004) identified and introduced *ANXC4*, as a new member of this family. At first these genes were identified by bioinformatics and sequencing, and then they were ascertained in the lab (Khalaj *et al.*, 2004). Disruption of *ANXC4* gene didn't show any particular phonotypical changes under different growth conditions, but in Khalaj*et al*. (2011) study, many considerable changes of protein expression were observed in *ANXC4* mutant and then with proteomics studies it was determined

*Corresponding author E-mail: elhamerami@gmail.com

that these proteins were often involved in responding to oxidative stress (Khalaj *et al.*, 2011).
Understanding the genome and its polymorphisms is a way to comprehend gene function in cellular processes. Despite the importance of the genomics studies, cellular mechanism of cell function in different situations cannot be predicted based on its gene sequence. To apprehend the dynamic and varied processes of cells, including those actions that interfere with the development of disease, we must study the proteins that contribute to these advancements by proteomics method (Anderson, *et al.*, 2000)(Van Eyk, 2001). If these changes are exclusive to a particular condition of a disease, it is possible that they would be used as a biomarker for diseases (Srinivas *et al.*, 2002)(Govorun and Archakov, 2002).The three main parts of proteomics include, the analysis of complex protein compounds, quantification of analyzed compounds and identification of analyzed compounds. There are different methods to reach these aims. Today, the most successful technology is the combination of 2-DE[1] and mass spectrometry (Karpievitch *et al.*, 2010).
2-DE is used to analyze complex proteins before mass spectrometry, but analysis with this method alone has its limitations, including the fact that most of the proteins involved in diseases or drug targets, are of low-abundant proteins. To observe these proteins, it is necessary to increase their amount in the sample (Neverova and Van Eyk, 2005)(Karpievitch *et al.*, 2010). Prefractionation of the protein complex is an efficient way to increase the power of separation. There has been a considerable amount of effort for the creation and development of prefractionation methods as tools, to enrich the level of low abundant proteins in the sample. Included in these methods are chromatography, electrophoretic and fractionation by centrifuge (Srinivas *et al.*, 2002)(Badock *et al.*, 2001)(Righetti *et al.*, 2003).
RP-HPLC[2] is a technique that along with other methods of purification of macromolecules, is used for the analysis and purification of biomolecules (Righetti *et al.*, 2005). In Vaziri*et al*. (2006) the efficiency of RP-HPLC prefractionation on baby hamster kidney cells infected by rabies virus was assessed. It was then determined that prefractionation of cell extract successfully increases the power of protein separation (Vaziri *et al.*, 2006).

In the present research, a combination of two methods including 2-DE and RP-HPLC were used, to compare the expression profiles of *ANXC4* gene in two mutant and wild samples. Through a comparative study the efficiency of prefractionation in the separation of protein complex was investigated.

Materials and Methods

Culture of microorganisms

Aspergillus fumigatus fungus strain AF293 was cultivated in the biotechnology department of Pasteur Institute of Iran, and annexin gene *ANXC4* was knocked out in it. Creation of this mutant strain, called 'treat 18', was repeated three times. The wild strain, as the control group, was called 27 I, II, III. Samples were taken from these two strains and they were lysed.

RP-HPLC

The mutant and wild lysed samples were prepared for fractionation. A microtube containing 300 µl of sample was centrifuged at 14,000 g for 15 min. To analyze the proteins based on hydrophobicity properties, 70 µl of centrifuged sample was injected onto NucleosilC8 HPLC 4.6 mm column (Knaver, Germany) that was equilibrated with 100% buffer A (Ultra pure water and 0.1 TFA%). The UV-visible detector (Pharmacia LKB, Sweden) was set at 220 and 280 nm. From minute 5 to 90, fractions were collected on 10 min intervals. Fractions were then dried in a vacuum refrigerated concentrator (Krist, Germany), and stored in a freezer at -20°C. At the end, 8 fractions were collected from each sample.
The optimized method used, is based on step gradient concentration of buffer B (5% acetonitrile containing 0.1% TFA) and buffer A, which is shown in Table 1. The method used in HPLC step is as follows: first detection wavelength λ1 220 nm, second detection wavelength λ2 280 nm, flow rate 0.5 ml/min. In each run approximately 70 µg was injected onto the column. (Knaver, Germany).

SDS-PAGE

Dried fractions from the RP-HPLC step were dissolved in 30 µl of loading buffer and were boiled for 10 min in 90°Cin heater block. After cooling down, the samples, and the molecular weight marker were injected into gel wells. The gel electrophoresis was run at 100 V, and gels were stained using Coomassie brilliant blue R-250 (Bio Rad, USA).

[1] Two dimensional electrophoresis
[2]Reverse phase high-performance liquid chromatography

Table 1. Optimized method used for protein prefractionation

	Buffer A (%)	Buffer B (%)
Step 1	100	0
Step 2	75	25
Step 3	73	27
Step 4	70	30
Step 5	65	35
Step 6	50	50
Step 7	40	60
Step 8	10	90
Step 9	100	0

2-DE

First dimension: A non-linear immobilized pH gradient 4-7 IPG 7 cm ReadyStrip, was used. Each strip was placed into a tray channel. Samples were loaded on the strips, which were soaked in hydrating buffer, and after an hour were covered with mineral oil and kept at room temperature for 16 hours. Based on concentration, 35 µg of each sample was collected, then with the aid of hydrating buffer, containing 0.0072 g DTT, each sample's volume was increased to 125 ml. All solutions were centrifuged for 15 min with 14000×g at 4˚c. Supernatant of each solution was separately poured into trays. Then 16 IPG strips were discharged and placed on an IEF cell based on a time schedule shown in Table 2.

Table 2. Time schedule for the first dimension of electrophoresis (IEF)

Step	Ramping Mode	Maximum Voltage(V)	Time (min)	Volt – Hour
1	Linear	250	20	-
2	Linear	4000	120	10000 – 14000
3	Rapid	4000	300	10000 – 14000

IPG strip preparation for the second dimension: Strips were placed in equilibration buffer in two steps, so that the SDS contained in the buffer would get loaded on sample proteins. On first step, to revive protein disulfide bonds, for each 7 cm strip, 0.06 mg of 2% DTT was added to 3 ml of equilibration buffer. On second step, 70 ml iodoacetamide was added (the same ratios). This step was done for the alkylation of the thiol group contained in the sample. 2-DE and SDS-PAGE tests were repeated three times for each fraction 4, 5 and 6 of the control and treat samples. Electrophoresis of reduced and alkylated samples was carried out using 7cm 12% SDS-PAGE gels (Mini-PROTEAN 3, Bio Rad) and finally was stained by silver nitrate EBT (Bio Rad, USA).

Image Analysis

For the analysis and enumeration of present protein stains ImageMaster software was used. First the gels were scanned using GS_800 Calibrated Densitometer (Bio Rad, USA). With the use of the obtained images and ImageMaster 2D software, spot detection matching and editing steps took place, and finally the gels were analyzed. Then, we made a report about all the spots that had changed expression.

Results

Fractionation of proteins using RP-HPLC

The obtained chromatogram from repeated analytical tests, using RP-HPLC, could be observed in figures 1 and 2.In Figure 1 the increased amount of acetonitrile buffer, of RP-HPLC of lysed *A. fumigatus* proteins is analyzed. This analysis was based on hydrophobicity. Fractions that were more hydrophobic were used for SDS-PAGE. In Figure 2, the graphs from RP-HPLC of the control and treat samples, at 220 nm wavelengths were compared. Proteomes of *A. fumigatus'* cells were analyzed in eight fractions. F: Fraction, A: Absorption at unit

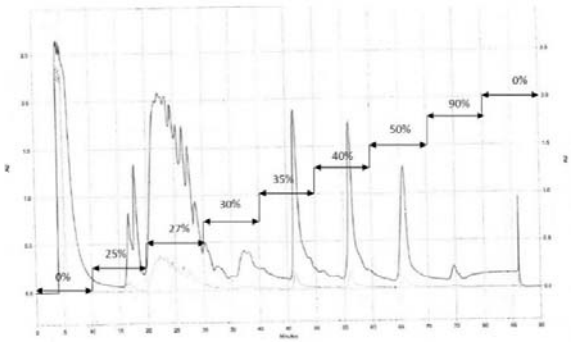

Figure 1.RP-HPLC chromatogram control

Results from SDS-PAGE method

After the RP-HPLC operation, each of the obtained fractions were analyzed using SDS-PAGE

method. The results are shown in Figure 3. The expression profile of the 8 fractions after chromatography was compared (A: Treat, B: Control). Analysis was done using 12% SDS-PAGE gels that confirm the RP-HPLC results.

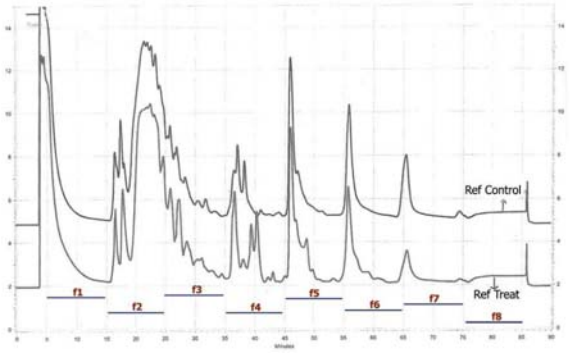

Figure 2. RP-HPLC chromatogram control and treat

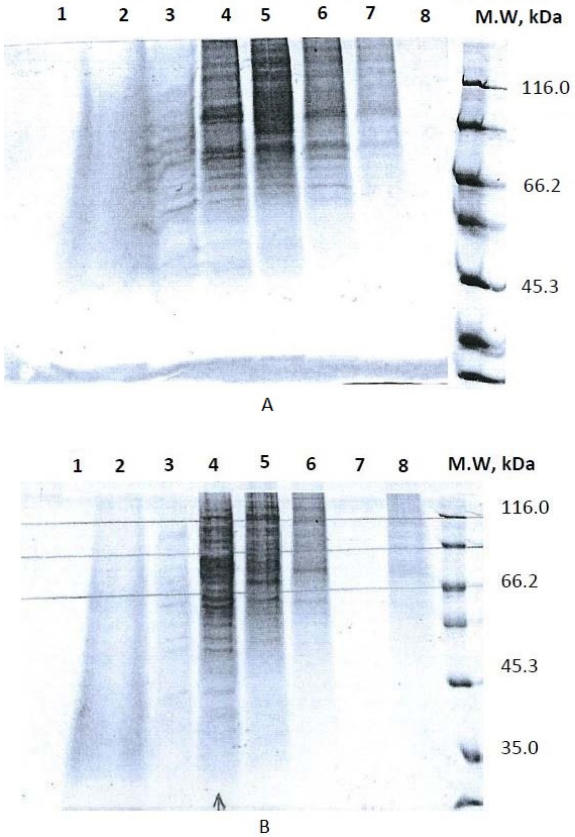

Figure 3. SDS-PAGE gel

2-DE Gel

After the fractionation and assessment of the sample concentration with the use of SDS-PAGE, fractions 4, 5, and 6 from control and mutant samples were selected and for each of them a two dimensional gel were used. The protein stains from 2-DE analysis are shown in Figure 4. 2-DE gels for the treat fractions 4, 5 and 6 are compared to the control samples using 12% large 2-DE gels.

Image analysis

With respect to the considered confidence level of this study (95%), based on the calculated degrees of freedom, the minimum t value was considered to be 2.77. Therefore, changes in which the t value was higher than 2.77 were considered statistically significant. The data from Image Master software was obtained with 5% confidence level consideration. In these settings, changed proteins in fractions 4 to 6 were assessed for increase or decrease. Table 3 contains the data that compare the changed protein stains in control and treat groups. CV: Coefficient variation, Fold: change of expression level, t: Average of three treatments, c: Average of three controls, F: Fraction

Discussion

Proteomics is an efficient technique for detection and identification of existing proteins in *Aspergillus fumigatus.* It is one of the pertinent methods to identify significant features of this fungus and classify its protein profile. In this study, to assess the expression profile of annexin gene ANXC4, and its changes as a result of a knockout, we used a prefractionation based RP-HPLC method. In order to compare the chromatograms, they were superimposed onto each other. The results of this comparison have been shown in Figure 3.2. Therefore, it was determined that this method has a satisfactory performance and it is replicable.

For the general analysis of the quality of fractionation for each fraction, SDS-PAGE was performed. In light of the SDS-PAGE results shown in Figure 3.3, it was determined that fractions 4 to 6 contain protein samples. Comparison of the peaks obtained from RP-HPLC with gels from SDS-PAGE shows that, firstly initial fractions, especially fractions 1, 2 and 3 that were from minute 5 to 35, contain very high amount of salt, so much that it has impaired the SDS-PAGE gel. Secondly, taking into account the protein content and the existing protein bands in each fraction, it was determined that, with respect to quality and quantity, SDS-PAGE gel is consistent with the acquired peaks from RP-HPLC. With the satisfactory results from the power of RP-HPLC in

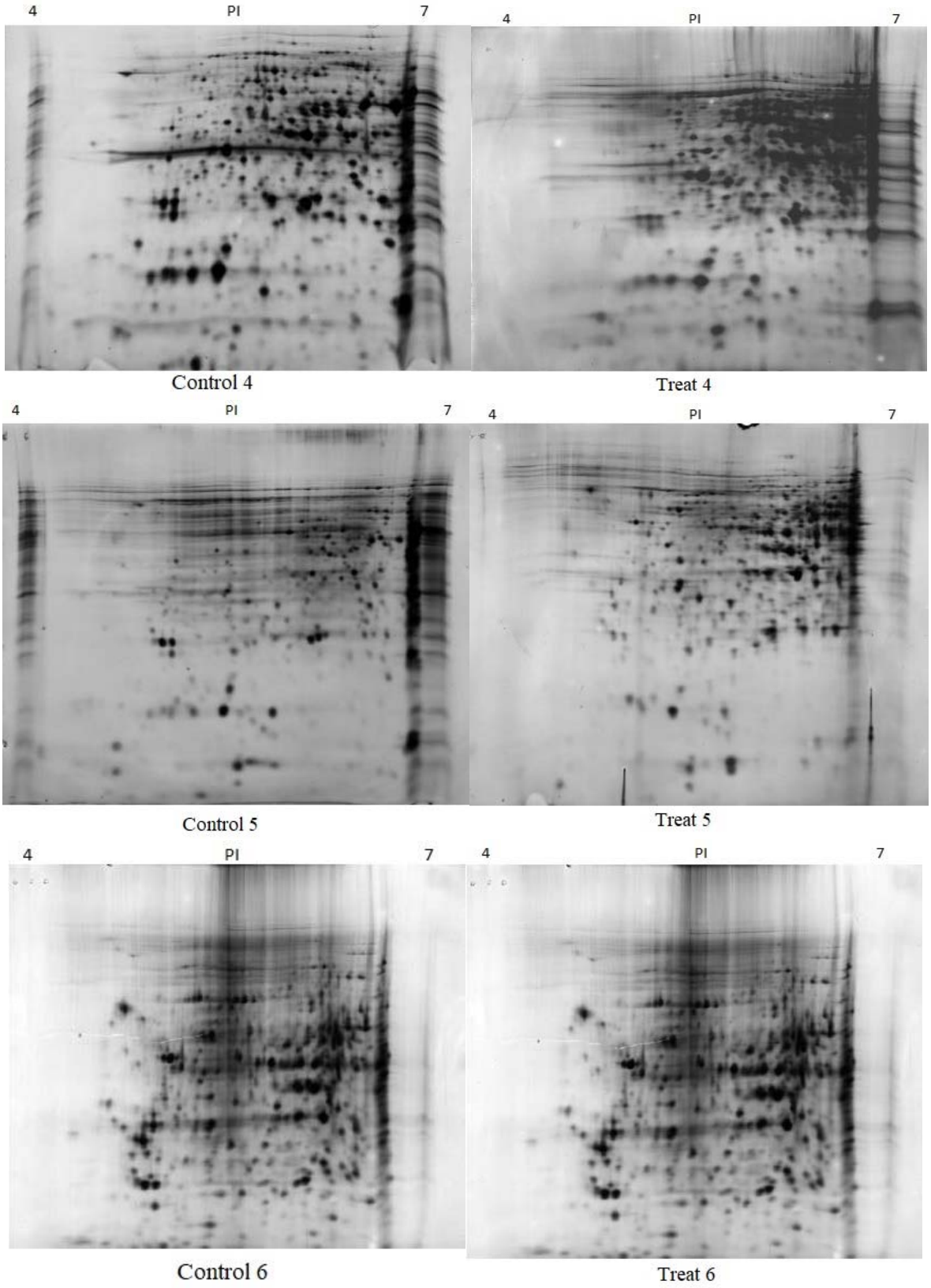

Figure 4. 2-DE gels for control and treat fractions 4, 5, 6

Table 3. Statistical analysis of observed protein stains from2-DE gel

Match ID	c (vol %)	t (vol %)	Coefficient Variation c	Coefficient Variation t	t -student	Fold change c/t
970 F4	0.368655	-	15.422	-	3.86304	-
1036 F4	1.010225	0.566525	9.851612	7.870546	7.05	1.783196
1272 F5	1.20446	0.57773	8.154575	5.015742	10.2693	2.021693
1174 F5	0.321039	0.10402	25.36911	41.45974	3.76044	3.086297
1055 F5	0.901037	0.602063	10.5398	21.6898	3.20709	1.496584
1044 F5	0.322710	0.230281	16.18483	10.65181	2.77666	1.401378
924 F5	0.468550	0.335923	9.25208	4.882869	6.3104	1.552839
1153 F5	1.051612	0.616247	8.723319	13.09232	6.17248	1.706478
1036 F5	1.103101	0.872303	9.539745	3.871478	3.61706	1.264585
1176 F5	0.960174	0.540951	13.8282	6.784911	5.27109	1.774973
1354 F6	0.724183	0.331232	22.28373	23.02627	3.07	1.804723
1496 F6	0.443131	0.159491	22.16693	22.14439	4.70641	2.778406
1517 F6	0.441796	-	9.851612	-	2.91	-

protein analysis, the two-dimensional electrophoresis was performed afterward. As SDS-PAGE gel compared with fraction 5 has several protein bands, while the gels obtained from 2-DE compared with SDS-Page have much higher analytical power. For analysis and enumeration of protein stains, ImageMaster software was used. With the attained results from the software, the number of changed proteins in fractions 4 to 6 was assessed for increase or decrease of expression. Among the 1654 identified proteins in these fractions, and in view of the considered t-test, 11 proteins in treat group had decreased expression, and two emerged proteins were encountered.

Although 2-DE is a powerful system to analyze proteins, it is unable to analyze low abundant, very small and very large proteins. In prefraction RP-HPLC proteins were separated based on hydrophobicity. In light of the other added protein characteristics in this analysis before 2-DE, this technique could be an efficient method used to increase the power of analysis and separation of complex protein mixtures in *Aspergillus Fumigatus* proteome. Therefore, the analysis and fractionation prior to doing 2-DE caused increased accuracy in identifying changes in protein profile expression of *ANXC4* gene. In fact, with this method, another dimension is added to the analysis of proteins. In order to accurately identify proteins with changed expression, the use of mass spectroscopy methods is necessary. With the results of the present study, we can identify the proteins involved in genomes of *Aspergillus Fumigatus* more precisely, and benefit from it in future research projects.

Acknowledgements

Authors acknowledge Dr. Vahid Khalajin biotechnology department of Pasteur Institute of Iran, for Giving samples of mutant strain of *Aspergillus fumigatus*. The authors also express their gratitude to Dr. Behrouz Vaziri for their valuable advices.

Conflict of Interest

The authors declare that there is no conflict of interest regarding the publication of this article.

References

1. Anderson, N. L., Matheson, A. D. and Steiner, S. (2000) Proteomics: Applications in basic and applied biology. Current Opinion in Biotechnology, pp. 408–412.

2. Badock, V. Steinhvsen,V.,Bommert,K.,Otto,A. (2001) Prefractionation of protein samples for proteome analysis using reversed-phase high-performance liquid chromatography. Electrophoresis, 22(14), pp. 2856–2864.
3. Dagenais, T. R. T. and Keller, N. P. (2009) Pathogenesis of Aspergillus fumigatus in invasive aspergillosis. Clinical Microbiology Reviews. American Society for Microbiology (ASM), pp. 447–465.
4. Debeaupuis, J. P. Sarfati,J.,Chazlet,V.,and paullatge,.J.(1997) Genetic diversity among clinical and environmental isolates of Aspergillus fumigatus. Infection and immunity, 65(8), pp. 3080–5.
5. Gerke, V. and Moss, S. E. (2002) Annexins: From Structure to Function. Physiological Reviews, 82(2), pp. 331–371.
6. Govorun, V. M. and Archakov, A. I. (2002) Proteomic technologies in modern biomedical science. Biochemistry (Moscow), pp. 1109–1123.
7. Karpievitch, Y. V ,.polpitiya,A.D.,Anderson,G.D.,Smith,R .D.,andDabney,A.R. (2010) Liquid chromatography mass spectrometry-based proteomics: Biological and technological aspects. Annals of Applied Statistics, 4(4), pp. 1797–1823.
8. Khalaj, K., Aminollahi, E., Bordbar, A., and Khalaj, V., Fungal annexins: a mini review (2015)
9. Khalaj, V. Smith,L.,Brookman,J.,Tuckwell,D. (2004) Identification of a novel class of annexin genes. FEBS Letters, 562(1–3), pp. 79–86.
10. Khalaj, V. Azarian,B.,Enayati,S.,Vaziri,B. (2011)Annexin C4 in A. Fumigatus: A proteomics approach to understand the function. Journal of Proteomics, 74(10), pp. 1950–1958.
11. Latgé, J. P. (2001) The pathobiology of Aspergillus fumigatus. Trends in Microbiology, pp. 382–389.
12. Maryam, M., FU, M, S., Alaiano, A., Camacho, E., Diego, G., Faneuff, E. E. (2019)The enigmatic role of fungal annexins: the case of cryptococcus neoformans
13. Moss, S. E. and Morgan, R. O. (2004) The annexins. Genome Biology. BioMed Central, p. 219.
14. Neverova, I. and Van Eyk, J. E. (2005) Role of chromatographic techniques in proteomic analysis. Journal of Chromatography B: Analytical Technologies in the Biomedical and Life Sciences, pp. 51–63.
15. Righetti, P. G. Castagna, A.Herbert,B. Reymond,F.Rossier,J.S.(2003) Prefractionation techniques in proteome analysis. in Proteomics, pp. 1397–1407.
16. Righetti, P. G. Castagna, A.AntonioliL, P.(2005) Prefractionation techniques in proteome analysis: The mining tools of the third millennium. Electrophoresis, pp. 297–319.
17. Ronning, C. M. Fedorova, N.D., Bowyer, P., Coulson, R., Goldman, G., Kim, H.S., Turner, G., Wortman, J.R., Yu, J., Anderson, M.J., Denning, D.W., Nierman, W.C. (2005)Genomics of Aspergillus fumigatus. Revista Iberoamericana de Micologia, pp. 223–228.
18. Srinivas, P. R., Verma , M.,Zhao , Y., and Srvastava, S. (2002) Proteomics for cancer biomarker discovery. Clinical Chemistry, pp. 1160–1169.
19. Van Eyk, J. E. (2001) Proteomics: unraveling the complexity of heart disease and striving to change cardiology. Curr Opin Mol Ther, 3(6), pp. 546–553.
20. Vaziri, B. ,Rahimpour,M.,Eslami,N.,Fayaz,A.,Rah imian,H. (2006) RP-HPLC prefractionation and its application in expressional proteomics analysis of an in vitro viral infection model. Journal of Separation Science, 29(15), pp. 2284–2291.

Journal of Cell and Molecular Research (2019) 10 (2), 97-101 DOI: 10.22067/jcmr.v10i2.73964

Research Article

Kinetic Study of Erythrose Reductase Extracted from *Yarrowia lipolytica*

Masoud Mohammadi Farsani[1], Mohammad Mohammadi[1*], Gholam Reza Ghezelbash[1], Ali Shahriari[2]

[1] *Department of Biology, Faculty of Science, Shahid Chamran University of Ahvaz, Ahvaz, Iran*
[2]*Department of Basic Sciences, Faculty of Veterinary Medicine, Shahid Chamran University of Ahvaz, Ahvaz, Iran*

Received 6 July 2018 Accepted.17 March 2019

Abstract

Erythritol as a non-caloric and non-cariogenic sweetener is safe for diabetics. Both microbial fermentation and chemical methods can be used to produce erythritol, but chemical methods failed to be industrialized due to their low efficiency. *Moniliella tomentosa*, *Aureobasidium* sp. and *Yarrowia lipolytica* are industrial producers of erythritol. Erythrose reductase (ER) is a key enzyme in the biosynthesis of erythritol and catalyzes the final step in this pathway. Enzyme extract was obtained from *Y. lipolytica* by grinding cells with 0.5mm glass beads and ER activity was performed using 10 µl enzyme extract, 7.5 mM NADPH and 12 mM D-erythrose in potassium phosphate buffer (pH 7.5). Reaction was monitored with decreasing of NADPH absorbance in OD_{340} at 37 ˚C for 8 min by a microplate analyzer. In order to determine the activation energy (E_a), activity of enzyme was measured in 4-45 ˚C and results were analyzed with Kinetic software according to Arrhenius equation. The best enzyme activity of ER was 6.268 mU. One unit of ER activity was defined as the amount of enzyme that catalyzes the oxidation of 1µmol of NADPH per minute. Specific activity of enzyme was equal to 3.24U/mg and finally the E_a was determined to be 29.6208 KJ.ER specific activity in this study was lower than the only similar study that used *Y. lipolytica*. Purification, overexpression and optimizing the reaction can help to increase enzyme performance.

***Keywords*:** Erythrose reductase, *Yarrowia lipolytica*, Enzyme kinetics

Introduction

Polyols are compatible solutes and effective in osmotic adjustment. Among polyols, glycerol and erythritol are more effective in osmotic adjustment because of their lower molecular weights (Ghezelbash et al., 2012).

Erythritol (MW 122.12) as a non-caloric four-carbon sugar alcohol or polyol is safe for diabetics, cause no gastric side effects and its use in foods and drugs is approved (Ghezelbash et al., 2014; Moon et al., 2010; Tomaszewska et al., 2012) erythritol has 60-70 percent of the sucrose sweetness and both are similar in taste profile (Tomaszewska et al., 2014b) without changing blood glucose and insulin levels, erythritol is excreted in the human urine or by renal processes. Because the bacteria causing dental caries cannot utilize erythritol as a carbon source, it might be safe for human teeth health(Park et al., 2011). Microbial fermentation and chemical methods can be used to produce erythritol. A high-temperature chemical reaction is necessary to synthesis erythritol from dialdehyde starch and this reaction needs a metal as it's catalyzer and therefor the costs of chemical reactions are high(Lee et al., 2010).Nowadays, fermentative methods reach to industrialization due to their high efficiency (Ghezelbash et al., 2014). Producers of erythritol can be osmophilic yeasts belonging to genus *Aureobasidium*, *Candida*, *Moniliella*, *Pichia*, *Pseudozyma*, *Trigonopsis*, *Trichosporon*, *Trichosporonoides* and *Yarrowia* (Moon et al., 2010). A mutant of *Aureobzidium* sp. is being used industrially to produce erythritol at a high yield of 44% in a medium with 40% glucose(Ishizuka et al., 1989). Erythritol can also be produced by the yeast *Yarrowialipolytica* (Rymowicz et al., 2009) which is known as a safe producer of polyols, proteins, lipids and organic acids (Janek et al., 2017). In yeasts, the final step of the pentose phosphate pathway (PPP) is catalyzed by erythrose reductase (ER), a key enzyme to produce erythritol by reducing erythrose. In this reaction, NAD(P)H is used by ER as co-enzyme(Lee et al., 2003b). Finally, yeast uses erythritol as an osmo protectant (Janek et al., 2017). The aim of this study was to determine kinetic parameters of ER and optimizing the enzyme activity.

*Corresponding author E-mail: mohamadi74@yahoo.com

Materials and Methods

Microorganism and culture media

Yarrowia lipolytica DSM70562 (Leibniz Institute DSMZ, Germany) was used in this study as an industrial producer of erythritol. The growth medium for activation contained 10% glucose, 0.5% yeast extract, 0.5% KH2PO4, 0.2% (NH4)2SO4 and 0.04% MgSO4(Merck, Darmstadt, Germany). We kept yeast cultures at 4°C and sub-cultured them every 4 weeks. The production medium used for this study contained 1% yeast extract, 0.5% KH2PO4, 0.025% MgSO4, and 20% glucose (Merck, Darmstadt, Germany). The initial pH of both mediums was adjusted to 5.5 (Ghezelbash et al., 2012; Ghezelbash et al., 2014).

Culture conditions

We inoculated a single colony of *Y. lipolytica* into 10 ml of production medium in 100ml Erlenmeyer flask and it was incubated at 30 ˚C and 120 rpm for 48 h. In the next step, we aseptically transferred 2.5 ml of the seed culture into 250ml Erlenmeyer flask containing 50ml of production medium and incubated it at 30 ˚C and 120 rpm for 168 h (Ghezelbash et al., 2012; Ghezelbash et al., 2014).

Preparation of cell extract

Yeast cells from the culture were harvested by centrifugation at 6,000 rpm for 10 min. After washing twice with 50mM potassium phosphate buffer (pH 7.5) containing 5 mM mercaptoethanol, cells were re-suspended in homogenization buffer containing 50 mM potassium phosphate buffer(pH 7.5), 10mMMgCl2, 1mMdithiothreitol (DTT) (Merck, Darmstadt, Germany), and 1 mM phenylmethylsulfonyl fluoride (PMSF) (Sigma, Northbrook, USA).In the next step, cell suspension was incubated at room temperature for 1h and then disrupted by grinding with glass beads (0.5 mm in diameter; Sigma, Northbrook, USA) and immediately kept on ice. The ruptured cells were removed by centrifugation at 12,000 rpm for 30 min at 4˚C. The supernatant was used for kinetic assays and further analysis.

Enzyme activity

Erythrose reductase enzyme activity was determined as reported previously (Ghezelbash et al., 2014),with some modifications given below. We determined ER activity using 12mM D-erythrose and 0.75mM NADPH (Sigma Aldrich, Germany) in 50 mM phosphate buffer (pH=7.5) and 10 µl enzyme extract in a microplate chamber (total volume 200 µl). Before reaction, the mixture was kept for 1 min at room temperature to eliminate the endogenous oxidation of NADPH. Then, reaction was monitored for NADPH absorbance in OD_{340} at 37˚C for 15 min using Microplate Analyzer (Bio-Rad, America). One unit of ER activity is the amount of enzyme that catalyzes the oxidation of 1 µmol of NADPH per min at 37 ˚C (Ghezelbash et al., 2014). Enzyme activities were estimated with micro plate analyzer (MPA) software.

Optimization of enzyme activity

Before starting the enzyme kinetic assays, we decided to optimize the reaction by finding the best concentration of NADPH and D-erythrose for determination of optimum enzymatic activity. For this purpose, erythrose reductase activity was investigated at different concentrations of NADPH (0.5 to 2 mM) and D-erythrose (1 to 15 mM).Then the lowest volume of enzyme extract giving highest activity was determined. As the $4^{th}$and 5^{th} steps, we estimated the effect of different temperatures (4-40˚C) and the effect of pH (2-9) on enzyme activity respectively. After any step, we used the optimized variable of the previous step.

Enzyme kinetic assay

The kinetic assay was performed using D-erythrose as substrate with concentrations between 0 to 15mM in optimized reaction. Activities of each concentration were measured with MPA software and the Michaelis-Mentenplot, Lineweaver-Burk plot, K_m and V_{max} was obtained with Graph-Pad Prism7 software (Fig.3).

Results

Optimizing the reaction conditions

The best concentration of NADPH with a higher amount in enzyme activity was 1.5mM (Fig.1). Then it was observed that the amounts beyond 10 µl of enzyme extract could not increase the activity of ER. There was no need to determine the optimized concentration of D-erythrose as the substrate of the reaction, because it is used in different concentrations in order to make the Michaelis-Menten plot. (In this study no NADPH to $NADP^+$interconversion activity or vice versa was observed in the crude extract of ER).

Effect of temperature and pH

Optimum assay condition was used to determine the effect of temperature and pH. As showed in Fig. 2, the best activities of ER were in

pH=3 and 28˚C

The lowest dose that was able to induce the significant increase in MnBi frequency in this experiment was 1.5 ng.ml^{-1}. To minimize the probability of cell damage, we used this dose throughout the rest of the experiment.

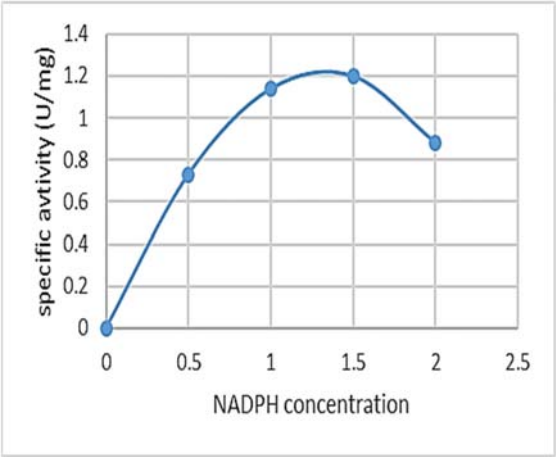

Figure1. Optimization of NADPH concentraion

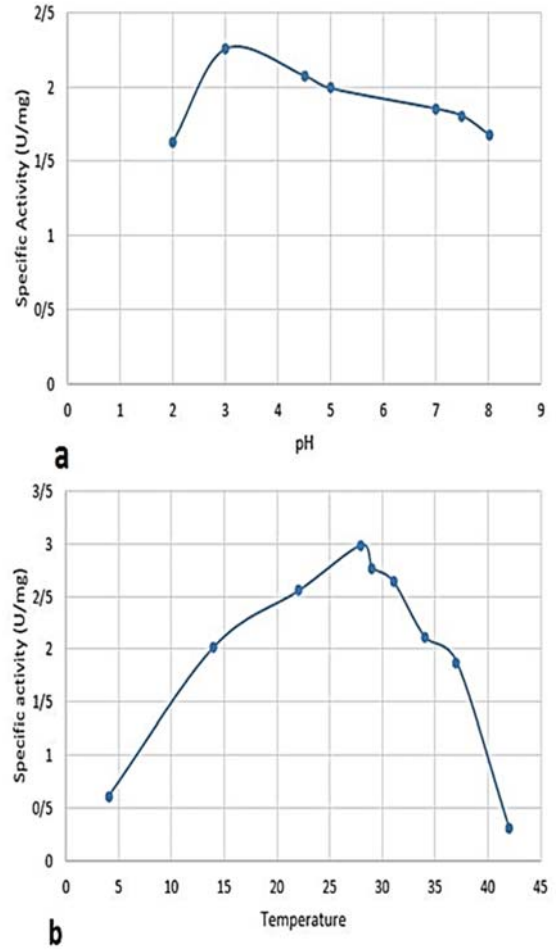

Figure 2. Optimization of pH (a) and temperature (b)

Enzyme kinetic parameters

Enzyme kinetic assay was performed using concentrations between 0 to 15mM of D-eryhtrose in optimum conditions of the reaction. An activity was calculated with MPA software and results were analyzed with Kinetic software. Michaelis-Menten plot and Lineweaver-Burk plot are given in Fig.3. Kinetic parameters were determined using nonlinear regression (Table 1).

Table 1. Results obtained from enzyme optimization

Variable	Range	Best activity
NADPH concentration(mM)	0.5 to 4	1.5
D-erythrose concentration(mM)	1 to 15	12
Enzyme extract valume(µl)	5 to 100	10
Effect of Temprature (˚C)	4 to 40	28
Effect of pH	2-9	3

[a]: Statistical difference with control (P<0.05)

Discussion

Temperature and pH optimization: the effect of temperature and pH on ER activity revealed that 28℃ and pH=3 are the best conditions for optimum enzyme activity. The best temperature for *Y. lipolytica*'s growth is 28-32℃(Groenewald et al., 2014),but it seems that the best activity of ER should be around 28℃. However, other studies on ER revealed different results. The optimum reported temperature for ER activity in *Candida magnolia* is 40 or 42℃ in different studies(Lee et al., 2010)(Lee et al., 2003a). Recently in a study which used a wild-type of *Y. lipolytica* (A101), results shows the best activity in37℃, but differences between 28℃ and 37℃ was low (only 0.5 U/mg-protein in specific activity) (Janek et al., 2017). As seen in Fig. 2a, the best activity of ER was in pH=3. Higher and lower amounts of pH can significantly decrease the enzymatic activity. As reported before, the optimum activity in low pH can be caused by the phenomenon of high titer of erythritol in acidic pH (Janek et al., 2017). However, producing erythritol by *Y. lipolytica* at low pH has been shown previously (Dobrowolski et al., 2016; Kamzolova et al., 2015; Morgunov et al., 2013; Rymowicz et al., 2009).In another study it has been revealed that the increasing of pH can help decrease amounts of erythritol (Tomaszewska et al., 2014a) and it can be considered as a consequence

of ER inactivation (Janek et al., 2017).

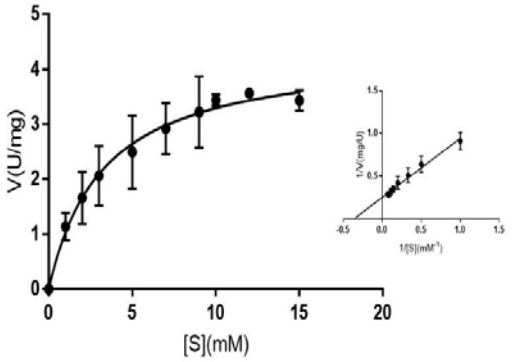

Figure 3. michaelis-menten and Lineweaver-Burk plot

Table 2. Kinetic parameters of erythrose reductase from yarrowia lipolytica

Kinetic parameter	Value (±SEM)	Unit
Km	3.254±0.654	mM
Vmax	4.362±0.2963	U/mg
Kinetic parameter	Value (±SEM)	Unit
The assays were conducted at 28℃ and data are presented as the mean ±standard error of the mean, (n=3). Km, Michaelis- Menten constant; Vmax , maximum velocity		

Table 3. Kinetic parameters of erythrose reductase from yarrowia lipolytica

Microorganism	Km (mM)	Reference
*Yarrowia lipolytica*DSM70562	3.254 ± 0.654	-
*Candida magnoliae*JH110	8.5 ± 0.4	(7)
Torula corallina	7.12	(11)
*Aureobasidium*sp. mutant.	8.0	-
Schizophyllum commune	5.0	-
Candida magnoliae	7.9	(13)

Enzyme activity and kinetics :among all substrates which can be used to be oxidized with ER, D-erythrose showed much better activities(Ishizuka et al., 1992; Jovanović et al., 2013; Lee et al., 2010; Lee et al., 2003a; Lee et al., 2003b). In our study, the best initial velocity occurred in 12mM concentration of D-erytrose in the optimum condition. Specific activity of ER isolated from *Y. lipolytica* in our study was about 60% compare to ER isolated from a wild-type *Y. lipolytica* in a study which used purified enzyme for the reaction (Janek et al., 2017). But in current study we used crude enzyme to promote the reaction and it may be the reason that enzyme activity was lower than the other measurement. In the optimum condition, kinetic parameters (K_M= 3.254 mM and V_{max}=4.362 U/mg protein) were obtained from Prism 7software. Compare to the other studies using different microorganisms containing ER, affinity of the ER isolated from *Y. lipolytica* seems to be more and desirable (Table 3). These properties may be important for using of *Y. lipolytica* in industrial purposes.

Acknowledgments

The current study was supported by the Grant from Shahid Chamran University of Ahvaz to Masoud Mohammadi Farsani for obtaining M.Sc. degree.

References

1. Dobrowolski A., Mituła P., Rymowicz W. and Mirończuk A. M. (2016) Efficient conversion of crude glycerol from various industrial wastes into single cell oil by yeast *Yarrowia lipolytica*. Bioresource technology 207:237-243.
2. Ghezelbash G., Nahvi I. and Rabbani M. (2012) Study of polyols production by *Yarrowia lipolytica* in batch culture and optimization of growth condition for maximum production. Jundishapur Journal of Microbiology 5:546-549.
3. Ghezelbash G. R., Nahvi I. and Emamzadeh R. (2014) Improvement of erythrose reductase activity, deletion of by-products and statistical media optimization for enhanced erythritol production from *Yarrowia lipolytica* mutant 49. Current microbiology 69:149-157.
4. Groenewald M., Boekhout T., Neuvéglise C., Gaillardin C., Van Dijck P. W. and Wyss M. (2014) *Yarrowia lipolytica*: safety assessment of an oleaginous yeast with a great industrial potential. Critical reviews in microbiology 40:187-206.
5. Ishizuka H., Tokuoka K., Sasaki T. and Taniguchi H. (1992) Purification and some properties of an erythrose reductase from an *Aureobasidium* sp. mutant. Bioscience, biotechnology, and biochemistry 56:941-945.

6. Ishizuka H., Wako K., Kasumi T. and Sasaki T. (1989) Breeding of a mutant of *Aureobasidium* sp. with high erythritol production. Journal of Fermentation and Bioengineering 68:310-314.
7. Janek T., Dobrowolski A., Biegalska A. and Mirończuk A. M. (2017) Characterization of erythrose reductase from *Yarrowia lipolytica* and its influence on erythritol synthesis. Microbial Cell Factories 16:118.
8. Jovanović B., Mach R. L. and Mach-Aigner A. R. (2013) Characterization of erythrose reductases from filamentous fungi. AMB Express 3:43.
9. Kamzolova S. V., Vinokurova N. G., Lunina J. N., Zelenkova N. F. and Morgunov I. G. (2015) Production of technical-grade sodium citrate from glycerol-containing biodiesel waste by *Yarrowia lipolytica*. Bioresource technology 193:250-255.
10. Lee D. H., Lee Y. J., Ryu Y. W. and Seo J. H. (2010) Molecular cloning and biochemical characterization of a novel erythrose reductase from *Candida magnoliae* JH110. Microbial cell factories 9:43.
11. Lee J. K., Kim S. Y., Ryu Y. W., Seo J.H. and Kim J.H. (2003a) Purification and characterization of a novel erythrose reductase from *Candida magnoliae*. Applied and environmental microbiology 69:3710-3718.
12. Lee J. K., Hong K. W. and Kim S. Y. (2003b) Purification and properties of a NADPHdependent erythrosereductase from the Newly isolated *Torula corallina*. Biotechnology progress 19:495-500.
13. Moon H.J., Jeya M., Kim I.W. and Lee J.K. (2010) Biotechnological production of erythritol and its applications. Applied microbiology and biotechnology 86:1017-1025.
14. Morgunov I. G., Kamzolova S. V. and Lunina J. N. (2013) The citric acid production from raw glycerol by *Yarrowia lipolytica* yeast and its regulation. Applied microbiology and biotechnology 97:7387-7397.
15. Park E. H., Ryu Y. W. and Kim M. D. (2011) Role of osmotic and salt stress in the expression of erythrose reductase in *Candida magnoliae*. Journal of microbiology and biotechnology 21:1064-1068.
16. Rymowicz W., Rywińska A. and Marcinkiewicz M. (2009) High-yield production of erythritol from raw glycerol in fed-batch cultures of *Yarrowia lipolytica*. Biotechnology Letters 31:377-380.
17. Tomaszewska L., Rakicka M., Rymowicz W. and Rywińska A. (2014a) A comparative study on glycerol metabolism to erythritol and citric acid in *Yarrowia lipolytica* yeast cells. FEMS yeast research 14:966-976.
18. Tomaszewska L., Rymowicz W. and Rywińska A. (2014b) Mineral supplementation increases erythrose reductase activity in erythritol biosynthesis from glycerol by *Yarrowia lipolytica*. Applied biochemistry and biotechnology 172:3069-3078.
19. Tomaszewska L., Rywińska A. and Gładkowski W. (2012) Production of erythritol and mannitol by *Yarrowia lipolytica* yeast in media containing glycerol. Journal of industrial microbiology & biotechnology 39:1333-1343.

Scientific Reviewers

MANUSCRIPT PREPARATION

Manuscripts should be prepared in accordance with the uniform requirements for Manuscript's Submission to **"Journal of Cell and Molecular Research".**

Language: Papers should be in English (either British or American spelling). The past tense should be used throughout the results description, and the present tense in referring to previously established and generally accepted results. Authors who are unsure of correct English usage should have their manuscript checked by somebody who is proficient in the language; manuscripts that are deficient in this respect may be returned to the author for revision before scientific review.

Typing: Manuscripts must be typewritten in a font size of at least 12 points, double-spaced (including References, Tables and Figure legends) with wide margins (2.5 cm from all sides) on one side of the paper. The beginning of each new paragraph must be clearly indicated by indentation. All pages should be numbered consecutively at the bottom starting with the title page.

Length: The length of research articles should be restricted to ten printed pages. Short communication should not exceed five pages of manuscript, including references, figures and tables. Letters should be 400-500 words having 7-10 references, one figure or table if necessary. Commentaries and news should also be 800-1000 words having 7-10 references and one figure or table if necessary.

Types of Manuscript: JCMR is accepting original research paper, short communication reports, invited reviews, letters to editor, biographies of scientific reviewers, commentaries and news.

Statement of Human and Animal Rights: Author's should declare regulatory statement regarding the experiments using animals, human cells/tissues that all in vivo experiments have been performed according to the guidelines (explained by WHO, international animal rights federations or your respective institute) to use animals in their research work.

Conflict of Interest Statement: Authors or corresponding author should declare statement of conflict of interest at the last of manuscript.

Manuscript Evaluation Time: All submitted manuscripts will be evaluated and reviewed according to following evaluation schedule.
Pre-Editorial Evaluation: All submitted manuscripts, right after their submission to JCMR will be evaluation by Editors for being according to the journal scope and format. This evaluation can take 2-7 days of submission.
Reviewer's Evaluation: Selected manuscripts after pre-editorial evaluation will be sent to minimum two blind reviewers assigned by Editor-in-Chief. This process may take 21-27 days.
Post Editorial Evaluation: After receiving reviewer's comments, editors evaluate the manuscripts considering the comments and decide their first decision. This process takes 3-5 days and then authors are informed regarding the editorial decision.

GENERAL ARRANGEMENT OF PAPERS

Title: In the first page, papers should be headed by a concise and informative title. The title should be followed by the authors' full first names, middle initials and last names and by names and addresses of laboratories where the work was carried out. Identify the affiliations of all authors and their institutions, departments or organization by use of Arabic numbers (1, 2, 3, etc.).

Footnotes: The name and full postal address, telephone, fax and E-mail number of corresponding author should be provided in a footnote.

Abbreviations: The Journal publishes a standard abbreviation list at the front of every issue. These standard abbreviations do not need to be spelled out within paper. However, non-standard and undefined abbreviations used five or more times should be listed in the footnote. Abbreviations should be defined where first mentioned in the text. Do not use abbreviations in the title or in the Abstract. However, they can be used in Figures and Tables with explanation in the Figure legend or in a footnote to the Table.

Abstract: In second page, abstract should follow the title (no authors' name) in structured format of not more than 250 words and must be able to stand independently and should state the Background, Methods, Results and Conclusion. Write the abstract in third person. References should not be cited and abbreviations should be avoided.

Keywords: A list of three to five keywords for indexing should be included at bottom of the abstract. Introduction should contain a description of the problem under investigation and a brief survey of the existing literature on the subject.

Materials and Methods: Sufficient details must be provided to allow the work to be repeated. Correct chemical names should be given and strains of organisms should be specified. Suppliers of materials need only be mentioned if this may affect the results. Use System International (SI) units and symbols.

Results: This section should describe concisely the rationale of the investigation and its outcomes. Data should not be repeated in both a Table and a Figure. Tables and Figures should be selected to illustrate specific points. Do not tabulate or illustrate points that can be adequately and concisely described in the text.

Discussion: This should not simply recapitulate the Results. It should relate results to previous work and interpret them. Combined Results and Discussion sections are encouraged when appropriate.

Acknowledgments: This optional part should include a statement thanking those who assisted substantially with work relevant to the study. Grant support should be included in this section.

References: References should be numbered and written in alphabetical order. Only published, "in press" papers, and books may be cited in the reference list (see the examples below). References to work "in press" must be accompanied by a copy of acceptance letter from the journal. References should not be given to personal communications, unpublished data, manuscripts in preparation, letters, company publications, patents pending, and URLs for websites. Abstracts of papers presented at meetings are not permissible. These references should appear as parenthetical expressions in the text, e.g. (unpublished data). Few example of referencing patterns are given as follows:

Bongso A., Lee E. H. and Brenner S. (2005) Stem cells from bench to bed side. World Scientific Publishing Co. Singapore, 38-55 pp.

Irfan-Maqsood M. (2013) Stem Cells of Epidermis: A Critical Introduction. Journal of Cell and Molecular Research 5(1): 1-2.

Note: All the reference should be in EndNote format (JCMR EndNote Style is available on JCMR's web site, Author's Guideline)

Tables and Figures: Tables and Figures should be numbered (1, 2, 3, etc.) as they appear in the text. Figures

should preferably be the size intended for publication. Tables and Figures should be carefully marked. Legends should be typed single-spaced separately from the figures. Photographs must be originals of high quality. Photocopies are not acceptable. Those wishing to submit color photographs should contact the Editor regarding charges.

Black Page Charges: There is no black page charges for publication in the Journal of Cell and Molecular Research.

Color Page Charges: All color pages being printed in color will cost 1,000,000 Iranian Rials/page.

JCMR Open Access Policy: Journal of Cell and Molecular Research follows the terms outlined by the Creative Common's Attribution-Only license (CC-BY) to be the standard terms for Open Access. Creative Commons License.

Note: All manuscripts submitted to JCMR are tracked by using "Plagiarism Tracker X" for possible plagiarism before acceptance to JCMR

Table of Contents

Journal of Cell and Molecular Research

Volume 10, Number 2, Winter 2019